`

HUMAN FACE SHAPED MICROSTRIP PATCH ANTENNAS FOR ULTRA-WIDEBAND APPLICATIONS

By:

Anandhi Dharmarajan

Supervisor:

Dr. Pradeep Kumar

Co-Supervisor:

Prof. Thomas Joachim Odhiambo Afullo

A dissertation submitted in fulfilment of the requirements for the degree of Master of Science in Electronic Engineering

COLLEGE OF AGRICULTURE, ENGINEERING AND SCIENCE

UNIVERSITY OF KWAZULU-NATAL

November 2019

`

HUMAN FACE SHAPED MICROSTRIP PATCH ANTENNAS FOR ULTRA-WIDEBAND APPLICATIONS

by:

Anandhi Dharmarajan

A dissertation submitted in fulfilment of the requirements for the degree of Master of Science in Electronic Engineering

As the candidate's supervisors, we agree to the submission of this dissertation.

Dr. Pradeep Kumar

Signed: _____ Date: _____

Prof. Thomas Joachim Odhiambo Afullo

Signed: _____ Date: _____

`

DECLARATION 1: PLAGIARISM

I, Anandhi Dharmarajan, declare that:

1. The research reported in this dissertation, except where otherwise indicated or acknowledged, is my original work.
2. This dissertation has not been submitted in full or in part for any degree or examination to any other university.
3. This dissertation does not contain other persons' data, pictures, graphs or other information, unless specifically acknowledged as being sourced from other persons.
4. This dissertation does not contain other persons' writing, unless specifically acknowledged as being sourced from other researchers. Where other written sources have been quoted, then:
    a) Their words have been re-written, but the general information attributed to them has been referenced.
    b) Where their exact words have been used, their writing has been placed inside quotation marks and referenced.
5. Where I have used material for which publications followed, I have indicated in detail my role in the work.
6. This dissertation is primarily a collection of material, prepared by me, published as journal articles or presented as a poster and oral presentations at conferences. In some cases, additional material has been included.
7. This dissertation does not contain text, graphics or tables copied and pasted from the Internet, unless specifically acknowledged, and the source being detailed in the dissertation and in the References sections.

Signed: _____ Date: _____

`

DECLARATION 2: PUBLICATIONS

I, Anandhi Dharmarajan, declare that the following is the list of publications from this dissertation:

1. A. Dharmarajan, P. Kumar, T. J. O. Afullo, "A human face shaped microstrip patch antenna for ultra-wideband applications", *Proceedings of ICTSES 2018, Lecture Notes in Electrical Engineering*, Springer (in press).
2. A. Dharmarajan, P. Kumar, T. J. O. Afullo, "A human face shaped ultra-wideband microstrip patch antenna with enhanced bandwidth", *Proceedings of the IEEE International Multidisciplinary Information Technology and Engineering Conference (IMITEC 2019)*, South Africa, IEEE Xplore (accepted).
3. A. Dharmarajan, P. Kumar, T. J. O. Afullo, "A high gain UWB human face shaped MIMO patch antenna with high isolation", *Progress in Electromagnetic Research Journals* (under review).

Signed: _____ Date: _____

<Anandhi Dharmarajan>

`

ABSTRACT

Wireless communication is a promising technology in recent years and the future communication devices needs to accommodate large number of users with high data rate. This proves that the antennas must be wideband to cover the large frequency band. Ultra-wideband (UWB) technology offers very high bandwidth using little power. The allocated frequency range for the UWB technology is from 3.1 GHz to 10.6 GHz for the unlicensed use. This study presents the design and development of the novel human face shaped microstrip patch antennas which cover the entire UWB frequency range with a notch band for eliminating wireless local area network (WLAN) signals.

The initial design of the human face shaped microstrip patch antenna with rectangular Defected ground structure (DGS) operates for the bandwidth from 5.9 GHz to 11.2 GHz. The human face shaped antenna has an overall size of $25.2\ mm \times 38.2\ mm$. To enhance the bandwidth of the system, the design of a human face shaped microstrip patch antenna with rectangular and triangular DGS, that operates for the bandwidth from 3 GHz to 14.7 GHz with a notch band of $5\ GHz - 6.3\ GHz$ is presented. The human face shaped antenna with enhanced bandwidth has the overall size of $24.6\ mm \times 38.6\ mm$. To enhance the capacity of the wireless system, the design of a human face shaped multiple input multiple output (MIMO) microstrip patch antenna, that uses polarization diversity technique, is also presented in this study. The MIMO antenna has two orthogonal human face shaped patches for achieving dual polarization. The MIMO antenna can operate for the bandwidth from 2.8 GHz to 16.1 GHz and has a notch band of $5\ GHz - 6.4\ GHz$. The overall size of the MIMO antenna is $39.1\ mm \times 70.2\ mm$. The proposed antennas utilize the concept of the DGS along with the human face shaped patch to achieve the wideband characteristics. The antennas are fed by 50Ω microstrip line and is optimized using CST microwave studio. The notch rejects the interference from WLAN signals at $5 - 6\ GHz$ frequency band.

The antenna parameters like reflection coefficient, radiation pattern, gain, efficiency etc. are presented and discussed for each antenna configuration. Each antenna with the optimized dimensions is fabricated and measured. The maximum gain, minimum reflection coefficient and maximum directivity of the human face shaped antenna with rectangular DGS are $6.219\ dB$, $-35.11\ dB$ and $6.268\ dBi$, respectively. The maximum gain, minimum reflection coefficient and maximum directivity of the human face shaped antenna with rectangular and triangular DGS are $5.945\ dB$, $-35.4\ dB$ and $6.411\ dBi$, respectively. The maximum gain, minimum reflection coefficient and maximum directivity of the human face shaped MIMO antenna with polarization diversity are $7.079\ dB$, -22 dB and $7.609\ dBi$, respectively. The

`

isolation between the ports for MIMO antenna is high over the entire operating bandwidth. The proposed antennas are simple in configuration, compact in size and easy to fabricate. The antennas operate over a wide bandwidth with high gain, high efficiency and high directivity. The MIMO antenna also has good isolation between the ports. The simulated and measured results prove that the proposed antennas are suitable for UWB communication systems.

`

ACKNOWLEDGEMENT

The work presented in this dissertation would not be possible without people who encouraged me and supported me. Firstly, I convey my sincere gratitude to my supervisor **Dr. Pradeep Kumar** of the University of KwaZulu-Natal (UKZN) for his constant support and guidance. He pointed me in the right direction and always had his door open for all my questions. He motivated me to complete my research by providing timely advice. I would also like to convey my regards to **Prof. Thomas Joachim Odhiambo Afullo** of the University of KwaZulu-Natal (UKZN) for making sure that I do not divert from the topic of the research. I convey my sincere respect to my Employer **Mr. Paul Michael Alcock** who motivated me and gave me time for my research.

I thank GOD for blessing me proficiency and perseverance to complete the dissertation. I thank my parents who always believed in me and wished me success. I wish to thank my Mother-in-Law for her encouraging and motivating words at times of difficulty. I find no words to thank my husband who was a great pillar of support to complete my research. He gave me confidence and showed me light amidst dark. I also like to thank my kids who encouraged me with their kind words.

`

TABLE OF CONTENTS

`

`

`

LIST OF TABLES

`

LIST OF FIGURES

`

`

`

LIST OF ABBREVIATIONS

BSF	Band Stop Filter
CST	Computer Simulation Technology
DGS	Defected Ground Structure
DMS	Defective microstrip structure
DRA	Dielectric Resonator Antenna
HIPERLAN	High Performance Radio LAN
HPDGS	Horizontal Periodic DGS
ITU	International Telecommunications Union
MIMO	Multiple Input Multiple Output
MMIC	Monolithic Microwave Integrated Circuit
MPA	Microstrip Patch Antenna
PICA	Planar Inverted Cone Antenna
PFDGS	Periodic Fractal DGS
UWB	Ultra-wideband Antenna
VPDGS	Vertical Periodic DGS
VSWR	Voltage Standing Wave Ratio
WiMAX	Worldwide Interoperability for Microwave Access
WLAN	Wireless Local Area Network

`

CHAPTER 1: INTRODUCTION

This chapter discusses the importance of antennas in wireless communication systems and the background of microstrip patch antennas. The chapter also introduces the importance of defected ground structure in microstrip antennas. The problem statement, research motivation and research questions are presented. The contribution of the dissertation, research methodology and dissertation outline are also discussed.

1.1 Background

Wireless communication is between the devices which are not connected using wired signals. This helps the users around the globe and those in rural areas to communicate with one other. Local Wi-Fi networks and cellular networks are two main types of wireless communication systems. Wi-Fi networks allow systems to communicate with each other over a short distance. This technology is used in laptops, tablets and printers to communicate with the internet. Cellular networks involve communication over long distance that enables the use of mobile phones.

Antennas play a vital role in wireless communication systems as it transforms the radio frequency signals into the current signals and vice versa. In 1890, only small number of antennas were there in the entire world. Today an average person uses a mobile phone to communicate. The mobile communication is not possible without the existence of antenna. Microstrip patch antenna (MSA) are used in various applications as these antennas are small in size and light in weight. These antennas can support dual polarization and the manufacturing cost for these antennas is low. The major disadvantages of these antennas are that these provide a very narrow bandwidth and poor gain [1]. In 2002, federal communication commission (FCC) authorized the use of unlicensed frequency band from 3.1 GHz to 10.6 GHz as ultra-wideband (UWB) for commercial purposes [2-3]. Large bandwidth, high data rate, high immunity to multi-path fading, low power etc are some of the advantages of UWB communication systems [4]. The UWB technology is limited to short range communications as it has low transmitted power [5].

Defected ground structure (DGS) is a technique to increase the impedance bandwidth of the microstrip antennas where defects or slots are etched in the ground plane under the transmission

`

line of the antenna. By changing the size of the defect, the required resonant frequency can be obtained [6]. Multiple input multiple output (MIMO) technique is used to increase channel capacity by providing reliable transmission with high data rates [7]. MIMO antennas must have high isolation between the ports to avoid mutual coupling. MIMO systems with UWB technology can provide high data rate and reliable transmission in wireless communication systems.

1.2 Problem statement

A microstrip antenna has low profile and light weight. In the basic configuration of MSA, the dielectric substrate is sandwiched between two metallic layers namely the ground plane and the patch. The patch can be of different shapes such as elliptical, circular, rectangular, square, ring, monopole, dipole etc. These antennas can easily be mounted on planar or non-planar surfaces. These antennas are used in many wireless applications as they are small and inexpensive. The major disadvantages of microstrip antenna are narrow impedance bandwidth and poor gain. Thus, designing an ultra-wideband microstrip patch antenna becomes a challenge as ultra-wideband antenna requires large bandwidth. There is also interference from other frequency bands existing within the ultra-wideband. If dual polarized antennas in MIMO system are used to increase the system capacity, these suffer from mutual coupling. Considering this view, this study aims to design and develop microstrip patch antennas for UWB applications, for UWB applications with elimination of 5 GHz - 6 GHz WLAN signals and for MIMO ultra-wideband applications with elimination of 5 GHz - 6 GHz WLAN signals.

1.3 Research motivation

As microstrip patch antennas offer very narrow bandwidth, ultra-wideband antennas are needed to accommodate more users and more applications, but UWB antennas require wide impedance bandwidth. When designing an ultra-wideband antenna, interference with existing bands occupied by wireless local area network (WLAN) from 5.1 to 5.35 GHz, high performance radio LAN (HIPERLAN/2) from 5.725 GHz to 5.825 GHz and worldwide interoperability for microwave access (WiMAX) service from 3.3 GHz to 3.6 GHz should be avoided. Therefore, it becomes necessary to design the antenna with wide impedance bandwidth that have band notches to reject interferences. The antenna must have lower reflection coefficient along with high gain and high directivity. The antennas must also have dual

`

polarization in order to use in MIMO systems to improve the system capacity. As dual polarized antenna suffers from mutual coupling, the designed antenna must have high isolation over the entire bandwidth. It is therefore necessary to design a MIMO ultra-wideband antenna that can provide a wide impedance bandwidth along with high isolation between the ports.

1.4 Research questions

The research work in this dissertation attempts to answer the following research questions:

- How can the bandwidth of the microstrip antennas be improved and the antennas be designed for UWB applications with elimination of WLAN signals?
- How can the microstrip antennas be designed to have lower reflection coefficient along with high gain and directivity?
- How can the microstrip antennas be designed for MIMO systems with high isolation between the ports?

1.5 Research contribution

This work presents the design, simulation and fabrication of human face shaped antennas for UWB applications. The first antenna is human face shaped microstrip patch antenna with a rectangular DGS that covers the bandwidth 5.9 GHz-11.2 GHz. The second antenna is human face shaped microstrip patch antenna with one rectangular DGS and two symmetrical triangular DGS that covers the bandwidth 3 GHz- 14.7 GHz with a notch band of 5 GHz- 6.3 GHz for the elimination of WLAN signals. The third antenna is a multiple input multiple output dual polarized human face shaped antenna that covers the bandwidth 2.8 GHz − 16.1 GHz with a notch band of 5 GHz − 6.4 GHz. The isolation between the ports of the MIMO antenna is more than 19.8 dB over the entire bandwidth. The presented antennas utilize the elliptical patch, which is modified to be like a human face to enhance the bandwidth. This work also uses the defected ground structure, which involves etching defects in the ground plane to increase the impedance bandwidth and to reduce the mutual coupling between the ports.

1.6 Research methodology

Various techniques for enhancing the bandwidth of the microstrip antennas are studied. Antenna dimensions such as patch size, width of the circular slots, width of the mouth, width of

`

the eyebrows is calculated using design concepts. The theoretical design is optimized using computer software simulation (CST) microwave studio. The antenna parameters like bandwidth, gain, reflection coefficient, coupling coefficient etc are analyzed. The antennas with the optimized results are fabricated and measured using vector network analyzer (VNA), signal generator, signal analyser, anechoic chamber etc. To increase the system capacity, the concept of polarization diversity is applied. The antennas are positioned properly to minimize mutual coupling. The various concepts for enhancing the antenna parameters are applied to improve the performance of the antenna for UWB applications.

1.7 Overview of chapters

Chapter 1: This chapter presents the basic concepts of the microstrip antenna along with the problem statement, research motivation, research contribution, research question, research methodology and the overview of chapters.

Chapter 2: The literature review of antenna, microstrip antenna concepts along with its limitations and feeding methods are discussed in this chapter. Antenna parameters, defected ground structure and the history of ultra-wideband antennas along with antenna types are also explained in detail.

Chapter 3: This chapter presents the design of human face shaped microstrip antennas which are simulated using CST microwave studio. Reflection coefficient graphs are plotted for various antenna configurations and are analyzed. The theory behind the human face (elliptical patch) is also described. Three-dimensional directivity patterns, gain patterns, normalized radiation patterns, gain and directivity plot, voltage standing wave ratio (VSWR) plot for various antenna configurations are presented and discussed. The gain and directivity plot are also presented for each antenna configuration. The performance of the proposed antennas is also compared with the existing antennas in literature.

Chapter 4: The design of a human face shaped multiple input multiple output antenna with polarization diversity is presented in this chapter. The concept of polarization diversity is explained. Three-dimensional directivity patterns, gain patterns, radiation patterns, gain and directivity plot, VSWR plot for the MIMO antenna are presented. The gain and directivity plot are also presented. The comparison of proposed UWB MIMO antenna with the existing antennas in literature is also presented.

`

Chapter 5: This chapter presents the conclusion of the dissertation along with the future scope of the work.

1.8 Chapter summary

The importance of antennas in the wireless communication systems, the problems with microstrip antennas, advantages of UWB communication systems have been presented. To achieve a wide bandwidth and high channel capacity, the concepts of DGS along with MIMO technique can be utilized. The need of designing an ultra-wideband microstrip patch antenna, ultra-wideband microstrip patch antenna with the elimination of 5 GHz - 6 GHz WLAN signals and ultra-wideband MIMO microstrip patch antenna with the elimination of 5 GHz - 6 GHz WLAN signals antenna have been addressed. The research questions, the contributions of the research and the research methodology used in this research work have also been presented. A brief overview of all chapters of the dissertation have been given.

`

CHAPTER 2: LITERATURE REVIEW

This chapter presents the introduction and importance of the antennas in wireless communication systems. The concepts of microstrip patch antennas along with the advantages, applications, feeding methods, limitations are discussed. Antenna parameters like gain, directivity, VSWR etc are presented and discussed. The different shapes and types of defected ground structures along with the working principle are explained. The literature review of various types of ultra-wideband antennas is also presented in this chapter.

2.1 Antennas in wireless communication systems

Antennas are vital in any wireless system and are used for radiating or receiving radio waves [1]. Antenna is a transducer that converts alternating current into electromagnetic radiations and vice versa. An antenna can be used as transmitter and receiver with the same characteristics. The voltage applied to the antenna terminals and the current flowing through them produce electromagnetic waves. The transmitting antenna converts electric current to electromagnetic waves, which are then propagated in the free space. These electromagnetic waves, at the receiving end, produce electric signals when they are received by the antenna. Thus, the receiving antenna converts the electromagnetic waves into currents, which are compatible for cables. Antennas are used in radar, television broadcasting, space communications, wireless communications etc. Various antenna types are wire antennas, array antennas, reflector antennas, microstrip antennas, aperture antennas, and lens antennas etc [1]. In this work, we will focus on the microstrip antennas. Microstrip patch antennas compact antennas and are suitable for wireless communications, missile, radar, aircraft, mobile communications etc.

2.2 Antenna parameters

The performance of the antenna is characterized based on the antenna parameters like gain, reflection coefficient, directivity, VSWR, bandwidth, radiation patterns, return loss, polarization etc. These parameters also determine the efficiency of the antenna. The antenna parameters are discussed below.

`

2.2.1 Directivity

Directivity is an estimate of how well an antenna can radiate in a direction. Directivity is measured in dB [1].

$$\text{Directivity} = \frac{\text{Maximum radiation intensity}}{\text{Average radiation intensity}} \tag{2.1}$$

Higher values of directivity indicate that the radiation from the antenna is focused in the particular direction. At the receiving side, the antenna will receive the power effectively from a direction in which the directivity is high.

2.2.2 Gain

Gain is defined as the capacity of the antenna to effectively radiate more or less in any direction when compared to the isotropic antenna. The gain of the antenna is a measure of the antenna efficiency and its directivity as given by [1]:

$$\text{Antenna gain} = \text{Directivity} * \text{Efficiency} \tag{2.2}$$

In the case of a transmitting antenna, gain is the measure of how effectively the antenna can radiate the transmitted power into free space in a direction. For receiving antenna, it indicates how effectively the antenna can transform the electromagnetic waves which are received from the space into electrical signals.

2.2.3 Voltage standing wave ratio (VSWR)

VSWR known as voltage standing wave ratio is an estimate of power transferred from source to the load via the transmission line. In ideal scenario, 100% of the power is transmitted, when there is perfect match between the impedance of the source, transmission line and the load. The voltage standing wave ratio is 1.0 or 1:1 in this case. In real life scenario, due to the impedance mismatch, some of the power is transmitted back to the source. The VSWR is higher than one for mismatched loads. Voltage standing wave ratio is given by the ratio of the maximum voltage in the transmission line to the minimum voltage as given below [1]:

`

$$\text{VSWR} = \frac{V_{max}}{V_{min}} \tag{2.3}$$

where V_{max} and V_{min} are the maximum voltage in the transmission line and minimum voltage in the transmission line, respectively.

2.2.4 Return loss

Return loss (R) is defined as the power loss in the signal that is transmitted back from the transmission line. This is generally used to express the mismatch. It is the difference between the incident power and the reflected power, which can be expressed as given below [8]:

$$\text{R (in dB)} = 10 \log_{10} \left(\frac{P_i}{P_r}\right) \tag{2.4}$$

where P_i and P_r are the incident power and the reflected power, respectively.

2.2.5 Reflection coefficient

Reflection coefficient (Γ) determines the amount of the signal propagating in a line that is reflected back to the source. The relation between the reflection coefficient and VSWR are given by the expression as given below [1]:

$$\Gamma = \frac{VSWR-1}{VSWR+1} \tag{2.5}$$

$$\text{VSWR} = \frac{1+\Gamma}{1-\Gamma} \tag{2.6}$$

When the reflection coefficient has the value of one it denotes the worst case as the signal is reflected back completely. In this case, VSWR will have the value of infinity as can be seen from above equation (2.6). This indicates that for higher values of VSWR, the reflection coefficient is higher. Return loss (L_R) in terms of reflection coefficient can be expressed by the following expression [8]:

$$\text{R (in dB)} = -20\, log_{10}\Gamma \tag{2.7}$$

`

2.2.6 Bandwidth

The bandwidth of an antenna refers to the frequency range in which the antenna can satisfy certain parameters like VSWR, reflection coefficient, return loss etc. Usually bandwidth of operation is measured for the frequency range in which the voltage standing wave ratio is lower than 2 and this is known as the impedance bandwidth. The percentage bandwidth (BW) is defined with regards to the centre frequency and is given by [1]:

$$\mathrm{BW} = 100\left(\frac{f_h - f_l}{f_c}\right) \tag{2.8}$$

where f_h , f_l and f_c are the highest frequency of the band, lowest frequency of the band and the center frequency of the band, respectively.

2.2.7 Radiation pattern

The radiation pattern represents the energy radiated by the antenna. Figure 2.1 represents the radiation pattern of a dipole antenna, where there is a main lobe and several back lobes [9]. The radiation pattern of Figure 2.1 is a directive radiation pattern and indicates the directions of high directivity and low directivity. The major lobe represents the direction of high directivity. The other lobes are minor lobes and represent the directions of low directivity. The nulls in the pattern represent zero directivity. It is a radiation lobe having the direction of maximum radiation [1]. Side lobes denote the direction where the radiation is distributed sideways. These indicate the directions, where the power is not desired. The lobe in the anti-direction of the main lobe is denoted as back lobe**.** A substantial amount of energy is dissipated in back lobe and side lobes.

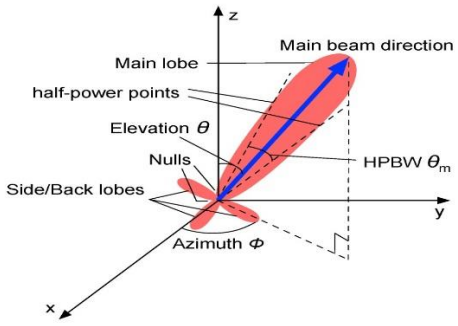

Figure 2.1: Radiation pattern [9]

`

2.2.8 Polarization

Polarization of an antenna defines the direction of the electric field. There are three types of the polarization as following [1]:

- Linear polarization
- Circular polarization
- Elliptical polarization

If the electric field moves in a linear path, it is termed as linear polarization. There are two types of linear polarization namely vertical and horizontal. In case of vertical polarization, the electric field is perpendicular to the earth. It is achieved by the antenna, that is placed vertically to the earth. In the horizontal polarization, the electric field is parallel to the earth and is achieved by the antenna, that is placed horizontal to the earth.

If the electric field moves in a circular path, it is termed as circular polarization. If the electric field has the clockwise rotation, then it is called as right-hand circular polarization. If the electric field has the anti-clockwise rotation, it is called the left-hand circular polarization. If the electric field moves in an elliptical path, it is termed as elliptical polarization. The quality of receiving signals also depends upon the direction of polarization of transmitting and receiving antennas. For the better quality of wireless system, the polarization of transmitting and receiving antennas should be aligned properly.

2.3 Microstrip patch antenna

A microstrip antenna has a radiating patch mounted on the ground plane as shown in Figure 2.2 and therefore referred as patch antennas. The patch is usually etched on the dielectric substrate [10]. The patch is built of material like gold, copper and can be in different shapes namely circular, elliptical, rectangular, triangular, square, or any other shape.

`

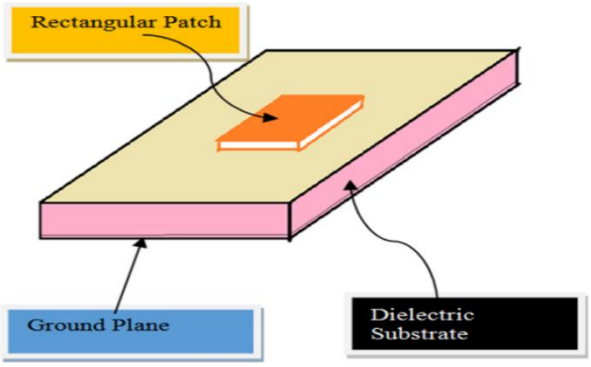

Figure 2.2: Structure of MPA [10]

For a rectangular patch, the electric field does not exist in the centre of the patch but is positive on one side of the patch and negative on the other side. The electric field also extends to the periphery of the patch and is known as fringing field. The patch antenna radiates due to the fringing field which is on the antenna's surface in the positive y direction as shown in Figure 2.3. The current also adds up in phase on the patch antenna but an equal magnitude of current but in the opposite direction is on the ground plane, which effectively neutralizes the radiation. The antenna radiates because of the fringing field that is generated due to the distribution of the voltage on the patch antenna [1].

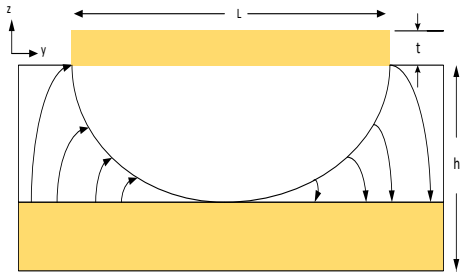

Figure 2.3: Fringing field effect in MPA [1]

The height of the patch is usually $0.003\lambda \leq h \leq 0.05\ \lambda$, where λ is the free space wavelength. The dielectric constant of the substrate is usually $2.2 \leq \epsilon \leq 12$ [1]. Thick substrate has lower dielectric constant and provide greater efficiency with large bandwidth. The antenna's resonant frequency depends on the length of the patch and is given by [11]:

$$f_c = \frac{c}{2L\sqrt{\epsilon_r}} = \frac{1}{2L\epsilon_0\mu_0\sqrt{\epsilon_r}} \tag{2.9}$$

`

From the above equation it is clear that the length of the rectangular patch L is approximately one half of the wavelength in the range of $\frac{\lambda}{3} < L < \frac{\lambda}{2}$.

2.3.1 Advantages of MPA

Microstrip patch antennas are very easy to fabricate, easy to install and so are common in devices like cell phones, satellite and missile communication, spacecraft etc. The advantages are listed below [1]:

- Compact size
- Inexpensive and easy to fabricate
- Robust when mounted on surfaces
- Support multi frequency bands (dual band, triple band)
- Support dual polarization types with compact size

2.3.2 Applications of MPA

Microstrip antennas are widely used in systems like mobile communications, satellites, medical science and rockets as discussed below.

2.3.2.1 Mobile communication

The fabrication of the microstrip antenna can be on the same printed circuit board along with the other components as it occupies only small space. Small size antennas have drawn interest from people around the world as these can fit in a compact device. These antennas are widely used in cellular phones, pagers, and in vehicles like car, airplanes, etc.

2.3.2.2 Satellite communication

The main requirement of the satellite communication is to have antennas with circular polarization. This can be achieved by using square or circular patch. The design of the microstrip antenna is trivial to achieve required polarization. These antennas can be used in satellite communication to broadcast from a satellite.

`

2.3.2.3 Healthcare applications

Human body needs to be monitored continuously sometimes to gather the biometric data. An antenna has to be attached to a human body to gather the data. An antenna constructed with textile material can be worn for long period and is known as wearable antenna. In this type of antenna, the radiating patch and the ground plane are made of textile material like flectron, shieldit and zelt. The substrate is a fabric material like jeans, polyester and cotton. This antenna forms a part of human clothing and is integrated into accessories like watches, helmets etc.

2.3.2.4 Direct broadcast satellite system

Direct broadcasting system provides satellite television services to the users around the world. A high gain antenna must be used to receive the signals. Parabolic reflectors are used, but these antennas are bulky and affected by rain. The arrays of microstrip antennas which are circularly polarized, are used in the recent times as these are easy to install, light weight and not affected by rain.

2.3.3 Feeding techniques

There are two types of feeding methods. One is the contacting type and the other is non-contacting type. The contacting type can be divided into line feeding technique and probe feeding technique. The non-contacting type can be divided into proximity feeding technique and aperture coupled feeding technique. The different feeding techniques are discussed below.

2.3.3.1 Microstrip (Offset microstrip) line feed

In this feed type, a microstrip line feeds the patch as shown in Figure 2.4. The feed line width is smaller than the width of the patch. Impedance matching is achieved by having an inset cut in the patch and by maintaining the inset position. It is the most commonly used feeding method as fabrication is easy and matching is simple. The increase in the substrate thickness increases the spurious feed radiation, which decreases the bandwidth of the antenna. This feed also suffers from cross polarization effects [12].

`

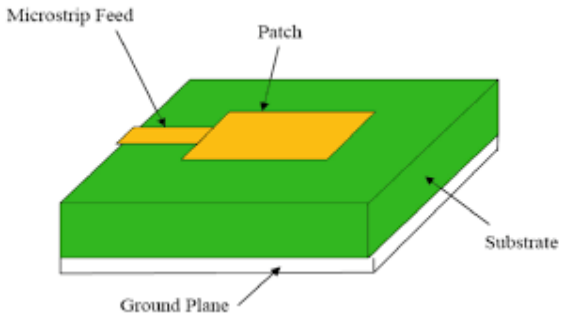

Figure 2.4: Microstrip feeding technique [12]

2.3.3.2 Coaxial feed

In this feeding technique, the inner conductor of coaxial cable is soldered to the patch and the outer conductor of the coaxial cable is attached to the ground plane as shown in Figure 2.5. The main advantage of this feed is that we can attach the inner conductor at the point of the feed where the input impedance is equal to the characteristic impedance of the feed line. Fabrication of coaxial feeding is simple but is difficult to model as a hole has to be drilled in the substrate. This also has low spurious radiation [13].

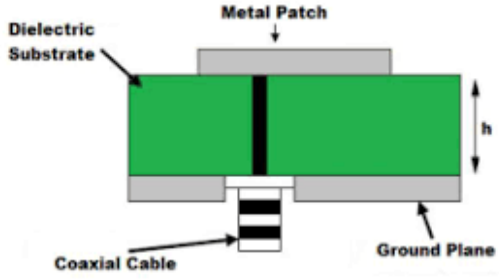

Figure 2.5: Coaxial feeding technique [13]

2.3.3.3 Proximity coupled feed

This feed is also known as electromagnetic coupling scheme and has two dielectric substrates. The feed line is present between the two substrates as shown in Figure 2.6. Energy from the feed line is coupled electromagnetically to the patch. The substrate's dielectric constant is chosen in such a way to widen the bandwidth and to reduce the spurious feed radiation. The

`

material for the upper substrate has a low dielectric constant as it has more radiations from the patch. This feeding gives the wide bandwidth among the other feeding techniques. Fabrication of proximity coupled feeding is difficult as it needs two dielectric layers which are properly aligned [13].

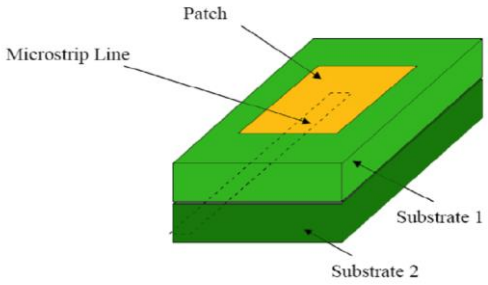

Figure 2.6: Proximity coupled feeding technique [13]

2.3.3.4 Aperture coupled feed

In this type of feed, the ground plane is in between the patch and the feed line. Slot or aperture present in the ground plane achieves the coupling between the patch and feed line as shown in Figure 2.7. The amount of coupling is dependent on shape, size and location of the aperture. Since the ground plane is present between the patch and the feed line, the spurious radiation is low [14].

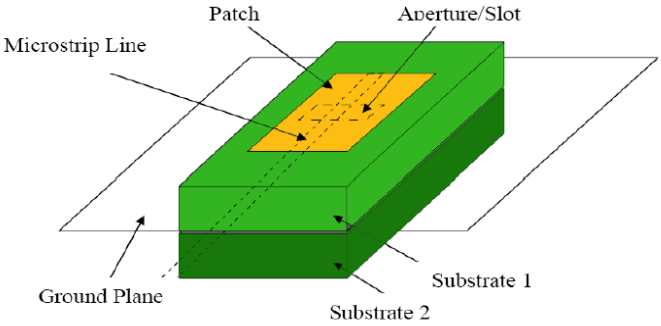

Figure 2.7: Aperture coupled feeding technique [14]

Thick substrate along with low dielectric constant is preferred for the upper substrate to get wide bandwidth. Thin substrate with high dielectric constant is preferred for lower substrate so that energy can be transferred efficiently from the feed line to the patch. This type of feed has

`

improved polarization purity, less spurious radiation and wide impedance bandwidth compared to coaxial and microstrip feed. Table 2.1 below compares the different feeds, where the aperture feed has an excellent polarization with low spurious radiation. Microstrip feed suffers from high spurious radiation and poor polarization but has the ease of fabrication.

Table 2.1: Comparison of various feeding techniques

Feed type	Polarization	Fabrication	Spurious Radiation
Microstrip feed	Poor	Easy	High
Coaxial feed	Poor	Difficult	Low
Proximity feed	Poor	Difficult	Low
Aperture feed	Excellent	Difficult	Low

2.4 Limitations of MPA

Although microstrip patch antennas have more advantages like compact size and easy to fabricate these antennas suffer from the following limitations:

- Cross polarization
- Poor gain and narrow bandwidth
- Low efficiency
- High dielectric and conductor losses
- Suffer from surface waves when high dielectric constant material is used.

Large number of researches have proposed techniques to increase the impedance bandwidth of the patch antenna and some of the common methods are decreasing the dielectric constant of the substrate [15], using stacked patches [16], defected ground structure [17], metamaterial [18], frequency selective surfaces (FSS) [19], electronic band gap (EBG) [20] [21].

2.5 Defected ground structure

Defects etched in the ground plane of microstrip patch antenna are known as defected ground structure (DGS). The defected ground structure is used to enhance the bandwidth and gain of the

`

microstrip antenna. The defects also reduce the return loss, size of the antenna, cross polarization etc.

2.5.1 Geometry and working principle

The ground plane of the microstrip antenna can have either single or multiple defects. These defects can be periodic or aperiodic. DGS has been used under the microstrip line to decrease the mutual coupling and higher order harmonics. Rectangular DGS elements on the ground plane increases the inductance and by changing the size of the defect, the inductance can be varied [22]. These defects disturb the current distribution, which alter the line inductance and capacitance thereby increasing the bandwidth [23].

2.5.2 Unit DGS

DGS has many shapes [24] such as rectangular dumbbell [25], H [26], spiral [27], U [28], V [28]. Other complex shapes are meander lines [29], split ring resonators [30], [31] and fractals [32]. These shapes are shown in Figure 2.8.

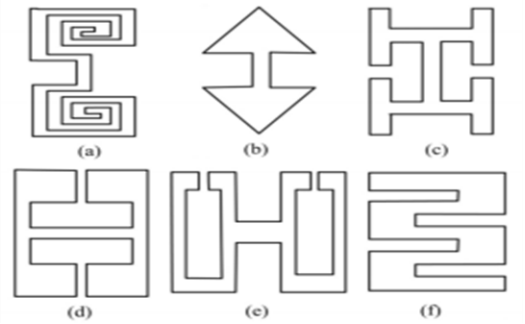

Figure 2.8: DGS shapes: (a) spiral (b) arrowhead (c) H shaped (d) square shaped with slot in center (e) dumbbell with open loop (f) interdigital [24]

2.5.3 Periodic DGS

In periodic DGS, defects are repeated with a fixed spacing between them. When such defects are cascaded, the bandwidth is improved. Shape of defects, distance between the defects and the distribution of defects determine how well periodic DGS can perform. DGS is commonly used as a band stop filter [33].

`

Periodic DGS can be classified as horizontal periodic DGS (HPDGS) and vertical periodic DGS (VPDGS) as shown in Figure 2.9. Applications, advantages and disadvantages of DGS are shown in Table 2.2 [34]. The dumbbell DGS has a simple structure while HPDGS and VPDGS helps in size reduction. U slot and V slot help to improve the Q factor but suffers from a single stop band.

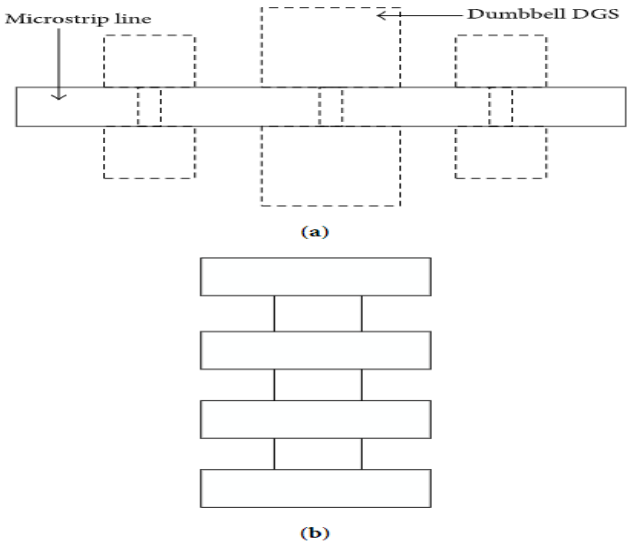

Figure 2.9: Periodic DGS (a) HPDGS (b) VPDGS [34]

Table 2.2: Advantages and disadvantages of various DGS shapes [34]

Shape	Advantage	Disadvantage	Applications
Dumbbell	Basic structure, easy to design and analyze	Single stop band	Band-stop filter
HPDGS	Reduction in size	Bigger size than VPDGS, dispersion problem	Matching networks of amplifier
VPDGS	Reduction in size	Dispersion problem	Matching network of amplifier
U-slot	Q -factor improvement	Single stop band	Band-stop filter
V-slot	Q -factor improvement	Single stop band	Band-stop filter

`

2.5.4 DGS based MSA

DGS based microstrip antennas are used in satellite communication, radio frequency identification systems etc as listed below.

2.5.4.1 Circularly polarized DGS antenna

Circular polarization is produced by the defects in the ground plane. These circularly polarized antennas are used in radio frequency identification systems, satellite communication, and wireless local area networks etc. An arrowhead shaped slot [35] in the square patch generates two orthogonal modes with a phase difference of 90°.

2.5.4.2 Wideband antenna

DGS has also been used for designing wideband antennas. A square shaped defect in the ground plane is used for enhancing the bandwidth of the microstrip antenna [36]. A parasitic square element in the center of the square defect is used for achieving an impedance bandwidth of about 80%. Two L shaped slots and parasitic structures are used to increase the bandwidth [37].

2.5.4.3 Antenna with notched band

A simple ultra-wideband antenna with triple band notch characteristic is presented in [38]. By introducing defected ground structure along with fork shaped stubs, three sharp notch bands are achieved at frequencies of 3.5 GHz, 5.68 GHz, and 7.48 GHz. The antenna operates from 2.8 GHz to 11.3 GHz with a VSWR < 2 except for the above notched bands.

2.5.4.4 Size reduction of antenna using DGS

Compact size of the antenna is achieved by using DGS, where the size of the antenna is reduced by 50% using meandering slots in ground plane [39]. Hybrid techniques of H shaped slot and defected ground structure are employed in [40]. The defected structures consist of combination of U and L shaped slots. This results in the size reduction of 86%.

2.5.4.5 Cross-polarization suppression of antenna using DGS

DGS reduces the cross polarization of microstrip antenna [41]. The periodic fractal DGS (PFDGS) reduces the mutual coupling between the antenna elements. About 20 dB mutual

`

coupling reduction is achieved thereby increasing the antenna efficiency [42]. A rectangular microstrip patch antenna with defected ground structure has been studied to improve polarization purity [43]. A huge improvement in cross polarization isolation is achieved with this configuration.

2.6 Ultra-wideband antennas

Ultra-wideband antennas are becoming popular as there is a great demand for high data rate, along with less power consumption at low cost. A single UWB antenna can replace multiple narrow band antennas thus saving antenna space, reducing interference between multiple antennas [44]. Main features for UWB antenna are given below [45]:

- The antenna's bandwidth should be from 3.1 GHz to 10.6 GHz with sensible efficiency and acceptable omnidirectional patterns.
- The emission power level should be extremely low over the entire ultra-wideband in the limits of -41.3 dBm/MHz.
- The antennas should be able to propagate short pulses with low distortion over the entire frequency range.

2.6.1 History of UWB antennas

In 1898, Oliver Lodge [46] developed the biconical antenna used in transmit and receive links as shown in Figure 2.10. Carter [47] improved Oliver's design using a tapered feed which paved way for the design of broadband antennas as shown in Figure 2.11. In 1941, Lindenblad [48], designed a coaxial horn which was based on the design of sleeve dipole [49] as shown in Figure 2.12.

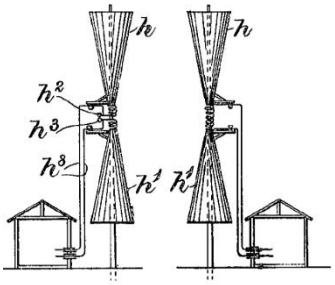

Figure 2.10: Biconical antenna by Lodge [46]

`

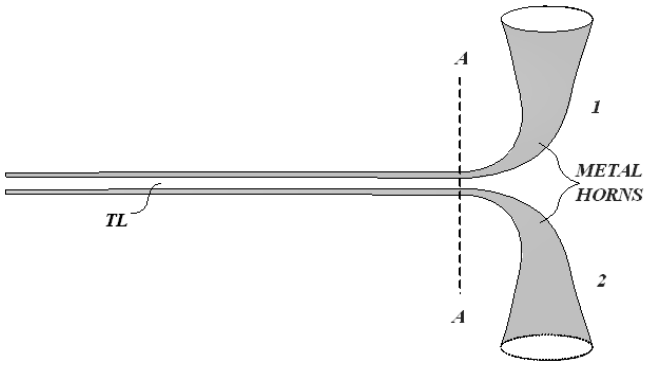

Figure 2.11: Biconical antenna by Cater's [47]

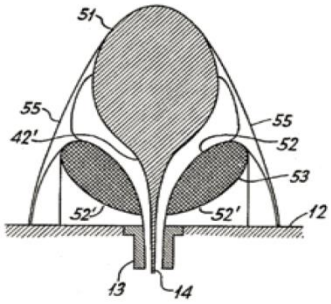

Figure 2.12: Coaxial horn by Lindenblad [48]

J. C. Kraus [50] developed a bulbous structure in 1940 that yielded an impedance bandwidth ratio of 5:1 as shown in Figure 2.13. This played a critical role for television development. He named that antenna as volcano smoke antenna. In 1942, King [51] patented traditional horns. The antennas were complex to manufacture as they are wide in structure as shown in Figure 2.14 [52]. Thus, cost of manufacture and complexity of procedures involved became very important in designing an antenna.

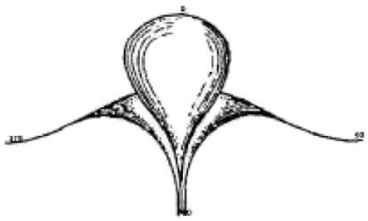

Figure 2.13: Volcano smoke antenna [50]

`

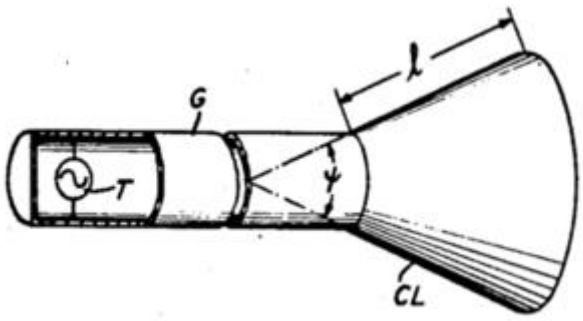

Figure 2.14: Conical horn by King's [52]

In 1968, W. Stohr [53] developed the monopole and dipole antennas which are elliptical in shape. The monopole and dipole antennas are shown in Figure 2.15(a) and Figure 2.15(b), respectively. The antennas proposed in the earlier century were not suited for high frequency applications due to solid structure. This led to the development of novel omnidirectional antennas.

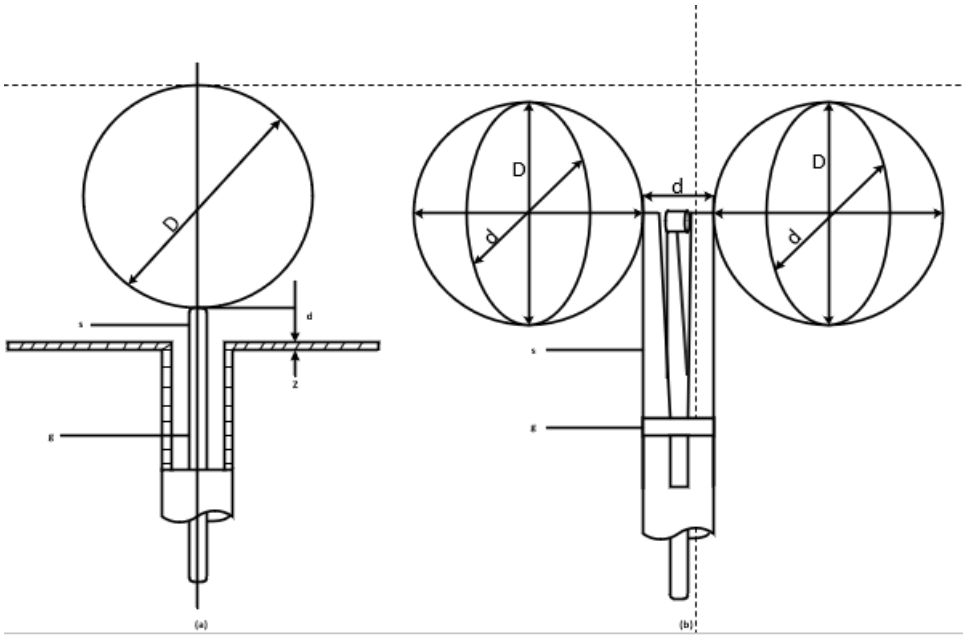

Figure 2.15: Ellipsoidal monopole and dipole by Stohr's [53]

`

2.6.2 Omnidirectional UWB antennas

There are two types of monopole antennas namely UWB planar monopoles and UWB printed monopoles. The UWB planar monopole is mounted on a large ground plane that is perpendicular to the plane of the monopole resulting in a three-dimensional structure and is complex to integrate with monolithic microwave integrated circuits (MMIC). The UWB printed monopoles are easier to integrate than the planar monopole antennas. Using several techniques for enhancing bandwidth, size reduction, these antennas can provide same bandwidth and radiation performance like UWB antennas.

2.6.2.1 UWB planar monopoles

In 1976, Dobust and Zisler [54] designed the first monopole antenna. The conventional monopole is replaced with the planar monopole positioned above a ground plane and fed using a coaxial probe. The structures of various planar monopoles are shown in Figure 2.16. These antennas have the bandwidth ratio from 2:1 to 10:1. Agrawall etal. [55] compared the bandwidth of several monopole structures and the results prove that circular and elliptical monopoles have wide bandwidth than the other structures with a bandwidth ratio exceeding 10:1. Evans and Amunann [56] proposed a trapezoidal monopole antenna with bandwidth ratio of 11:1. Suh etal. [57] proposed planar inverted cone antenna (PICA) with bandwidth ratio of more than 10:1. Later, Bai etal. [58] proposed a modified PICA where a plate which is shaped like leaf with three circular holes as shown in Figure 2.16 (f). The feed gap and location of the feed point determine the impedance matching. Techniques such as notching, double feed, square feed, triangle shaped feed, trident shaped feed, beveling and shorting feed are the various techniques used to enhance the bandwidth of planar square monopole antennas as shown in Figure 2.17.

`

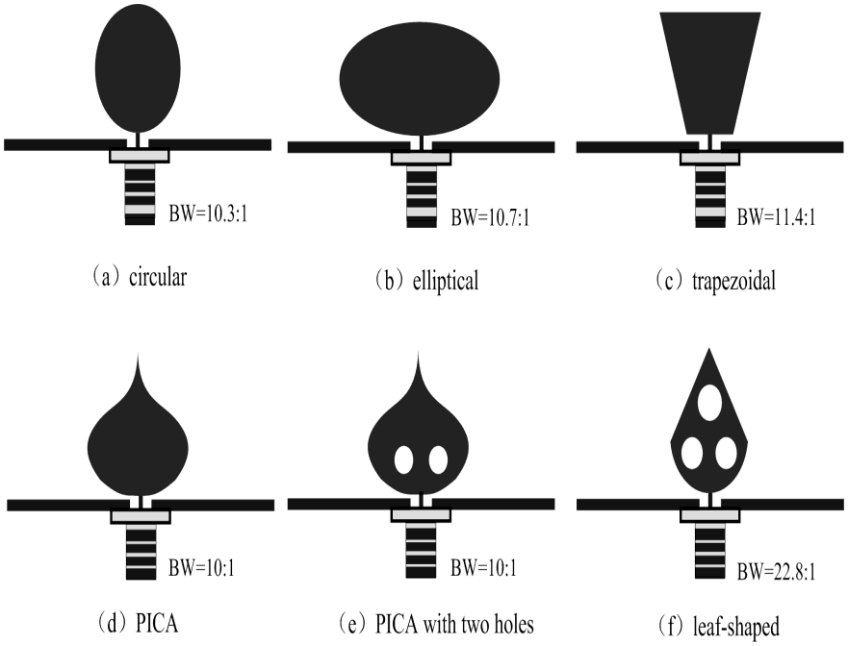

Figure 2.16: Different shapes of planar monopole antennas [55-58]

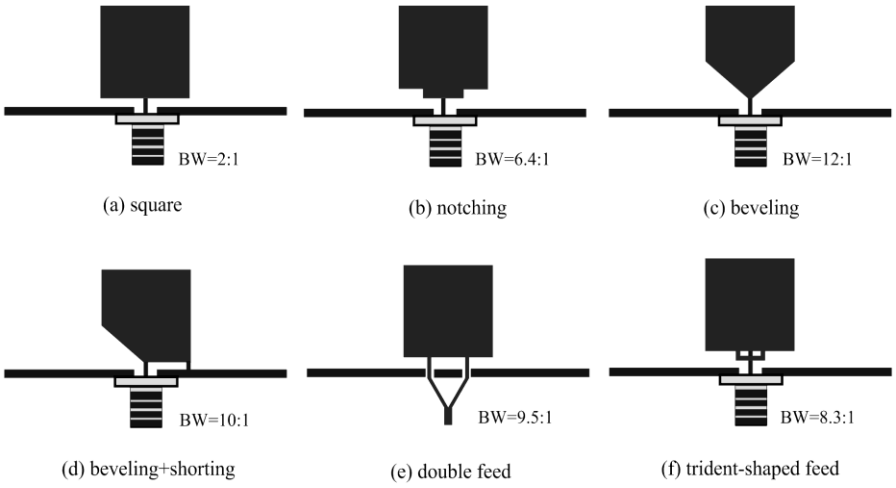

Figure 2.17: Bandwidth enhancing techniques for planar square monopole antennas [49]

2.6.2.2 UWB printed monopoles

The printed antenna has the monopole patch and the ground plane which are printed on the same side or opposite side of the substrate and are excited by microstrip or coplanar waveguide feed (CPW) [59]. Various monopole structures are shown in Figure 2.18. The circular monopole [60] is the simplest with an impedance bandwidth of 3.8:1. Other shapes such as octagon

`

monopole [61], spline-shaped monopole [62], U-shaped monopole [63], knight's helm shape monopole [64], two steps circular monopole [65] are also studied. The octagon [60] monopole antenna has impedance bandwidth of 3.8:1. Spline-shaped monopole [61] supports wireless standards covering personal communication service (PCS), Industrial, Scientific and Medical band (ISM) bands.

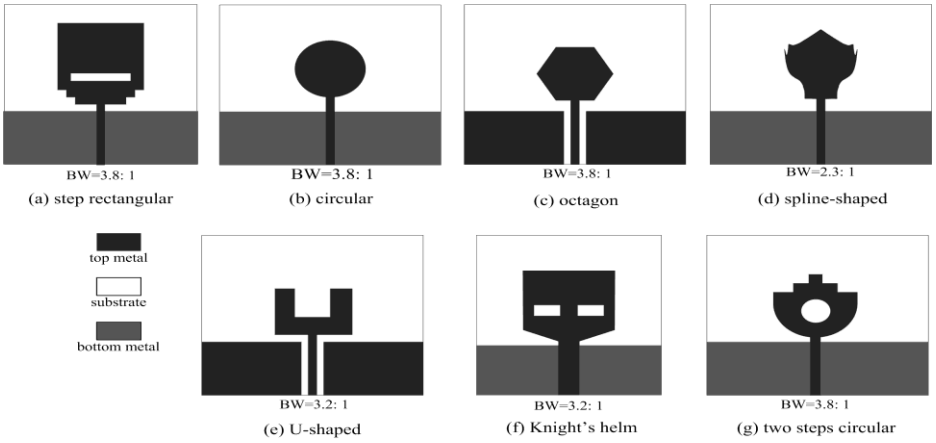

Figure 2.18: Various monopole structures [59-65]

2.6.3 Directional UWB antennas

The directional UWB antenna have higher gain than omnidirectional antenna in a particular direction than other directions. Various directional antennas such as UWB printed wide-slot antennas, the UWB dielectric resonator antenna (DRA), and the DRAs with radiation reconfiguration are discussed below:

2.6.3.1 UWB printed wide-slot antenna

This type of antenna consists of a broad slot, tuning stub which is connected to a microstrip line or coplanar waveguide. Several types of tuning stubs are studied as shown in Figure 2.19. Jang [66] proposed two rectangular slot antennas fed by cross shaped stub and π shaped stub and these antennas achieved bandwidth 1.7 GHz - 4.9 GHz and 1.7 GHz - 6 GHz, respectively. Yao et al. [67] presented fan shaped microstrip stub which has the bandwidth 0.5 GHz - 5.7 GHz.

`

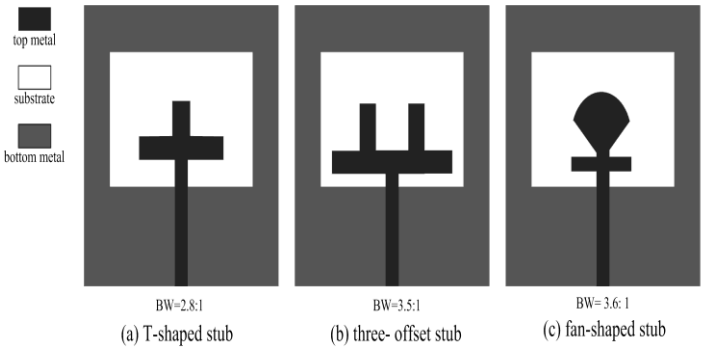

Figure 2.19: Various tuning stubs [66-67]

2.6.3.2 UWB dielectric resonator antenna

This antenna has the small size and greater efficiency compared to UWB printed monopole and wide slot antennas. The effective way to enhance DRA's bandwidth is to combine DRA and monopole antenna as shown in Figure 2.20. Lappiere et al. [68] proposed an antenna by combining monopole antenna with annular dielectric resonator antenna. Using the hybrid technique, monopole antenna can achieve UWB performance. To enhance the bandwidth further, Ruan et al. [69] proposed an annular ring dielectric resonator antenna which produces a bandwidth ratio of 3.7:1. Jazi and Denidni [70] introduced a skirt monopole antenna which excites an inverted conical ring shape resonator.

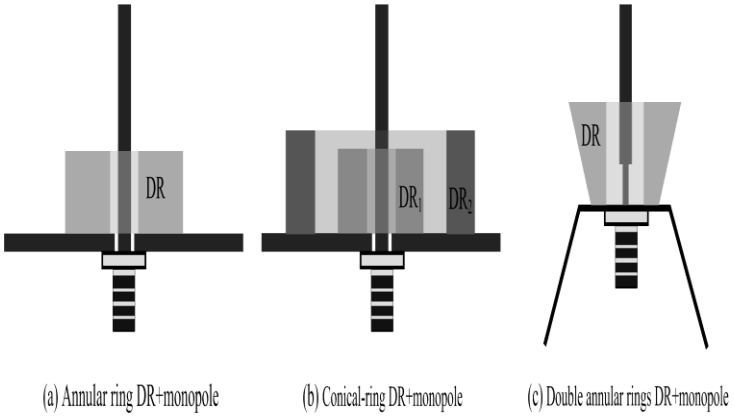

Figure 2.20: UWB hybrid DRAs [68-70]

2.6.4 Band-notched UWB antennas

Some of the frequency bands in UWB band are occupied by WLAN IEEE 802.11a in 5.1-5.35 GHz and HIPERLAN/2 WLAN from 5.725-5.825 GHz bands. Some Asian and European

`

countries also have the WiMAX service from 3.3-3.6 GHz. This causes interference between the UWB system and the existing narrow band systems. Filters can be used to notch unnecessary interfering bands, but filters increase the system complexity, insertion loss and the weight. To overcome these issues, UWB antennas have been designed with notches to eliminate the interfering bands. Different notching techniques are embedding slot, parasitic stub, band stop transmission line etc as discussed below.

2.6.4.1 Embedding slot

One simple way of notching technique is to embed slots on the ground plane or on the patch. Many shapes of slots are shown in Figure 2.21. Kim and Kwon [71] proposed a UWB antenna with a hexagonal patch which has a V shaped slot embedded in the patch. This slot creates a narrow frequency notch.

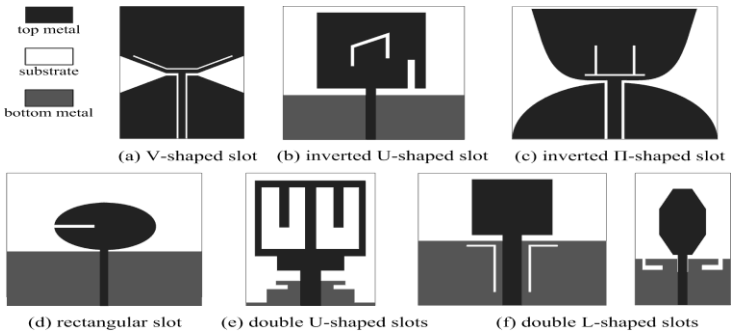

Figure 2.21: Various notch shapes [71-76]

Chung et al. [72], Ojaroudi et al. [73] introduced the inverted U-shaped slot, rectangular slot or π shaped slot in the printed UWB monopole antenna to create a notch effect. In [74], a band notch effect is provided by the U-shaped slot which acts as half wave resonant structure. Sim et al. [75], Tang et al. [76], introduced pair of inverted L shaped slots to achieve the notch effect. Ghimire and Choi [77] proposed a U-shaped slot etched on a circular patch to achieve the notch band.

2.6.4.2 Parasitic stub

Another way to create a notched band is to use parasitic stubs in the aperture area of the antenna that forms a resonant structure. This produces a change of impedance in the notched

`

band. Liu et al. [78] introduced a band notched UWB antenna with a T shaped stub. A pair of parallel parasitic microstrip lines are added to ground plane out of which one is shorted by a short pin to the patch as shown in Figure 2.22. These parasitic units are used to produce a notch band from 3.3 GHz to 3.7 GHz and from 5.15 GHz to 5.85 GHz.

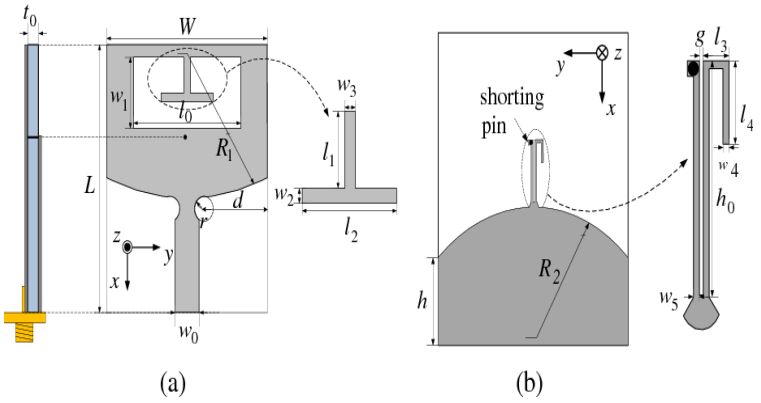

Figure 2.22: Parasitic stub [78]

Guichi et al. [79] presented a novel UWB monopole antenna which has dual band-notch characteristics. The antenna has V shaped patch with a staircase defect and a semi-circular defected ground plane. The notch bands are obtained by having two parasitic stubs on the patch and an inverted U slot in the transmission line. This antenna rejects the WiMAX band from 3.17 GHz to 3.85 GHz and the international telecommunications union (ITU) band from 7.9 GHz to 9.1 GHz. The geometry of this antenna is shown in Figure 2.23.

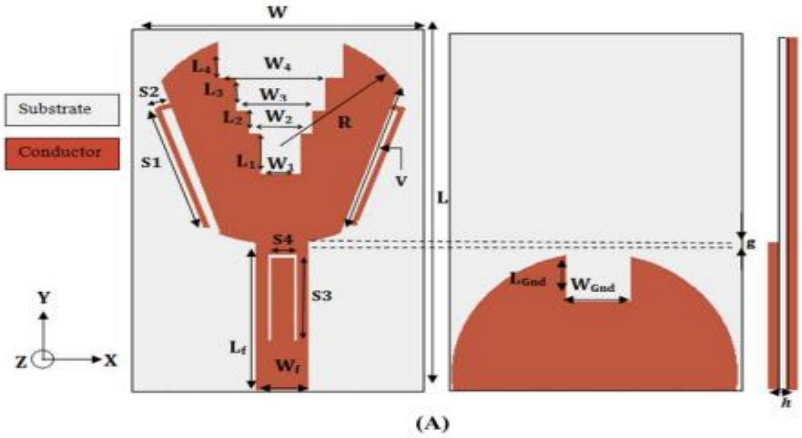

Figure 2.23: Band notched antenna with parasitic stub [79]

`

2.6.4.3 Bandstop transmission line

Band notched techniques will affect the antenna radiation as it increases the cross polarization. A transmission line with band stop characteristic will have little effect on the antenna radiation. A printed UWB antenna with triple band notch bands is presented in [80]. The band notches are obtained by using a defected microstrip structure (DMS) band stop filter (BSF) placed in the feed line along with inverted π shaped slot in the patch. The antenna operates in the frequency band 3.1 GHz - 14 GHz with three notch bands 4.2 GHz - 6.2 GHz, 6.6 GHz - 7.0 GHz and 12.2 GHz - 14 GHz. The antenna configuration is shown in Figure 2.24.

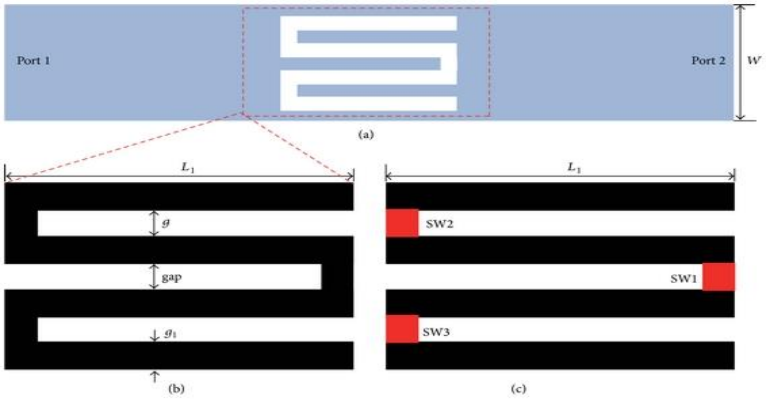

Figure 2.24: Notched antenna with band stop transmission line [80]

2.7 Chapter summary

In this chapter, the geometry of the microstrip patch antenna along with the advantages and limitations have been presented. The application of microstrip patch antennas are also explained. Different feeding techniques involved in microstrip patch antennas are discussed and analyzed. Various antenna parameters like gain, directivity, radiation pattern etc are discussed in detail. The working principle of defected ground structure along with various applications of DGS is presented. The comparative study of different types of DGS is discussed. The history of ultra-wideband antennas along with various types of ultra-wideband antennas are discussed as well.

`

CHAPTER 3: HUMAN FACE SHAPED MICROSTRIP PATCH ANTENNAS WITH DGS

The design of two human face shaped microstrip patch antennas that can be used for ultra-wideband applications are presented in this chapter. The initial design of the human face shaped antenna operates from 5.9 GHz to 11.2 GHz and the improved design of the human face shaped antenna operates from 3 GHz to 14.7 GHz with a notch band from 5 GHz to 6.3 GHz for the elimination of 5 GHz - 6 GHz WLAN signals. The antennas have a human face shaped patch, partial ground plane and are fed by 50Ω microstrip line. The use of defected ground structure enhances the bandwidth of the antenna. The antennas are simulated and optimized using CST microwave studio and various antenna parameters like gain, directivity, radiation pattern, VSWR etc are discussed. The human face shaped antennas with optimized dimensions are then fabricated and measured. The measured and simulated input and directional parameter of the proposed antennas are presented. The antennas are simple in configuration, and provide wide bandwidth, high gain, high efficiency and low reflection coefficient.

3.1 Introduction

Ultra-wideband technology has attracted much attention in modern telecommunication systems as it can transmit a lot of data (high bandwidth) over a short distance without using large power. Microstrip antennas used for designing UWB antennas suffer from narrow bandwidth and poor gain. The concept of defected ground structure along with slotted elliptical patch is used to enhance the bandwidth of the microstrip antenna. The defects are integrated on the ground plane of microwave planar circuits thus modifying the continuity of the ground plane. These defects also supress mutual coupling [81-82]. These slots are placed under the transmission line so that it can provide better coupling with the line. The initial design presented in this chapter utilizes the rectangular defects for enhancing the antenna bandwidth. The proposed microstrip antenna with rectangular DGS operates from 5.9 GHz to 11.2 GHz. The improved design uses triangular and rectangular defects to improve the bandwidth of the antenna. The proposed human face shaped microstrip antenna with rectangular and triangular DGS operates from 3 GHz to 14.7 GHz with a notch band from 5 GHz to 6.3 GHz. The proposed human face shaped antennas are suitable for UWB applications.

`

3.2 Human face shaped microstrip patch antenna with rectangular DGS

In this section, the design of a human face shaped microstrip patch antenna with rectangular DGS is presented. The design of the ultra-wideband antenna began with an elliptical patch as shown in the Figure 3.1. The ground plane of the antenna shown in Figure 3.1 is similar to Figure 3.2 except that it has no DGS. The antenna does not have any defects in the ground plane. The antenna produces two frequency bands i.e $5.9\ \text{GHz} - 6.2\ \text{GHz}$ and $8.4\ GHz$ - $10.8\ GHz$.

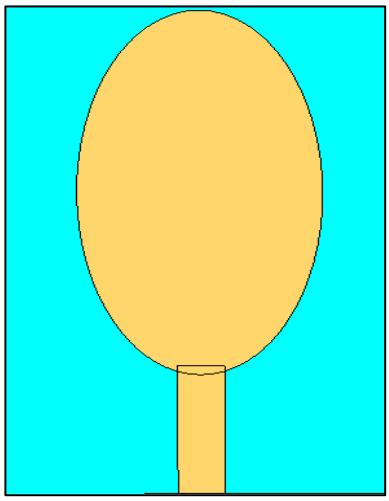

Figure 3.1: Top view of the antenna without human face and defects in ground plane

The following analytical equations are used for designing elliptical patch antenna [83]:

$$f_{11}^{e,o} = \frac{15}{\pi e a}\left(\frac{q_{11}^{e,o}}{\varepsilon_r}\right)^{0.5} \tag{3.1}$$

where $f_{11}^{e,o}$, a, e, $q_{11}^{e,o}$ and ε_r are the dual resonant frequency (TM_{11}^{e} and TM_{11}^{o} mode), semi major axis, eccentricity, approximated Mathieu function of the dominant mode (TM_{11}^{e} and TM_{11}^{o}) and dielectric constant of the substrate, respectively. The $q_{11}^{e,o}$ of the dominant $TM_{11}^{e,o}$ mode for even mode resonance is given as [83]:

$$q_{11}^{e} = -0.0049e + 3.788e^2 - 0.7278e^3 + 2.314e^4 \tag{3.2}$$

and for odd mode resonance is given by the below [83]:

`

$$q_{11}^{o} = \text{-0.0063e+3.8613e}^{2}\text{-1.3151e}^{3}\text{+5.2229e}^{4} \quad (3.3)$$

The eccentricity e of the elliptical patch is given by [83]:

$$\mathrm{e} = \sqrt{\left[1 - \left(\frac{b}{a}\right)^{2}\right]} \quad (3.4)$$

where b is the semi minor axis.

Due to fringing effect, the resonant frequency calculated from equation (3.1) is less than the actual resonant frequency as the effective size of the patch is bigger than the actual size. Considering the effective major axis due to fringing effect, the actual dual resonant frequency can be given as [83]:

$$\mathrm{f}_{11} = \frac{15}{\pi \mathrm{e} a_{eff}} \left(\frac{\mathrm{q}_{11}}{\varepsilon_{\mathrm{r}}}\right)^{0.5} \quad (3.5)$$

The relation between actual semi major axis and the effective major semi axis is given by [83]:

$$a_{eff} = \left[a^{2} + \frac{ha}{0.3525\pi\varepsilon_{\mathrm{r}}}\left(\ln\left(\frac{a}{2h}\right) + 1.41\varepsilon_{\mathrm{r}} + 1.77 + \frac{h(0.268\varepsilon_{\mathrm{r}}+1.65)}{a}\right)\right]^{0.5} \quad (3.6)$$

where a_{eff} and h are the effective semi major axis and thickness of dielectric substrate, respectively. The dimension of the eyebrows can be optimised using the above equation using CST microwave studio.

The microstrip line feeding technique is used to excite the patch. The characteristic impedance (z_c)of the transmission line is given by [1]:

$$z_{c=} \frac{60}{\sqrt{\varepsilon_{\mathrm{reff}}}}\left[ln\left(\frac{8h}{W_0} + \frac{W_0}{4h}\right)\right] \qquad (\text{for } \frac{W_0}{h} \leq 1)$$

$$z_{c=} \frac{120\,\pi}{\sqrt{\varepsilon_{\mathrm{reff}}}\left[\frac{W_0}{h}+1.393+0.667\,ln\left(\frac{W_0}{h}+1.444\right)\right]} \ (\text{for } \frac{W_0}{h} > 1)$$

Where W_0, and h are the width of the microstrip feeding line and thickness of the substrate, respectively. $\varepsilon_{\mathrm{reff}}$ is the effective dielectric constant of the substrate and is given by [1]:

`

$$\varepsilon_{reff} = \frac{\varepsilon_r + 1}{2} + \frac{\varepsilon_r - 1}{2}\left(1 + 12\,\frac{h}{W}\right)^{-1/2}$$

Using above equations, the width of the microstrip feed line is calculated for 50 Ω characterstic impedance. The dimensions of the microstrip feed line is optimized using CST Microwave Studio to achieve good matching.

Two rectangular defects are added in the ground plane to increase the bandwidth as shown in Figure 3.2. The DGS also acts as radiation element and radiate the power. So, the antenna with DGS radiates more power and the reflected power is reduced. Hence, the reflection coefficient is reduced. Further, the resonant frequencies of the DGS slots can be varied and optimized so that the bandwidths of slots and radiating patch is combined and provides a large impedance bandwidth.

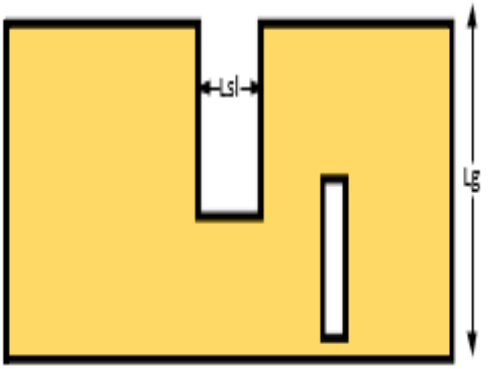

Figure 3.2: Two rectangular defects in ground plane

DGS is similar to LC resonator circuit as shown in dotted section in Figure 3.3, whose reactance is given by [84]:

$$X_{LC} = \frac{1}{\omega_0 C}\left(\frac{\omega_0}{\omega} - \frac{\omega}{\omega_0}\right) \tag{3.7}$$

where ω_0 is the angular resonant frequency of the parallel LC resonator.

`

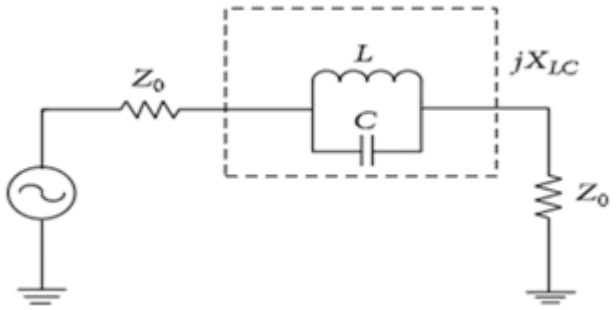

Figure 3.3: DGS equivalent circuit [84]

To enhance the bandwidth, two symmetrical circular slots (eyes) and a rectangular slot (nose) is added to the elliptical patch as shown in Figure 3.4. The slots in the patch also resonate. The dimensions of the slots are chosen in such a way such that the bandwidth of slots overlap to obtain wide bandwidth. Further, considering mutual coupling effects etc, the dimensions of each slot is optimized using CST Microwave Studio for optimum performance. The antenna produces two frequency bands i.e. 5.8 GHz − 7 GHz and 7.6 GHz − 10.7GHz. When two symmetrical elliptical slots (eyebrows) and an elliptical slot (mouth) are added to the patch as shown in the Figure 3.5, the antenna produces bandwidth from 8.4 GHz to 11.2 GHz .

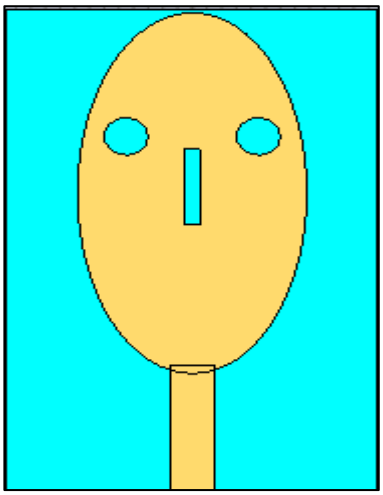

Figure 3.4: Human face shaped microstrip patch antenna with eyes and nose

`

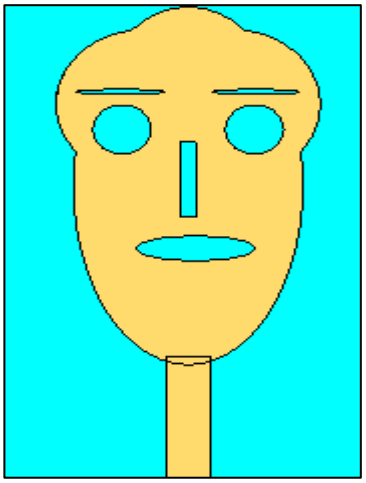

Figure 3.5: Human face shaped microstrip patch antenna with eyes, nose, eyebrows and mouth

3.2.1 Antenna dimensions and geometry

The proposed antenna is shown in Figure 3.6. The top view, bottom view and side view of the antenna are presented in Figure 3.6 (a), Figure 3.6 (b) and Figure 3.6 (c), respectively. The antenna has an elliptical patch with embedded slots in the patch. The elliptical patch is used as it provides larger flexibility in the design, more degree of freedom as compared to the circular geometry [85]. The antenna is designed on a 38.2 $mm \times 25.2$ mm FR4 substrate with the dielectric constant of 4.4 and substrate thickness of 1.6 mm. A thin 50Ω microstrip line of width 3.058 mm and length 10 mm feeds the antenna. The elliptical patch is made of copper foil and has the width of 15.6 mm and a length of 28.6 mm. The ground plane is modified as shown in Figure 3.6 (b). Slots are loaded in the conducting patch for reducing the size and improving the bandwidth and gain of the antenna [86]. These slots cause meandering of the patch surface current paths, thus lowering the resonant frequency causing the reduction in antenna size. The slots also help in improving the return loss [87]. Two slots are etched in the ground plane to increase the bandwidth of the antenna.

The width and length of the ground plane are 25.2 mm and 9.5 mm, respectively. Dimension along the length and width of the elliptical patch is considered as length and width of the ground plane. The copper layer in the ground and the patch has a very small thickness. The elliptical patch antenna without the human face and slots provides a very narrow bandwidth. The addition of human face with eyes, and nose reduces the reflection coefficient and improves

`

the bandwidth. The mouth in the structure further improves the bandwidth of the antenna. The addition of head and eyebrows significantly decreases the reflection coefficient and improves the bandwidth. The width and length of the eyebrows are 6 *mm* and 0.4 *mm*, respectively. Dimensions along the length and width of the elliptical patch are taken as length and width of the eyebrow. The width of the head is 12 *mm*. The width and length of the mouth are 8 *mm* and 2 *mm*, respectively. The width of the eye is 4 *mm*. The width and length of the nose are 1 *mm* and 6 *mm*, respectively. The dimensions The entire optimized antenna dimensions are shown in the Table 3.1.

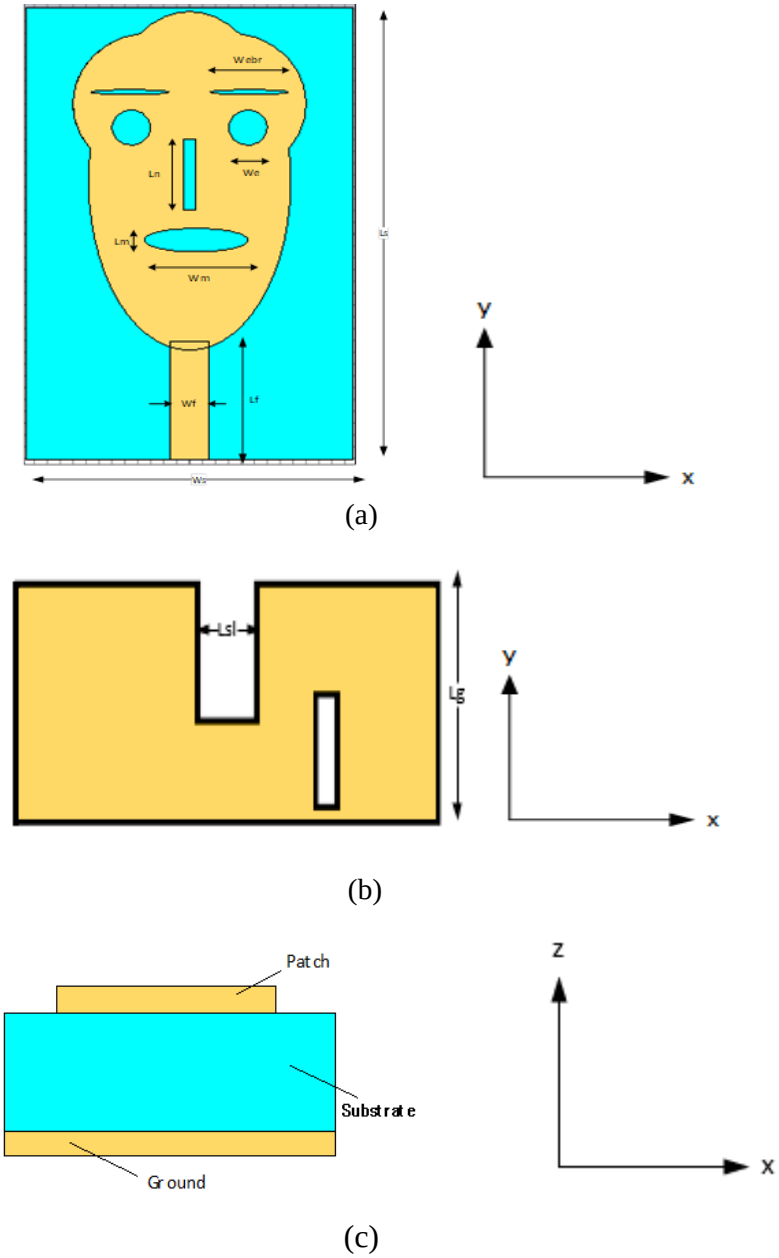

Figure 3.6: Geometry of the antenna (a) top view (b) bottom view (c) side view

`

Table 3.1: Optimized antenna dimensions

Parameter	Value (mm)	Description
L_s	38.2	Substrate length
W_s	25.2	Substrate width
L_f	10	Feed line length
W_f	3.05	Feed line width
W_m	8	Mouth width
L_n	1	Nose length
W_e	4	Eye width
L_m	2	Mouth length
W_{ebr}	6	Eyebrow width
L_g	9.5	Ground length
L_{sl}	5.2	Slot length
W_{sl}	3.4	Slot width

3.2.2 Results and discussion

The antenna is simulated using CST microwave studio and the simulated results of various parameters of the antenna like reflection coefficient, gain, directivity, VSWR, radiation patterns are discussed below.

3.2.2.1 Reflection coefficient (S_{11}) and antenna bandwidth

The bandwidth of the antenna is the frequency range in which the reflection coefficient is less than -10 dB. Figure 3.7 shows the S_{11} plot of the antenna without human face. It can be observed from the graph that the antenna without human face and defects provided two frequency bands i.e. 5.9 GHz – 6.2 GHz and 8.4 GHz – 10.8 GHz. The minimum reflection coefficient is -17.09 dB. When defects are added, the antenna without human face and defects provided two frequency bands i.e. 5.8 GHz – 7.0 GHz and 7.6 GHz – 10.7 GHz. The minimum reflection coefficient is -26.17 dB.

Figure 3.8 shows the S_{11} plot of the antenna with human face. It can be shown from the graph that the antenna with human face and without defects provides the bandwidth 8.4 GHz – 11.2 GHz. The minimum reflection coefficient is -16 dB. When defects are added, the antenna

`

with human face and defects provides the bandwidth 5.9 GHz – 11.2 GHz. The minimum reflection coefficient is -35.11 dB.

Table 3.2 summarizes the reflection coefficient and bandwidth of different antenna structures. It is evident that human face shaped antenna with eyes, nose, mouth, eyebrows having defects in the ground plane has a wide bandwidth 5.9 GHz – 11.2 GHz with a minimum reflection coefficient of -35.11 dB.

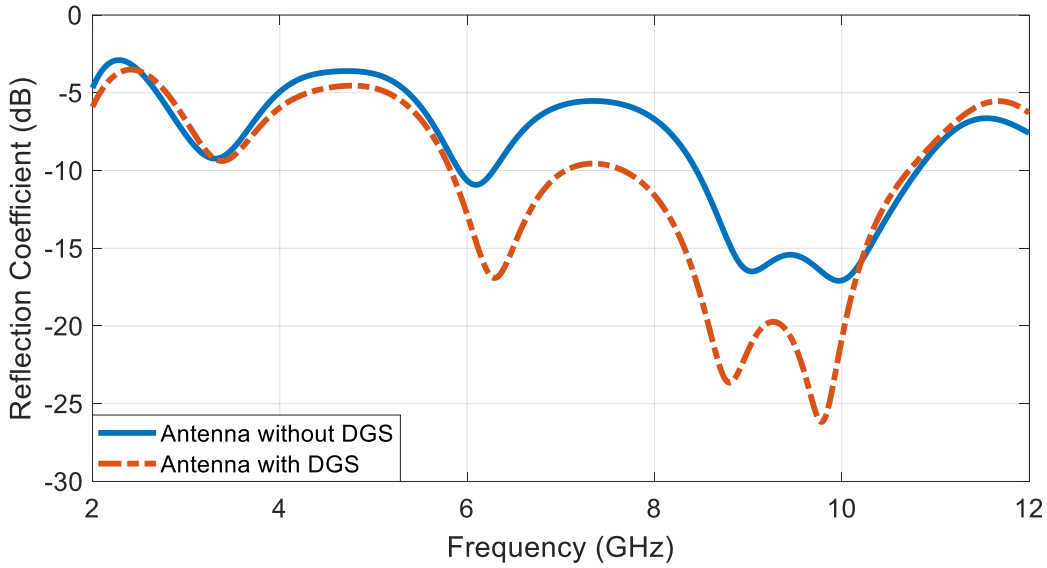

Figure 3.7: Reflection coefficient of the elliptical antenna without human face.

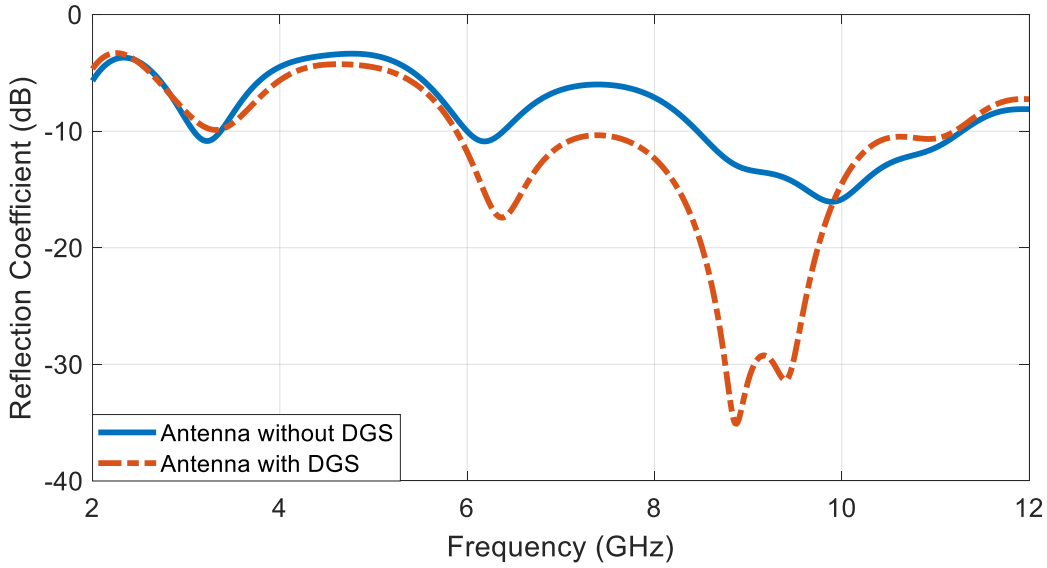

Figure 3.8: Reflection coefficient plot of the antenna with human face

`

Table 3.2: Reflection coefficient and bandwidth of different antenna structures

Antenna Structure	**Minimum Reflection Coefficient** (dB)	**Frequency range**
Elliptical patch without human face and without ground plane defects	-17.09	5.9 – 6.2 GHz 8.4 – 10.8 GHz
Elliptical patch without human face and with defects in ground plane	-26.17	5.8 – 7.0 GHz 7.6 – 10.7 GHz
Elliptical patch with human face having eyes and nose with defects in ground plane	-25	5.8 – 7.0 GHz 7.6 – 10.7 GHz
Elliptical patch with human face having eyes, nose, eyebrows, mouth and defects in ground plane	-35.11	5.9 – 11.2 GHz
Elliptical patch with human face having eyes, nose, mouth eyebrows without defects in ground plane	-16	8.4 – 11.2 GHz

3.2.2.2 Three-dimensional directivity pattern

The red portion in the directivity pattern shows the maximum radiation as shown in Figure 3.9. The maximum directivity of the human face shaped antenna without human face and defects in the ground plane at 10 GHz is 5.691 dBi. Figure 3.10 shows the directivity pattern of the antenna with human face with defects in ground plane. The maximum directivity at 10 GHz is 6.268 dBi. It is evident that addition of human face with eyes, nose, eyebrows and mouth helps to increase the directivity of the antenna.

`

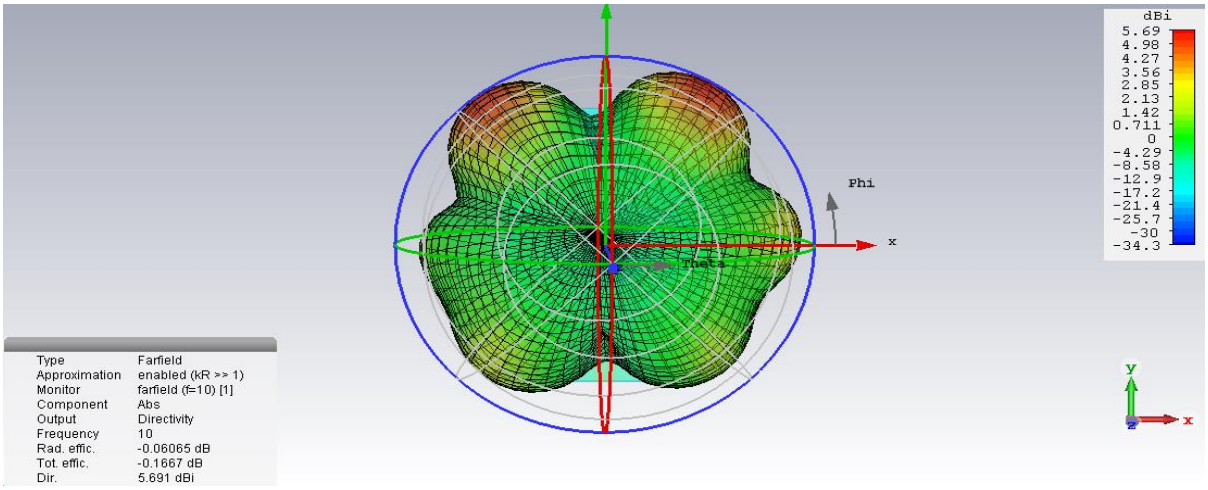

Figure 3.9: Directivity pattern of the antenna without human face and defects

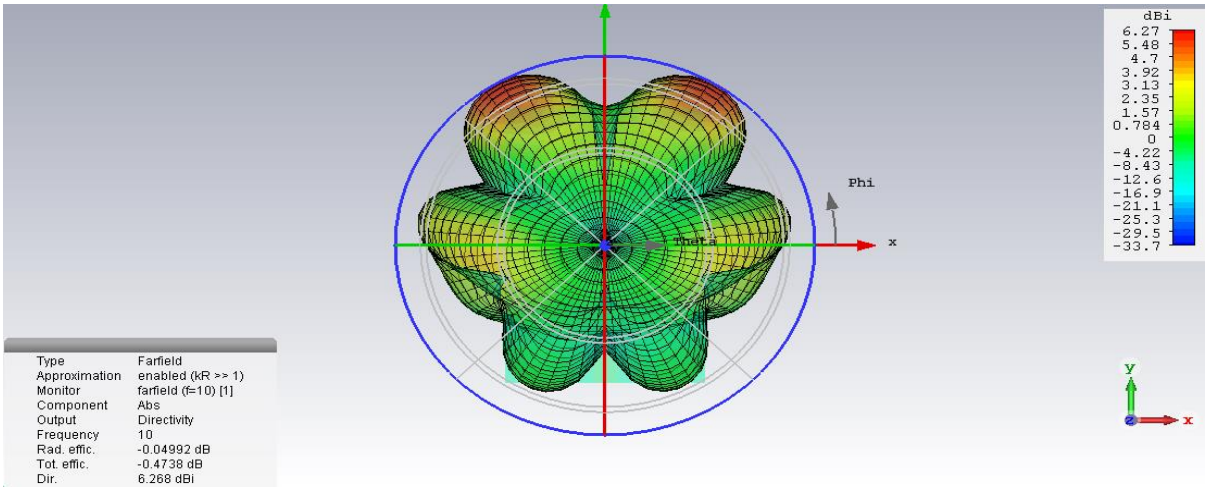

Figure 3.10: Directivity pattern of the antenna with human face having eyes, nose, eyebrows, and mouth and with defects in ground plane

3.2.2.3 Three-dimensional gain pattern

Figure 3.11 shows the gain pattern of the antenna without human face and defects. It is observed that the maximum gain at f=10 GHz is 5.630 dB. Figure 3.12 shows the gain pattern of the antenna with human face and with defects in ground plane. The maximum gain at f=10 GHz is 6.219 dB. Table 3.3 shows the gain and directivity of different antenna structures at f=10 GHz. From this table, it can be observed that the microstrip patch antenna with human face having eyes, nose, mouth, eyebrows and defects in ground plane has the maximum gain and maximum directivity of 6.219 dB and 6.268 dBi, respectively. Table 3.4 shows the gain,

`

directivity, radiation efficiency and total efficiency of the antenna at various frequencies, where the gain and directivity are maximum at f=10 GHz.

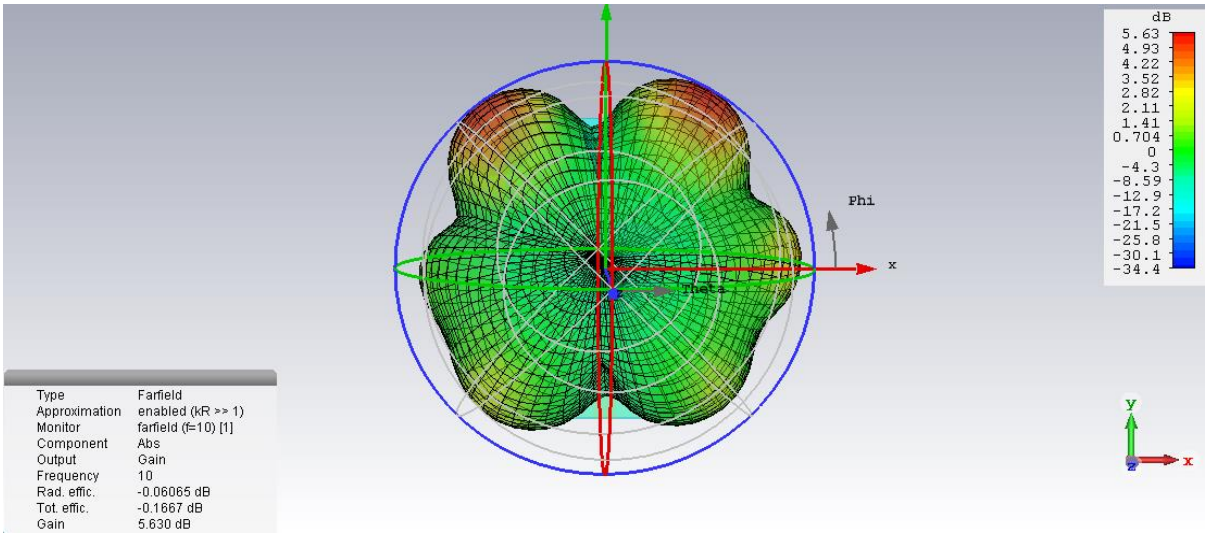

Figure 3.11: Gain pattern of the antenna without human face and defects

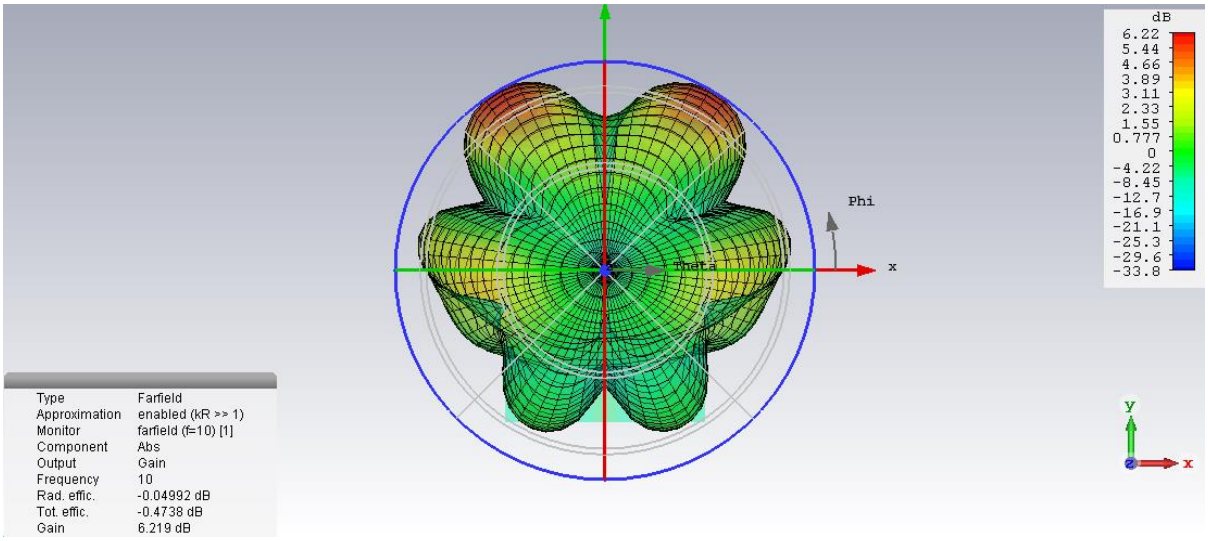

Figure 3.12: Gain pattern of the antenna with human face having eyes, nose, eyebrows and mouth with defects in ground plane

`

Table 3.3: Gain and directivity of different antenna structures

Antenna Structure	**Gain (dB) at f=10 GHz**	**Directivity (dBi) at f=10 GHz**
Elliptical patch without human face and without ground plane defects	5.630	5.691
Elliptical patch with human face having eyes and nose with defects in ground plane	6.091	6.176
Elliptical patch with human face having eyes, nose, mouth and defects in ground plane	5.662	5.763
Elliptical patch with human face having eyes, nose, mouth, eyebrows and defects in ground plane	6.219	6.268

Table 3.4: Gain, directivity, radiation efficiency, total efficiency at various frequencies

Frequency (GHz)	**f=2**	**f=4**	**f=6**	**f=8**	**f=10**	**f=12**
Gain (dB)	-0.0154	2.720	4.377	3.778	6.219	5.570
Radiation Efficiency (dB)	-1.929	-0.4820	-0.7422	-0.4294	-0.0499	-0.1508
Total Efficiency (dB)	-4.437	-2.271	-0.8475	-0.4915	-0.4738	-1.077
Directivity (dBi)	1.913	3.202	5.119	4.207	6.268	5.721

`

3.2.2.4 Two-dimensional radiation patterns

Figure 3.13 shows the normalized radiation patterns of the human face shaped microstrip patch antenna with defects in the ground plane for various frequencies. The normalized pattern in phi=0 degree plane and phi=90 degree plane at 8 GHz is shown in Figure 3.13 (a). The normalized pattern in phi=0 degree plane and phi=90 degree plane at 10 GHz is shown in Figure 3.13 (b).

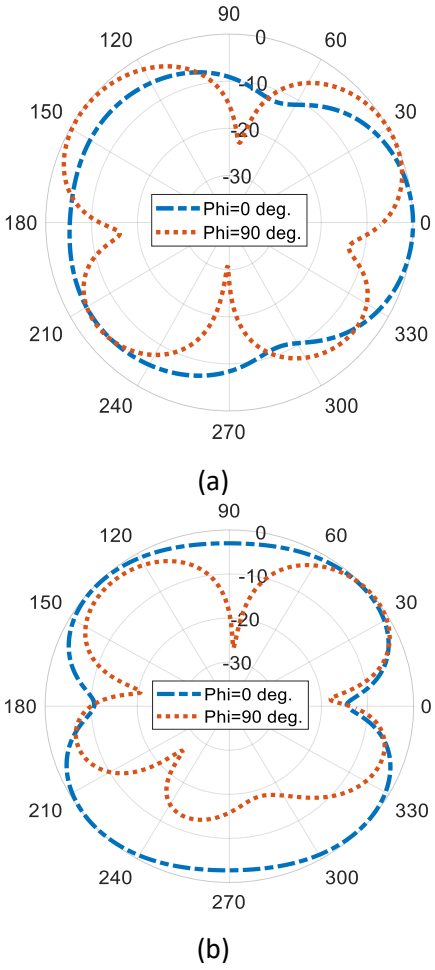

Figure 3.13: Radiation patterns of the human face shaped antenna with rectangular DGS (a) f=8 GHz (b) f=10 GHz

3.2.2.5 Gain and directivity plot

The gain and directivity of the human face shaped antenna at 10 GHz is shown in Figure 3.14. The maximum gain and maximum directivity of the human face shaped antenna are 6.2 dB and 6.268 dBi, respectively.

`

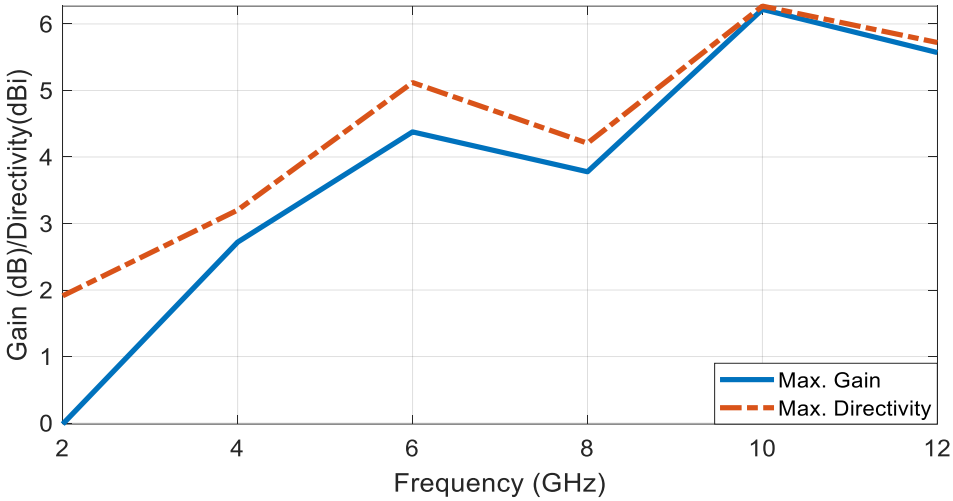

Figure 3.14: Gain and directivity of the human face shaped antenna with rectangular DGS

3.2.2.6 VSWR plot

Low VSWR indicates that the antenna is matched well, and the maximum power is delivered to the antenna. The VSWR plot of the human face shaped microstrip patch antenna with rectangular DGS is shown in Figure 3.15. As seen from this figure, the minimum value of VSWR is 1.035 at 8.8 GHz. From the VSWR plot, it is evident that the value of VSWR is less than 2 for the frequency range 5.9 GHz -11.2 GHz.

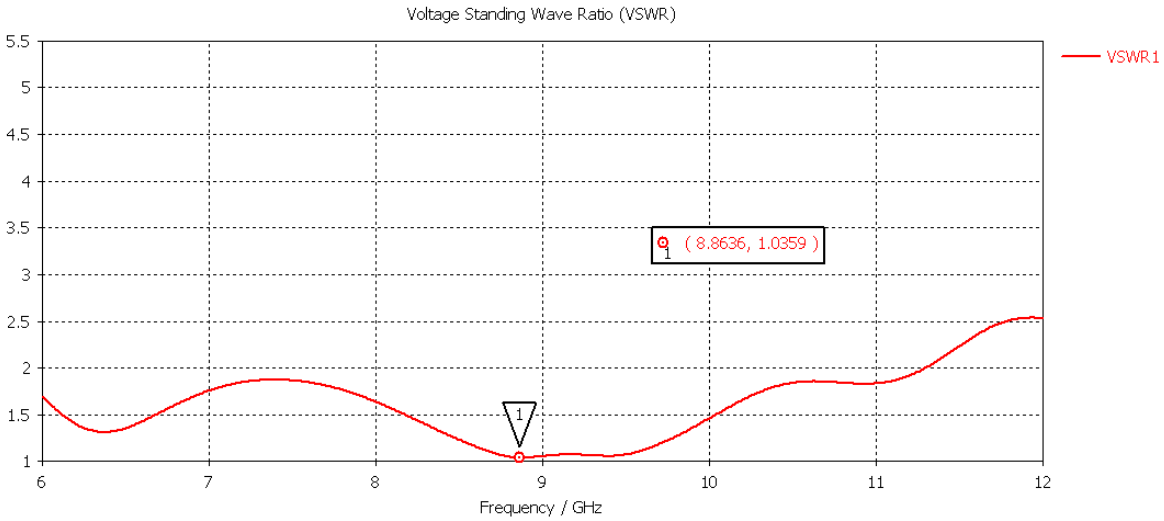

Figure 3.15: VSWR plot

`

3.2.2.7 Comparison of human face shaped microstrip patch antenna with existing antennas

Table 3.5 shows the comparison of human face shaped patch antenna with existing antennas. It can be seen that the proposed antenna is compact in size with a minimum reflection coefficient. The gain of the proposed antenna is high.

Table 3.5: Comparison of human face shaped antennas with some existing antennas

Reference	**[88]**	**[89]**	**[90]**	**[91]**	**Proposed Antenna**
Maximum Gain (dB)	3	1.49	7.362	3.778	6.219
Bandwidth	140%	77%	142%	119%	70%
Size (mm * mm)	40*40	20*18	70*82	30*30.82	25.2*38.2
Minimum reflection coefficient (dB)	-30	-16	-26.02	-28.49	-35

3.3 Human face shaped microstrip patch antenna with rectangular and triangular DGS

In this section, the design of human face shaped microstrip patch antenna with rectangular and triangular DGS is presented. A triangular defect is etched in the ground plane to increase the bandwidth of the human face shaped microstrip antenna as shown in Figure 3.16. This produces two frequency bands i.e. $5.4\ \text{GHz} - 8.6\ \text{GHz}$ and $10.1 - 14.7\ GHz$. To eliminate the interference from wireless local area network one more triangular defect (symmetrical to the other) is etched in ground plane as shown in Figure 3.17. This produces three frequency bands i.e. $3.2\ GHz - 5\ \text{GHz}$, $6.3\ GHz$ - $9.2\ GHz$ and $10.1 - 15\ GHz$. It is evident that the addition of the defects improves the bandwidth of the human face shaped microstrip patch antenna.

`

`

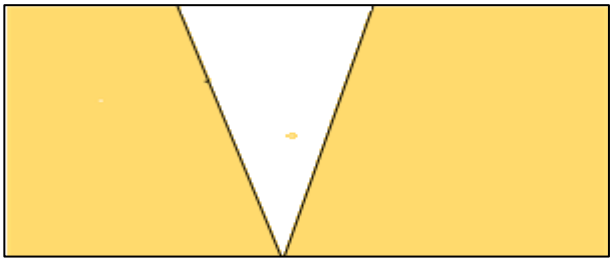

Figure 3.16: Ground plane with triangular defect

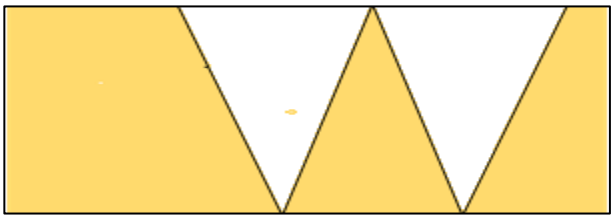

Figure 3.17: Ground plane with two triangular defects

To further cover the lower frequency band of the ultra-wideband, one rectangular defect is etched in the ground plane as shown in Figure 3.18. The addition of rectangular defect produces three frequency bands i.e. 3.1 GHz − 5 GHz , 6.3 GHz - 9.2 GHz and 10.1 − 14.7 GHz. To eliminate notch band from 9.3 GHz to 10 GHz a human face shaped patch is designed as shown in the Figure 3.19.

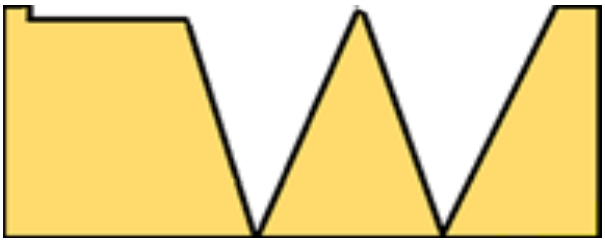

Figure 3.18: Ground plane with one rectangular slot, two triangular defects

`

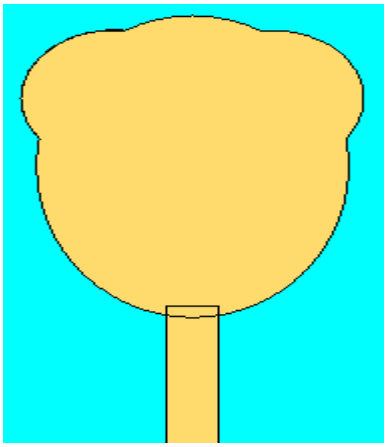

Figure 3.19: Elliptical patch with human face

This human face produces three frequency bands i.e. 3.2 GHz − 5 GHz , 6.3 GHz - 9.3 GHz and 9.5 − 14.3 GHz. To further increase the bandwidth, two symmetrical circular slots (eyes) and a rectangular slot (nose) are added to the elliptical patch as shown in Figure 3.20. The addition of eyes and nose to the antenna produces three frequency bands i.e. 3.1 GHz − 5 GHz, 6.3 − 9.3 GHz, 9.5 − 14.7 GHz. To remove the notch at 9.4 GHz frequency band, one elliptical slot (mouth) is added to the human face patch as shown in Figure 3.21. Finally, when two symmetrical elliptical slots (eyebrows) are added to the human face shaped microstrip antenna as shown in Figure 3.22, it produces the desired bandwidth 3.0 GHz − 5 GHz and 6.3 GHz - 14.7 GHz.

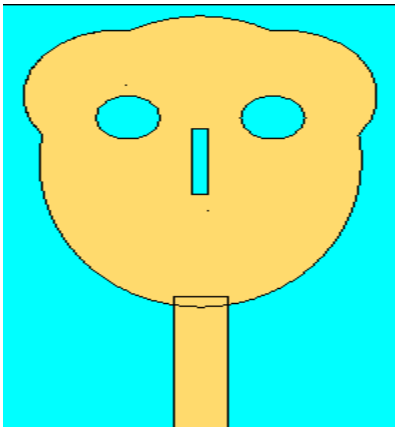

Figure 3.20: Elliptical patch with human face, nose and eyes

`

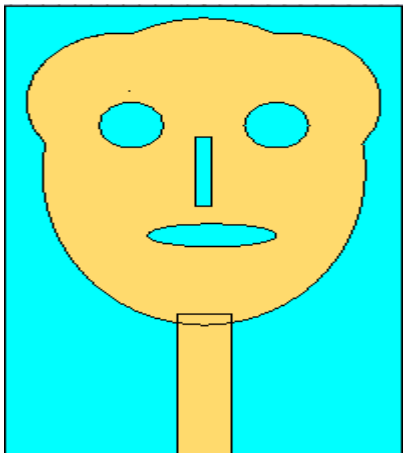

Figure 3.21: Elliptical patch with human face, nose, eyes and mouth

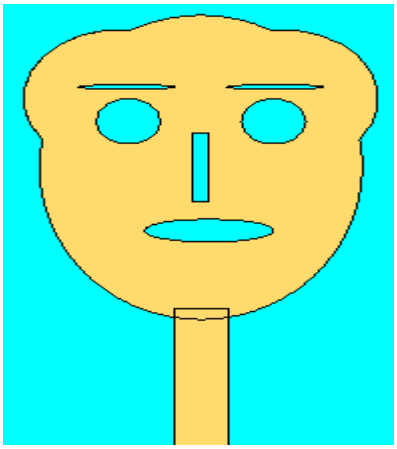

Figure 3.22: Elliptical patch with human face, nose, eyes, mouth and eyebrows.

3.3.1 Antenna geometry and dimensions

The antenna is designed on a $38.6\ mm \times 24.6\ mm$ FR4 substrate with a dielectric constant of 4.4 and thickness of $1.6\ mm$. The substrate parameters are summarized in Table 3.6. The width of the head is $12\ mm$. The width and length of the mouth are 8mm and $2\ mm$, respectively. The width and length of the eyebrows are $6\ mm$ and $0.4\ mm$, respectively. The width of the eye is $3\ mm$. The width and length of the nose are $1\ mm$ and $6\ mm$, respectively. The antenna structure is fed by a $50\ \Omega$ microstrip line. The width and the length of the microstrip line are $3.4\ mm$ and $12\ mm$, respectively.

One rectangular defect and two symmetrical defects are etched in the ground plane, which help to increase the gain and to reduce harmonics, mutual coupling and size of the antenna. The

`

width and length of the ground plane are 24.6 mm and 9.8 mm, respectively. The rectangular defect in the ground plane has the length of 8.6 mm and the width of 0.5 mm. The triangular defects have the length of 9. 6 mm and a width of 7.1 mm at the open end. The top view and the bottom view of the antenna are shown in Figure 3.23 (a) and Figure 3.23 (b), respectively. The optimized dimensions of the human face shaped microstrip patch antenna with rectangular and triangular defects are summarized in Table 3.7.

Table 3.6: Substrate specifications

Parameter	**Value**
Thickness of substrate	1.6 mm
Dielectric constant (ε_r)	4.4
Material	FR4

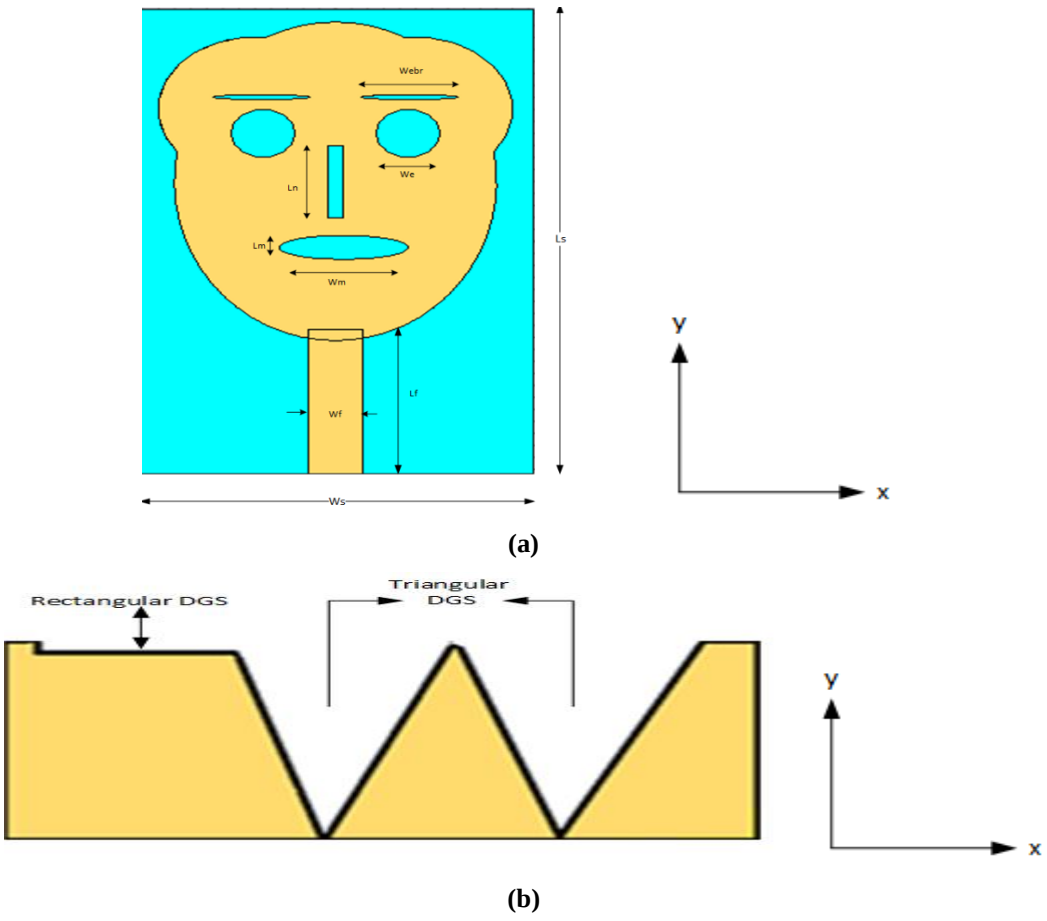

Figure 3.23: Geometry of the proposed antenna (a) top view (b) bottom view

`

Table 3.7: Optimized antenna dimensions

Parameter	Value (mm)	Description
L_s	38.6	Substrate length
W_s	24.6	Substrate width
L_f	12	Feed line length
W_f	3.4	Feed line width
W_m	8	Mouth width
L_n	6	Nose length
W_e	3	Eye width
L_m	2	Mouth length
W_{ebr}	6	Eyebrow width
L_g	9.8	Ground length

3.3.2 Results and discussion

The antenna is simulated using CST microwave studio and the simulated results of various parameters of the antenna like reflection coefficient, gain, directivity, radiation pattern, VSWR are discussed below.

3.3.2.1 Reflection coefficient (S_{11}) and antenna bandwidth

It can be seen from the Figure 3.24, the antenna without human face and defects in the ground plane has three frequency bands i.e. 5.4 GHz - 5.9 GHz, 9.5 GHz - 12 GHz and 13.6 GHz – 14.2 GHz. The minimum reflection coefficient is -12 dB. When the defects are added to the ground plane, the antenna has three frequency bands i.e. 3.1 GHz - 5 GHz, 6.3 – 9.2 GHz and 10.1 – 15 GHz. The minimum reflection coefficient is -39.8 dB.

Figure 3.25 shows the S_{11} plot of the antenna with human face. The antenna with human face and without defects in the ground plane has three frequency bands i.e. 5.5 GHz - 6 GHz, 9.5 GHz - 12 GHz and 9.3 GHz – 11.7 GHz. The minimum reflection coefficient is -14.82 dB. When the defects are added to the ground plane the antenna produces the bandwidth from 3.0 GHz to 14.7 GHz with a notch band of 5 GHz - 6.3 GHz. The minimum reflection coefficient is -35.4 dB. Table 3.8 summarizes the reflection coefficient and bandwidth of different antenna

`

structures, which indicates that the human face antenna with eyes, nose, mouth, eyebrows, and defects in the ground plane has the wide bandwidth from 3.0 GHz to 14.7 GHz with a notch band from 5 GHz to 6.3 GHz. The minimum reflection coefficient of -35.4 dB is achieved.

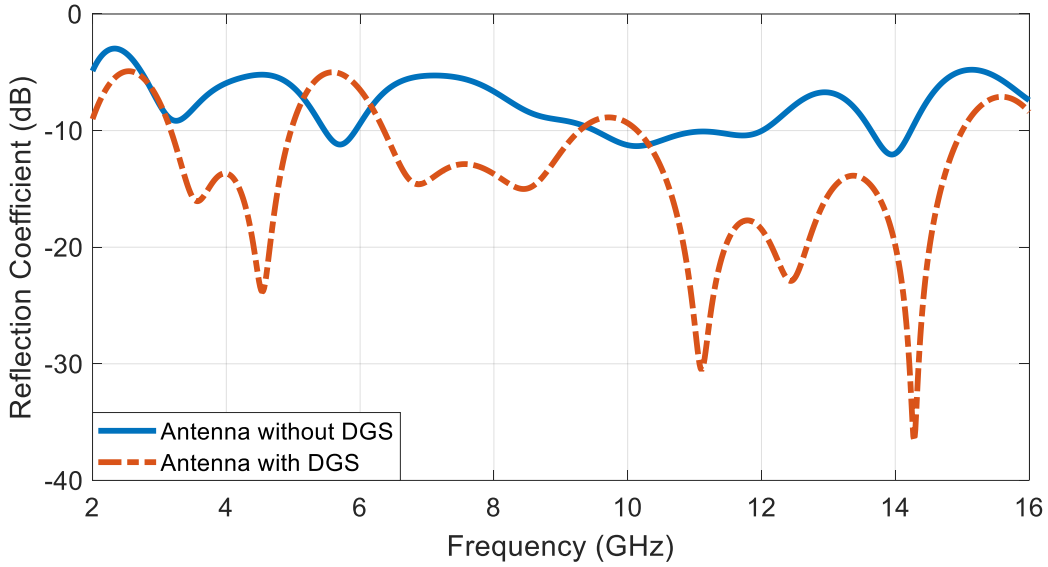

Figure 3.24: Reflection coefficient plot of the antenna without human face

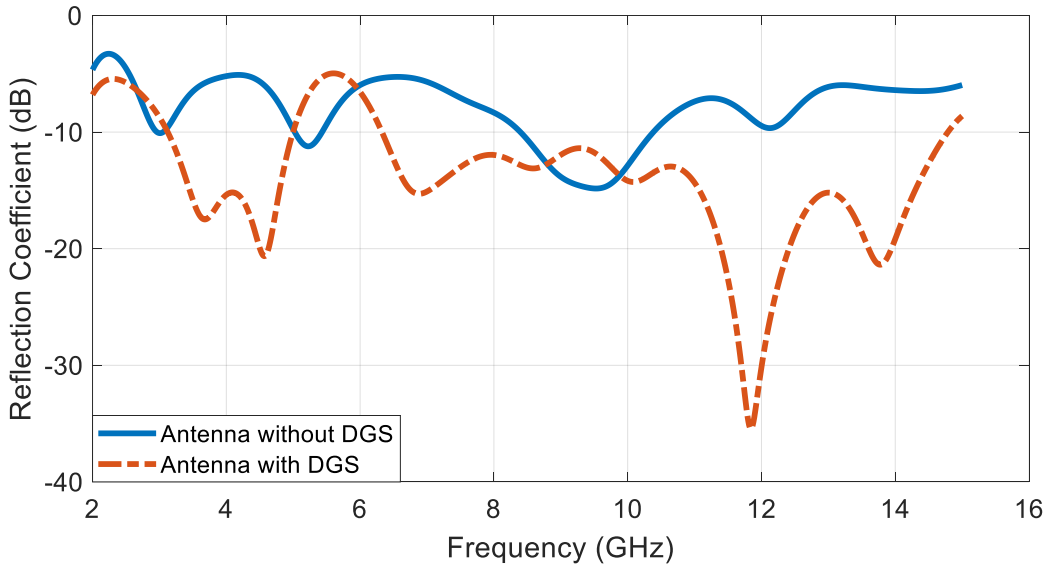

Figure 3.25: Reflection coefficient plot of the antenna with human face

`

Table 3.8: Reflection coefficient and bandwidth of different antenna structures

Antenna Structure	**Reflection Coefficient (dB)**	**Frequency range**
Elliptical patch without human face and without ground plane defects	-12	5.4 - 5.9 GHz 9.5 - 12 GHz 13.6 – 14.2 GHz
Elliptical patch without human face and with a triangular defect in ground plane	-57.16	5.3 - 8.6 GHz 10.1 – 14.7 GHz
Elliptical patch without human face and with two triangular defects in ground plane	-44.8	3.2 - 5.0 GHz 6.3 – 9.2 GHz 10.1 – 15.0 GHz
Elliptical patch without human face and all defects in ground plane	-39.8	3.1 - 5.0 GHz 6.3 – 9.2 GHz 10.1 – 15.0 GHz
Elliptical patch with human face (no slots) and all defects in ground plane	-36.5	3.2 - 5.0 GHz 6.3 – 9.3 GHz 9.5 – 14.3 GHz
Elliptical patch with human face having eyes and nose and all defects in ground plane	-35.5	3.1 - 5.0 GHz 6.3 – 9.3 GHz 9.5 – 14.7 GHz
Elliptical patch with human face having eyes, mouth, nose and all defects in ground plane	-31.5	3.1 - 5.0 GHz 6.3 – 14.7 GHz
Elliptical patch with human face having eyes, nose, mouth, eyebrows and all defects in ground plane	-35.4	3.0 - 5.0 GHz 6.3 – 14.7 GHz

3.3.2.2 Three-dimensional directivity pattern

Figure 3.26 shows the directivity pattern without human face and defects in the ground plane at 10 GHz. The red portion shows the maximum radiation which is 5.914 dBi at 10 GHz. Figure 3.27 shows the directivity pattern of the antenna with human face, eyes, nose, mouth,

`

eyebrows and all defects in ground plane. Maximum directivity of the human face shaped microstrip patch antenna with rectangular and triangular defects in the ground plane is 6.15 dBi at 10 GHz.

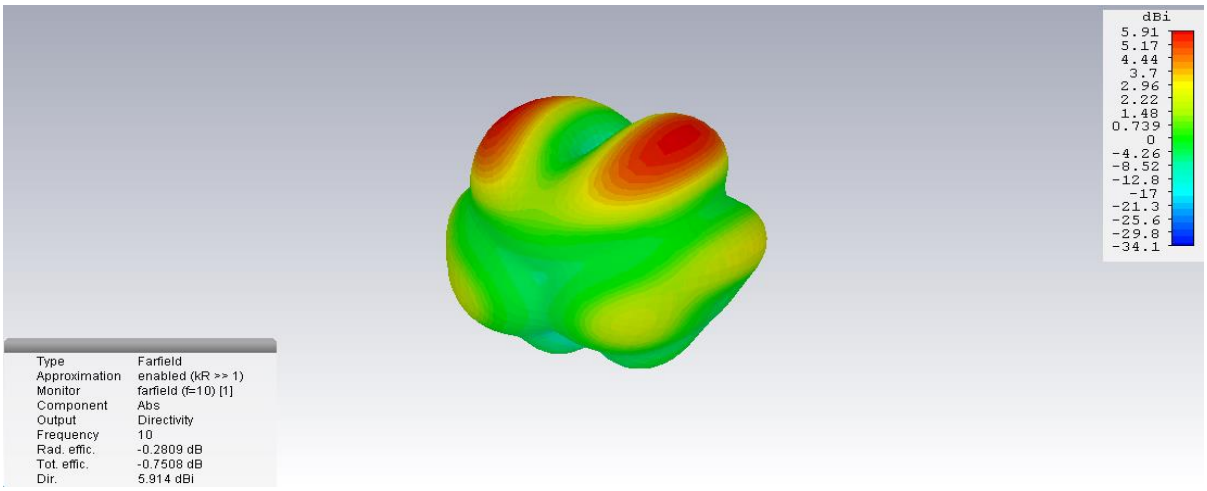

Figure 3.26: Directivity pattern of antenna without human face and defects in ground plane at 10 GHz

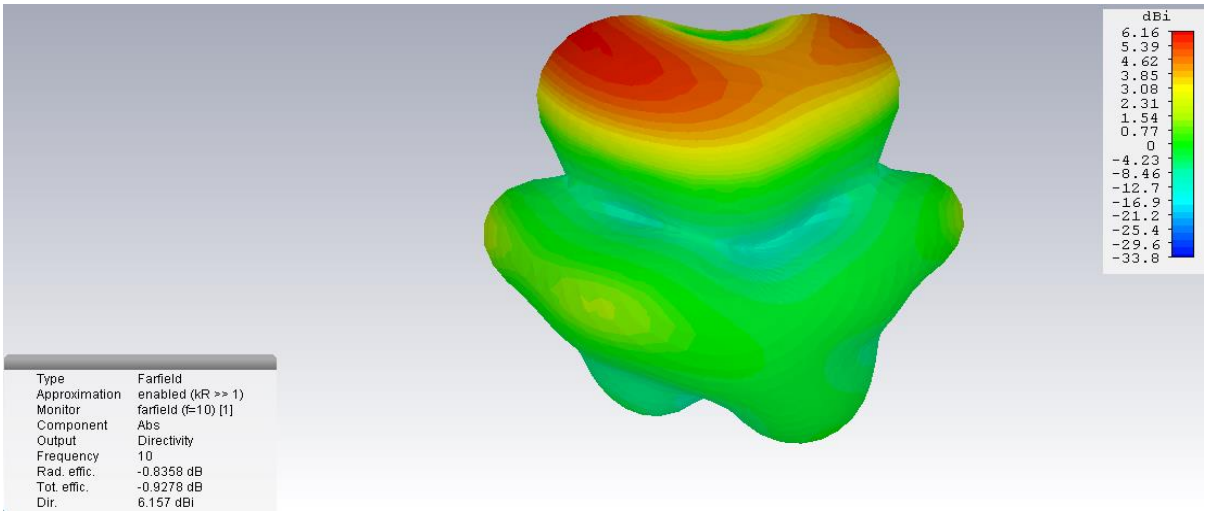

Figure 3.27: Directivity pattern of antenna with human face having eyes, nose, mouth, eyebrows and all defects in ground plane at 10 GHz

3.3.2.3 Three-dimensional gain pattern

Figure 3.28 shows the gain pattern for the antenna without human face and defects. The red portion shows the maximum gain, which is 5.633 dB at 10 GHz. Figure 3.29 shows the gain

`

pattern of human face shaped antenna with eyes, nose, mouth, eyebrows having two triangular defects and a rectangular defect in ground plane at 10 GHz. The maximum value of the gain is 5.321 dB. The gain and directivity of different antenna structures at 10 GHz is shown in Table 3.9. As shown in the table 3.9, the maximum gain and directivity of the human face shaped antenna with defects are 5.321 dB and 6.15 dBi, respectively. Table 3.10 shows the gain, directivity, radiation efficiency and total efficiency of the antenna at various frequencies. The maximum gain and maximum directivity of the human face shaped antenna at 14.7 GHz are 5.9 dB and 6.4 dBi, respectively.

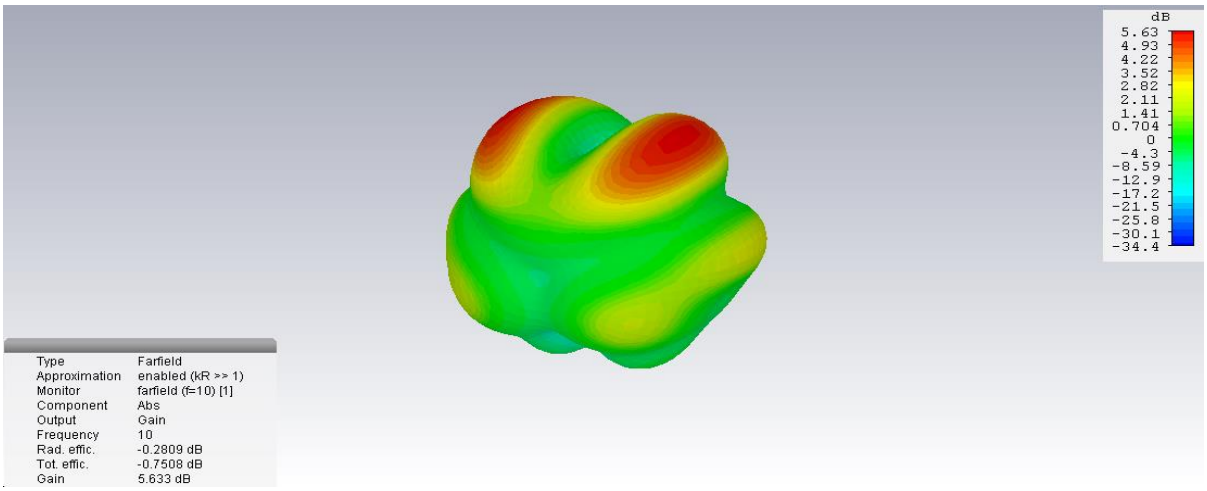

Figure 3.28: Gain pattern of antenna without human face and defects at 10 GHz.

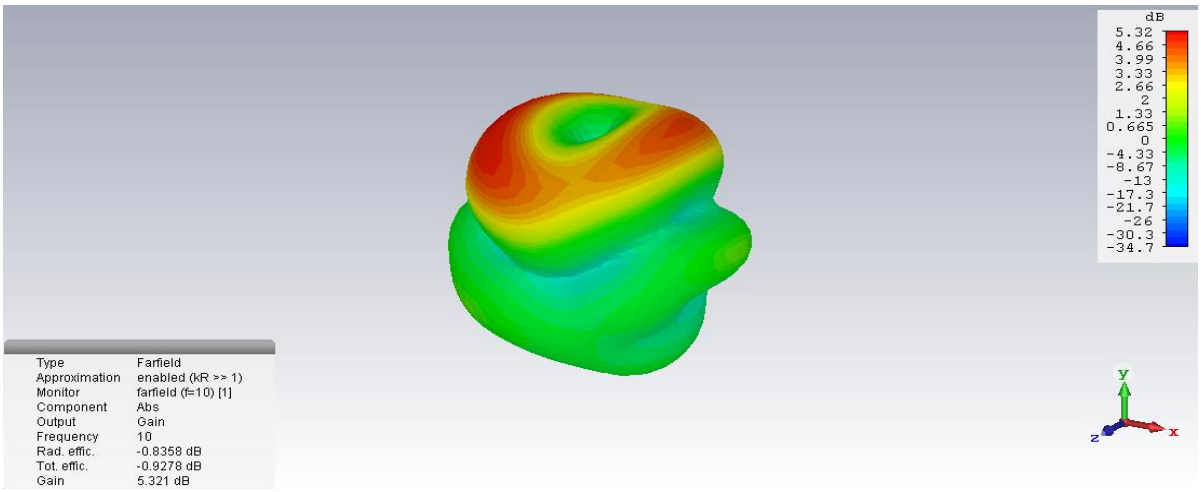

Figure 3.29: Gain pattern of antenna with human face having nose, eyes, mouth, eyebrows and two triangular defects and a rectangular defect at 10 GHz

`

Table 3.9: Gain and directivity of various antenna structures

Antenna Structure	**Gain (dB) at f=10 GHz**	**Directivity (dBi) at f=10 GHz**
Elliptical patch without human face and without ground plane defects	5.633	5.914
Elliptical patch without human face and with a triangular defect in ground plane	5.859	6.368
Elliptical patch without human face and with two triangular defects in ground plane	4.485	5.600
Elliptical patch without human face and all defects in ground plane	4.636	5.746
Elliptical patch with human face (no slots) and all defects in ground plane	5.117	6.003
Elliptical patch with human face having eyes and nose and all defects in ground plane	5.016	5.918
Elliptical patch with human face having eyes, mouth, nose and all defects in ground plane	5.392	6.216
Elliptical patch with human face having eyes, nose, mouth, eyebrows and all defects in ground plane	5.321	6.15

`

Table 3.10: Gain, directivity, radiation efficiency, total efficiency at various frequencies

Frequency (GHz)	**f=4**	**f=6**	**f=10**	**f=14.7**
Gain (dB)	1.977	2.377	5.32	5.945
Radiation Efficiency (dB)	-1.204	-2.845	-0.836	-0.4662
Total Efficiency (dB)	-1.422	-3.886	-0.928	-0.9207
Directivity (dBi)	3.180	5.222	6.156	6.411

3.3.2.4 Gain and directivity plot

The gain and directivity of the antenna are shown in Figure 3.30. The maximum gain and maximum directivity of the human face shaped microstrip patch antenna are 6 dB and 6.41 dB, respectively.

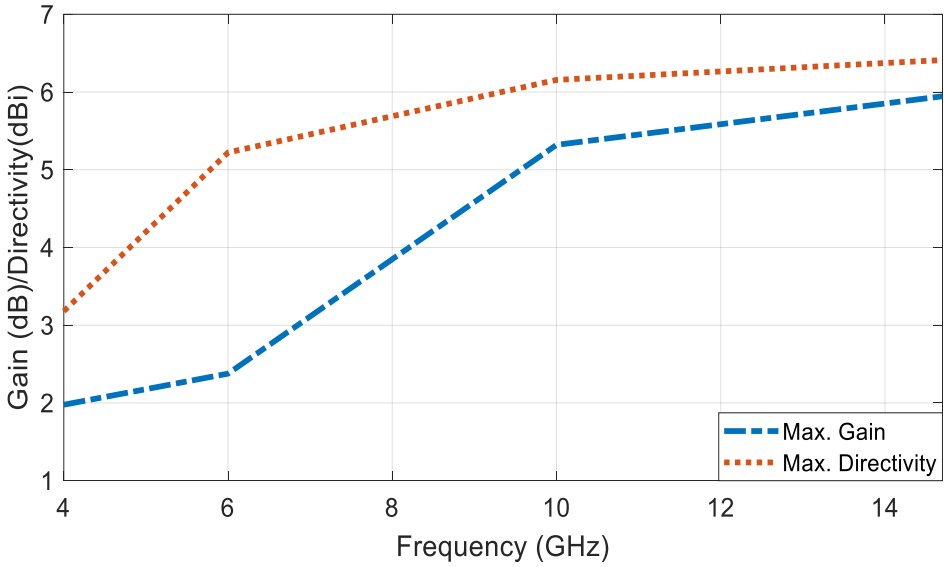

Figure 3.30: Gain and directivity of human face shaped antenna with triangular and rectangular DGS

`

3.3.2.5 VSWR

Figure 3.31 shows the VSWR vs frequency plot. The maximum value is 3.6 which is at the notched frequency. The minimum value is 1.0363 at the resonance frequency of 11.76 GHz. From the VSWR plot, it is evident that the value of VSWR is less than 2 from 2.8 GHz - 16.1 GHz except from 5 GHz - 6.3 GHz.

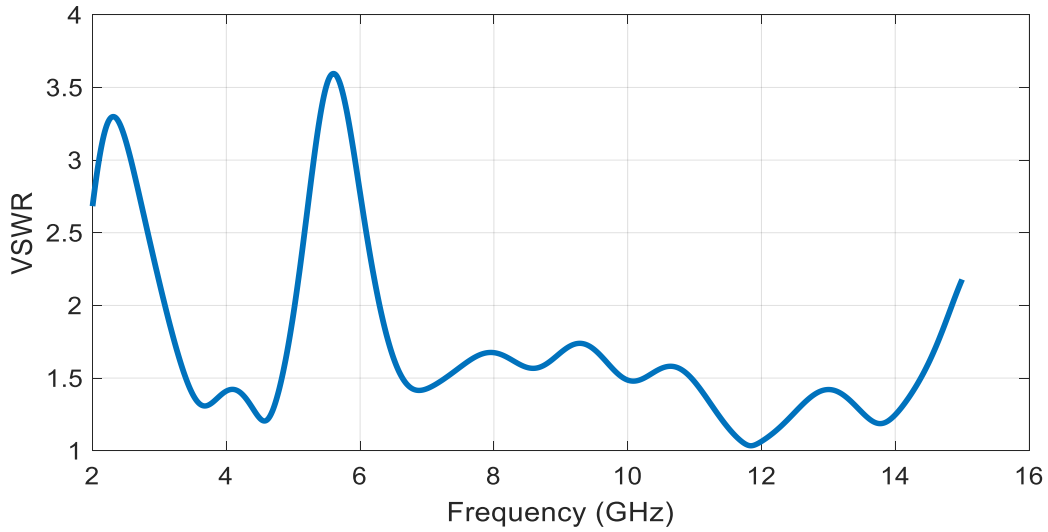

Figure 3.31: VSWR vs frequency plot

3.3.2.6 Comparison of human face shaped antenna having enhanced bandwidth with existing antennas

Table 3.11 shows the comparison of proposed human face shaped microstrip antenna with existing antennas in the literature. It is evident from the table that the proposed antenna has the maximum gain, wide bandwidth with minimum reflection coefficient.

Table 3.11: Comparison of human face shaped antenna having enhanced bandwidth with some existing antennas

Reference	**[88]**	**[89]**	**[90]**	**[91]**	**Proposed Antenna**
Max Gain (dB)	3	1.49	7.362	3.778	5.945
Bandwidth (%)	140	77	142	119	118
Size (mm*mm)	40*40	20*18	70*82	30*30.82	24.6*38.6
Min. Reflection Coefficient (dB)	-30	-16	-26.02	-28.49	-35.4

`

3.3.3 Fabrication and measured results

To verify the design of the antenna, the fabrication is done on a FR4 substrate having relative permittivity of 4.4 and thickness of 1.6 mm with area of 38.6 mm × 24.6 mm. FR4 is used as substrate as it is cheap and easily available. For fabrication, the gerber files for each layer of the antenna configuration are exported using CST microwave studio. Photo-lithographic method is used for the fabrication of the microstrip patch antenna. The undesired copper dust on the fabricated structure is removed. A SMA connector is connected with the structure using soldering. The inner connector of the SAM connector is connected to the feed line and the outer connector of the SMA connector is connected with the ground plane. The fabricated antennas are shown in Figure 3.32 (a) and Figure 3.32 (b).

Figure 3.32 (a) and Figure 3.32 (b) shows the images of top view and bottom view of the human face shaped antenna, respectively. On the top side of the antenna, a microstrip line having a width of 3.4 mm feeds the antenna. The antenna is excited by a 50 Ω SMA connector.

(a) (b)

Figure 3.32: Fabricated antenna (a) top view, (b) bottom view

3.3.3.1 Reflection coefficient

The reflection coefficient of the fabricated antenna is measured using vector network analyzer as shown in Figure 3.33. The frequency range of the VNA is from 100 KHz – 13 GHz.

`

Figure 3.33: Vector network analyzer

Figure 3.34 shows the simulated and measured reflection coefficient plot up to 13 GHz. As seen from the figure the human face shaped antenna has bandwidth from 3 GHz to 14.7 GHz with a notch band from 5 GHz to 6.3 GHz. The comparison between simulated and measured results shows good agreement except little deviation. It may be due to connector and other losses etc.

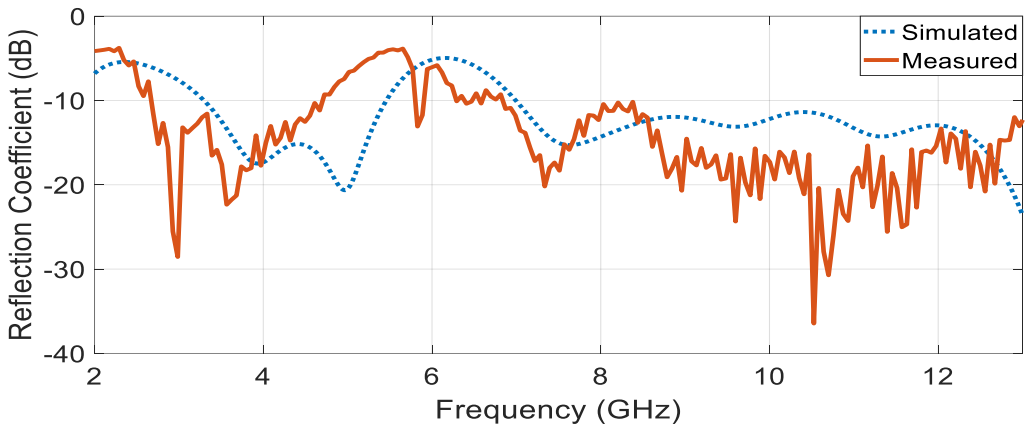

Figure 3.34: Measured and simulated reflection coefficient plot of the human face shaped microstrip antenna

3.3.3.2 Two-dimensional radiation patterns

Measurement of radiation pattern was done in an anechoic chamber. A horn antenna is used as a receiving antenna and is connected to a signal analyzer. The human face shaped antenna is connected to a transmitting device namely signal generator through a mount. The frequency in

`

the signal generator is adjusted and the peak value of the spectrum is noted by rotating the human face shaped antenna.

The normalized radiation patterns of the proposed human face shaped antenna with rectangular and triangular DGS are shown in Figure 3.35. The normalized pattern in phi= 0 degree and phi= 90 degree plane at 4 GHz, 8 GHz, 10 GHz, 12 GHz and 14 GHz are depicted in Figure 3.35 (a), Figure 3.35 (b), Figure 3.35 (c), Figure 3.35 (d) and Figure 3.35 (e), respectively. The simulated and measured patterns show reasonable agreement with minor deviation. It may be due to connector and other losses etc.

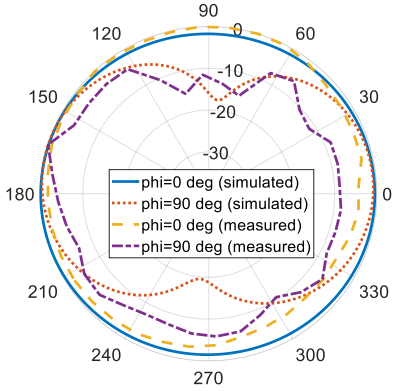

(a)

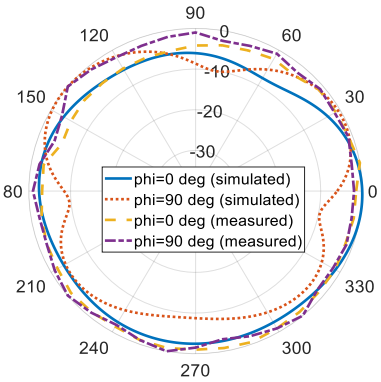

(b)

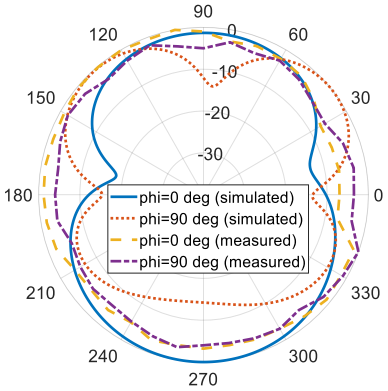

(c)

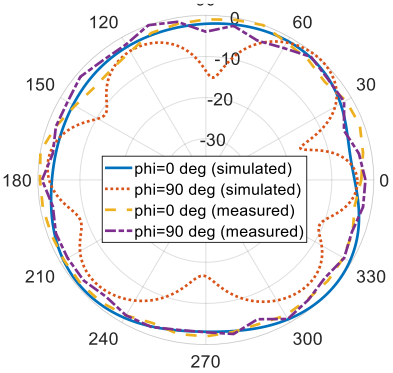

(d)

`

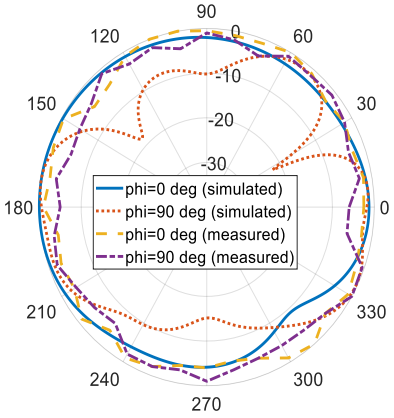

. (e)

Figure 3.35: Radiation pattern for antenna with defects (a) f=4 GHz, (b) f=8 GHz, (c) f=10 GHz, (d) f=12 GHz, (e) f=14 GHz

3.4 Chapter summary

An initial design of elliptical human face shaped antenna with eyes, nose, eyebrows, mouth that covers a bandwidth 5.9 GHz - 11.2 GHz has been presented. The improved design of the human face shaped antenna that covers a bandwidth from 3 GHz to 14.7 GHz with a notch band of $5\ GHz - 6.3\ GHz$ has been presented and discussed. The design evolution of the human face shaped antenna is explained for both the antenna configurations. The antennas are simulated using CST microwave studio and various antenna parameters like reflection coefficient, VSWR, radiation pattern, gain, directivity, total efficiency, radiation efficiency etc are presented and discussed. The proposed antennas are suitable for ultra-wideband applications.

`

CHAPTER 4: A HIGH GAIN UWB HUMAN FACE SHAPED MIMO PATCH ANTENNA WITH HIGH ISOLATION

A compact human face shaped multiple input multiple output microstrip patch antenna that covers the ultra-wideband from 2.8 GHz to 16.1 GHz is presented. The antenna has a notch from 5 GHz to 6.4 GHz to avoid interference from WLAN band (5 GHz - 6 GHz). The antenna has two orthogonal human face shaped antenna to achieve dual polarization. The antenna has the isolation of more than 19.8 dB over the entire bandwidth. The antenna is designed, simulated and optimized using CST microwave studio and various antenna parameters like gain, directivity, VSWR, coupling coefficient are presented. The human face shaped MIMO antenna is fabricated and measured. The gain and directivity plot are presented. The proposed UWB human face shaped MIMO antenna provides high gain and high isolation between the ports.

4.1 Introduction

Polarization plays an important role in antenna and usually denotes the direction of electric field of the radio wave. If the electrical field is horizontally oriented, it is referred as horizontal polarization and if it is vertically oriented, it is referred as vertical polarization. Antennas for MIMO systems require antennas with polarization diversity. To achieve spatial multiplexing the MIMO system uses multiple transmitting and receiving antennas [92]. Polarization diversity is of great importance and is needed for MIMO technique [93].

Many UWB MIMO antennas have been developed [94]-[96] in the recent years. In [94], asymmetric coplanar fed UWB MIMO antenna is discussed. The isolation obtained was >15 dB. In [95], two stubs and complementary split ring resonator (CSRR) were used to achieve UWB and isolation > 15dB. In [96], a disk-shaped MIMO antenna achieved high isolation > 15dB using a carbon black film. The proposed MIMO antenna operates from 2.8 GHz to 16.1 GHz with a notch from 5 GHz to 6.4 GHz. The antenna utilizes the concept of polarization diversity to increase the system capacity.

`

4.2 Design of MIMO human face shaped microstrip patch antenna

MIMO technique increases channel capacity without using any additional bandwidth. MIMO technique is combined with UWB technology for reliable transmission and high data rate.

The MIMO human face shaped antenna consists of two human face shaped antennas placed orthogonally to each other in order to achieve dual polarization. The human face shaped MIMO antenna radiates two linearly polarized fields in two different directions, which are perpendicular to each other thus forming dual orthogonal polarized field [97]. Since the mutual coupling between the antennas is high with multiple antennas, designing a MIMO antenna with low mutual coupling is a challenge. Low mutual coupling is needed to achieve high efficiency and gain. Some of the techniques to reduce mutual coupling are to use DGS [98], resonators [99], slots [100].

One solution to mutual coupling is to space the antennas far apart, but it increases the size of the antenna. The edge to edge spacing between the human face shaped MIMO antennas is 0.39 λ0, where λ0 is the free space wavelength corresponding to center frequency of 9.45 GHz. The antenna elements are placed on the same substrate and have separate ground planes on the same substrate. One rectangular defect and two symmetrical triangular defects are etched in the ground plane, which provides impedance matching and also helps to reduce the mutual coupling.

The position of the second antenna along the horizontal dimension in Figure 4.1 is optimized to further improve the performance of the antenna. Three different positions as shown in Figure 4.1, Figure 4.2, Figure 4.3 are analyzed. For the antenna configuration of Figure 4.1, the minimum reflection coefficient is -28.8 dB. The antenna produces three frequency bands i.e. 2.8 GHz - 5 GHz, 6.4 GHz -14.5 GHz and 15.3 GHz - 16.1 GHz. The gain, directivity and the coupling coefficient of the human face shaped MIMO antenna are 5.7 dB, 6.3 dBi and -16.9 dB, respectively.

`

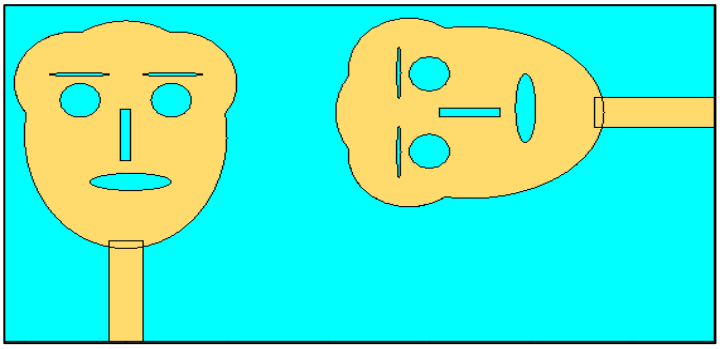

Figure 4.1: Human face shaped MIMO antenna in position 1

The position of antenna at port 2 is varied and optimized to obtain the optimized performance of the proposed MIMO antenna. The antenna structures for second antenna at different three positions are shown in Figure 4.1- 4.3. Various parameters for these three structures are analyzed and it is observed that the antenna configuration of Fig. 4.3 provides the optimum performance. For the antenna configuration of Figure 4.2, the minimum reflection coefficient is -22.34 dB. The antenna produces two frequency bands i.e. 2.8 GHz - 5 GHz and 6.4 $GHz -$ 16.1 GHz. The gain, directivity and coupling coefficient of the human face shaped MIMO antenna are 6.6 dB, 7.2 dBi and -19.5 dB, respectively. For the antenna configuration of Figure 4.3, the minimum reflection coefficient is -22.0 dB. The antenna covers the bandwidth from 2.8 GHz to 5 GHz and from 6.5 GHz to 16.1 GHz with a notch band from 5 GHz – 6.4 GHz. The gain, directivity and coupling coefficient of the human face shaped MIMO antenna are 7.1 dB, 7.6 dBi and -19.8 dB, respectively. The proposed antenna is a two port structure and provides very low mutual coupling between the ports with high gain. Hence, the proposed antenna is suitable for 2x2 MIMO system with low interference between the signals of two ports.

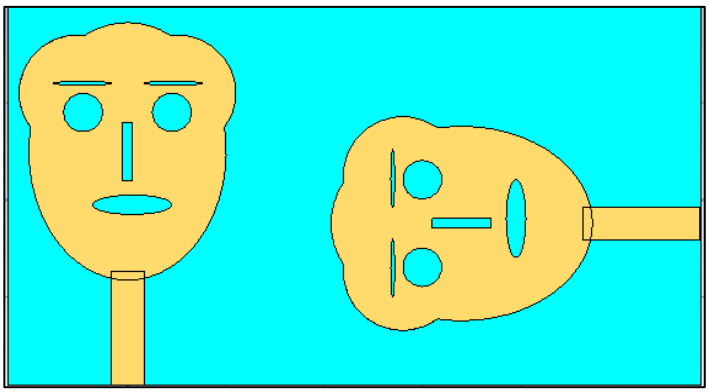

Figure 4.2: Human face shaped MIMO antenna in position 2

`

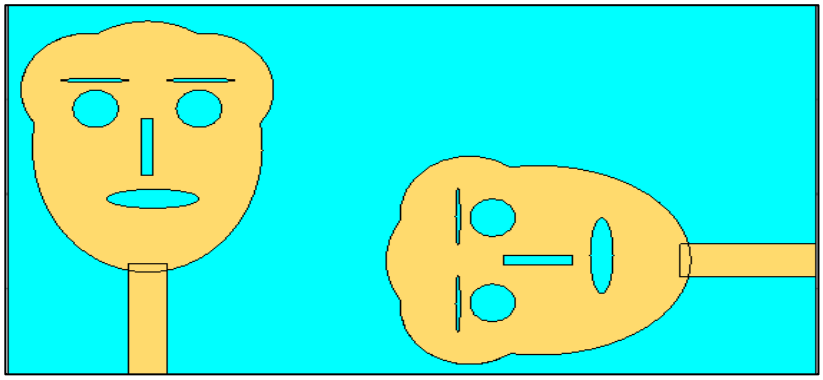

Figure 4.3: Human face shaped MIMO antenna in position 3

4.2.1 MIMO antenna geometry and dimensions

The geometry of the proposed human face shaped MIMO antenna is shown in Figure 4.4. Figure 4.4(a) and Figure 4.4(b) shows the top view and bottom view, respectively. The antenna is designed on a 39.1 *mm* x 70.2 *mm* FR4 substrate with a dielectric constant of 4.4 and a thickness of 1.6 *mm*. Each of the human face shaped antenna is fed by 50 Ω microstrip feed line having a width of 3.4 *mm* and a length of 11.8 *mm*. To increase the bandwidth, a rectangular defect and two triangular defects are etched in the ground plane of each antenna as shown in Figure 4.4 (b). The width and length of the rectangular defect are 8.6 *mm* and 0.5 *mm,* respectively. The width and length of the triangular defect are 7.1 *mm* and 9.6 *mm,* respectively.

The human face shaped patch in each antenna has two symmetrical circular defects (eyes), two symmetrical elliptical defects (eyebrows), one rectangular defect (nose), and a non-symmetrical elliptical defect (mouth) to achieve the desired wide bandwidth. The eyebrows in each human face shaped patch have the width of 6 *mm* and a length of 0.4 *mm*. The head in each human face shaped patch has the width of 12 *mm*, and the mouth has the width of 8 *mm* and length of 2 *mm* . The eye in each of the human face shaped patch has the width of 3 *mm*, and the nose has the width of 1 *mm* and a length of 6 *mm*. These defects are needed to increase the bandwidth of the antenna. The width and length of the ground plane are 24.2 *mm* and 9 *mm* respectively. The optimized dimensions of the MIMO antenna are summarized in Table 4.1.

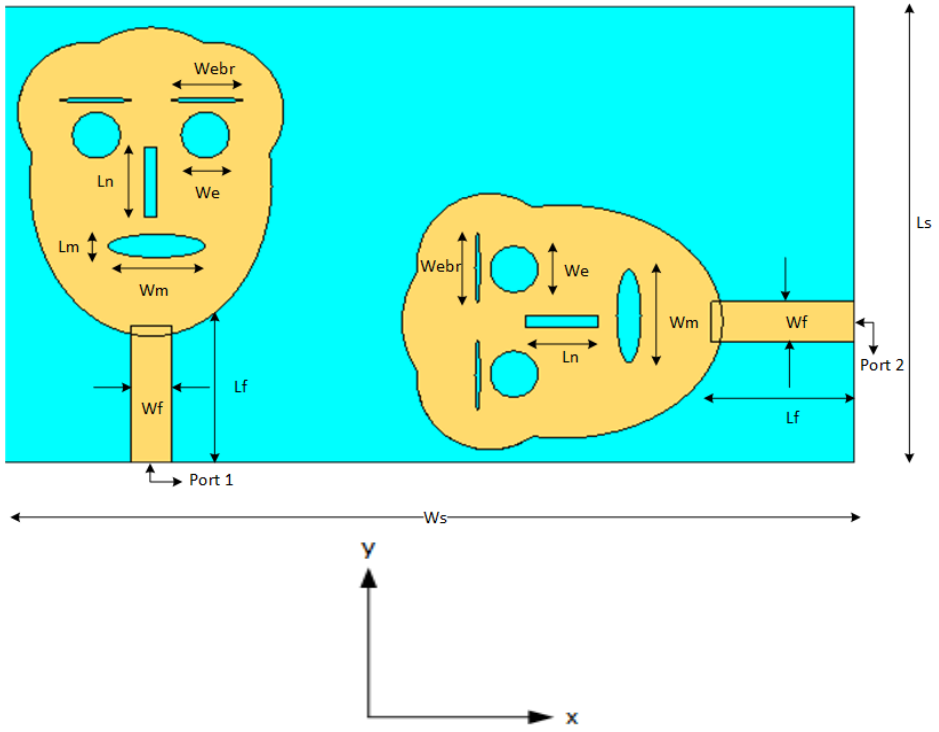

(a)

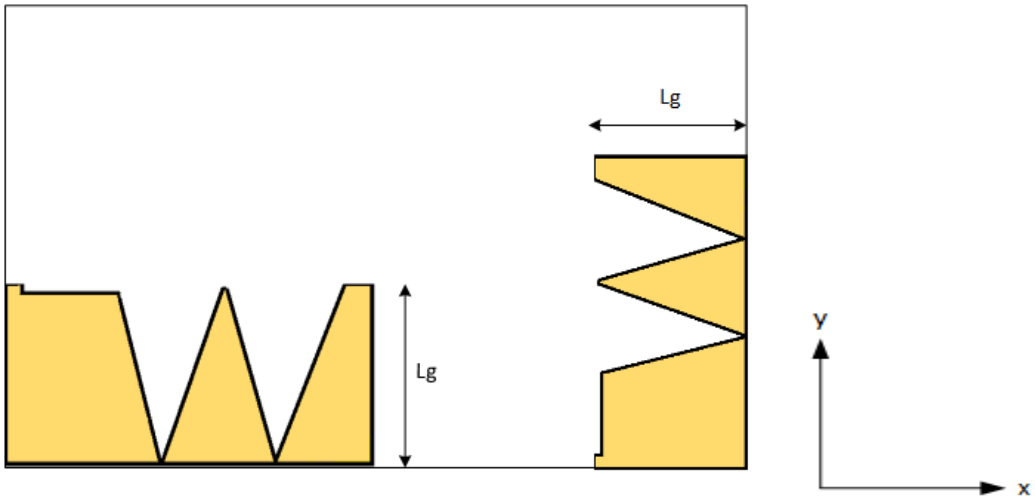

(b)

Figure 4.4: Geometry of MIMO human face shaped microstrip antenna (a) top view (b) bottom view

`

Table 4.1: Optimized antenna parameters

Parameter	Value (mm)	Description
Ls	39.1	Substrate length
Ws	70.2	Substrate width
Lf	11.8	Feedline length
Wf	3.4	Feedline width
Wm	8	Mouth width
Ln	6	Nose length
We	3	Eye width
Lm	2	Mouth length
Webr	6	Eyebrow width
Lg	9	Ground length

4.2.2 Simulation results and discussion

The antenna is simulated and optimized using CST microwave studio and the simulated results of various parameters of the antenna are discussed below.

4.2.2.1 Scattering parameters and antenna bandwidth

Figure 4.5 shows the reflection coefficient plot for port 1 of the MIMO antenna for various configuration. As observed from the figure below, the reflection coefficient of the antenna in position 1, position 2 and position 3 are -28.8 dB, -22.2 dB and -22 dB, respectively.

`

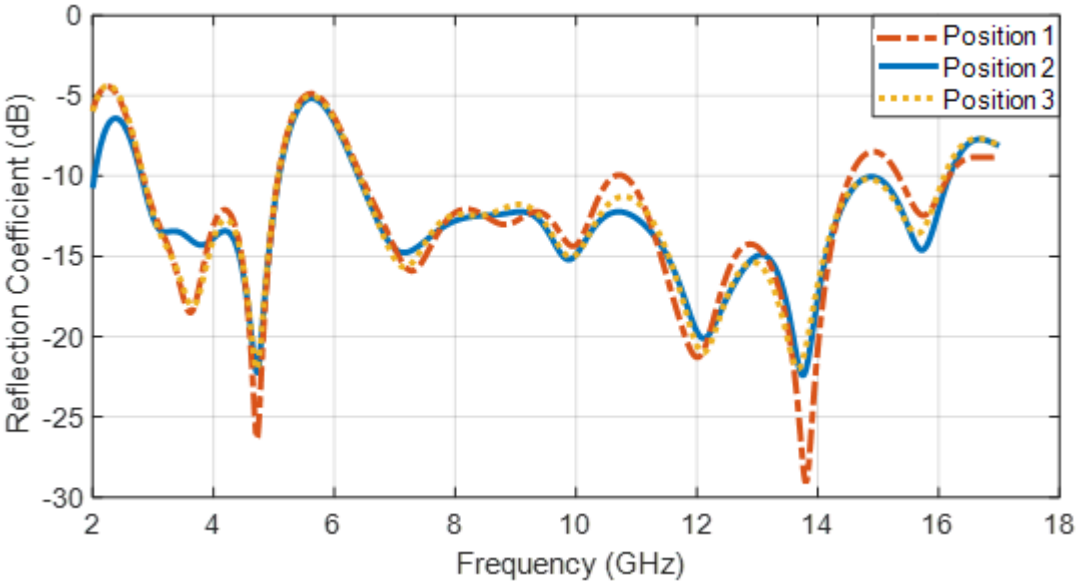

Figure 4.5: Reflection coefficient plot of the antenna

Figure 4.6 shows the coupling coefficient plot for port 1 of the MIMO antenna for various configuration. As shown from the figure below, the coupling coefficient of the human face shaped MIMO antenna in position 1, position 2 and position 3 are -16.9 dB, -19.5 dB and -19.8 dB, respectively. Figure 4.7 shows the transmission coefficient plot for port 1 of the MIMO antenna for various configuration. The S12 parameters for position 1, position 2 and position 3 are -17dB, -19.6 dB and -19.6 dB, respectively. The minimum value of the scattering parameters for various antenna configuration is shown in Table 4.2. As shown from the table that the coupling coefficient of the human face shaped MIMO antenna in position 3 is better than the antennas in position 1 and position 2.

`

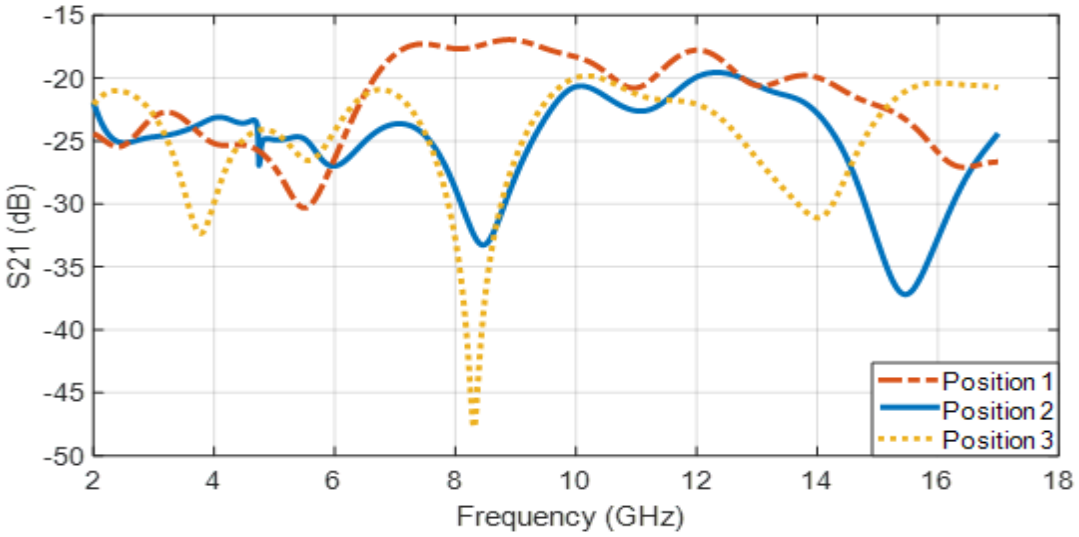

Figure 4.6: Coupling coefficient plot of the antenna

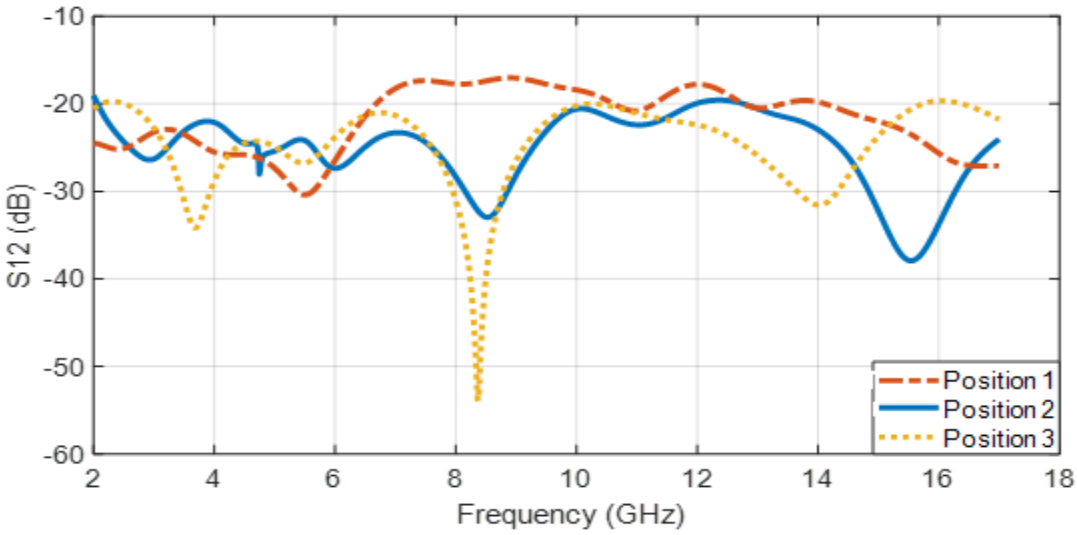

Figure 4.7: Transmission coefficient plot of the MIMO antenna

Table 4.2: Scattering parameters of various antenna structures

Antenna Positions	**Position 1**	**Position 2**	**Position 3**
Min. reflection coefficient for port 1(S11)	-28.8 *dB*	-22.2 *dB*	-22 *dB*
Min. coupling coefficient (S21)	-16.9 *dB*	-19.5 *dB*	-19.8 *dB*
Min. transmission coefficient (S12)	-17 *dB*	-19.6 *dB*	-19.6 *dB*
Min. reflection coefficient for port 2 (S22)	-26.5 *dB*	-30 *dB*	-23.6 *dB*

`

4.2.2.2 Three-dimensional directivity patterns

Figure 4.8 shows the directivity pattern of the human face shaped MIMO antenna in position 3 for port 1. As seen from the figure, the maximum directivity at 16 GHz is 7.61 dBi. Figure 4.9 shows the directivity pattern of human face shaped MIMO antenna in position 3 for port 2. As seen from the figure, the maximum directivity at 16 GHz is 7.21 dBi.

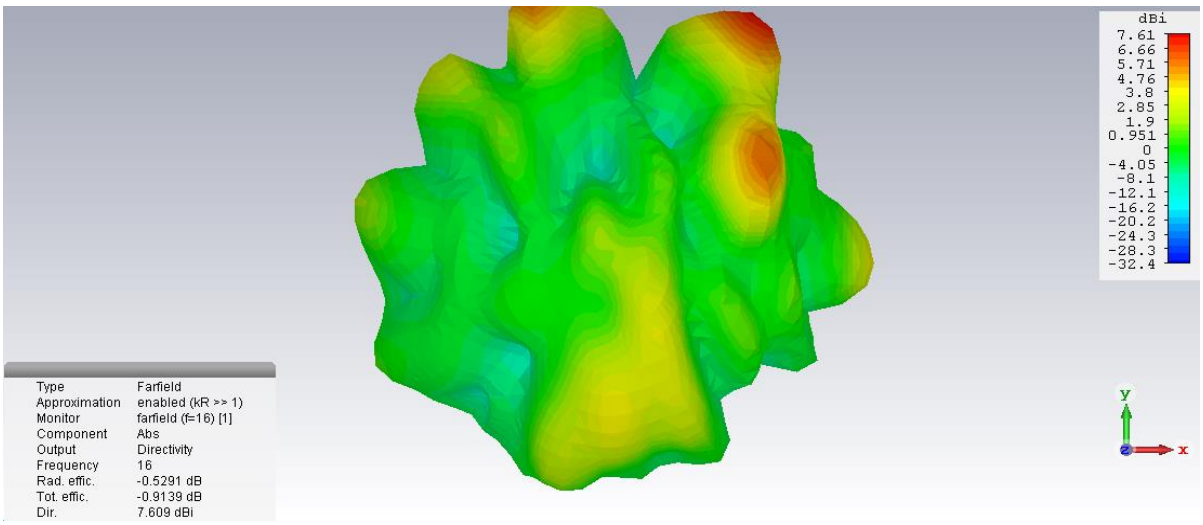

Figure 4.8: Directivity pattern of human face shaped MIMO antenna for port 1

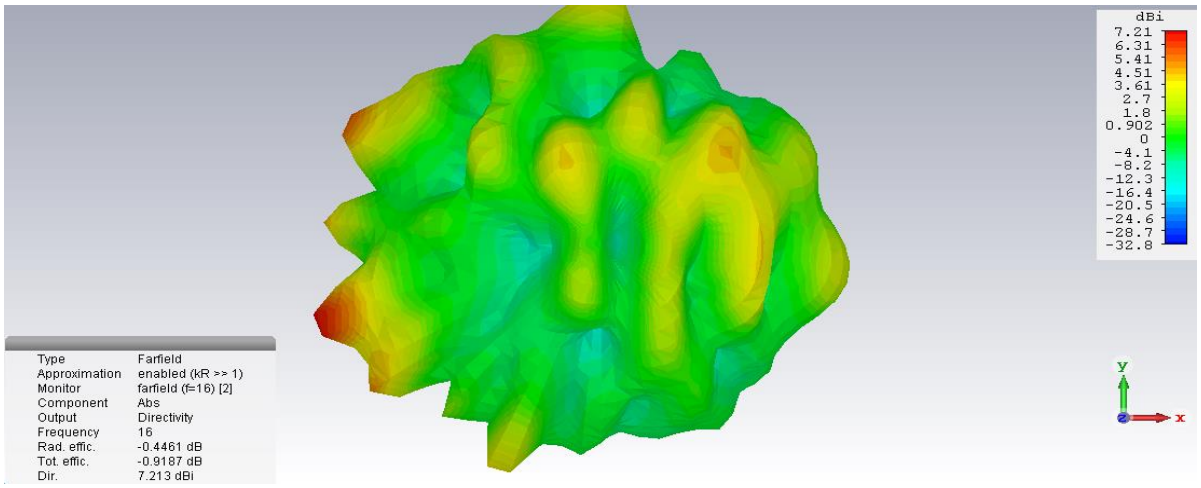

Figure 4.9: Directivity pattern of human face shaped MIMO antenna for port 2.

`

4.2.2.3 Three-dimensional gain pattern

Figure 4.10 shows the gain pattern of the MIMO antenna in position 3 for port 1. The MIMO antenna for port 1 has a maximum gain of 7.01 dB at 16 GHz. Figure 4.11 shows the gain pattern of the MIMO antenna in position 3 for port 2. The MIMO antenna for port 2 has a maximum gain of 6.71 dB at 16 GHz.

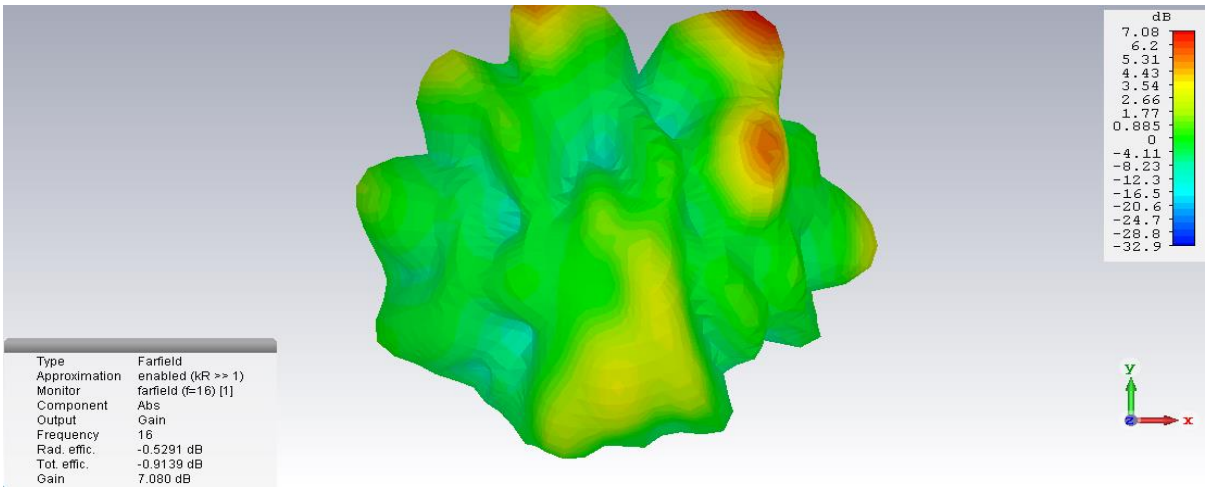

Figure 4.10: Gain pattern of human face shaped MIMO antenna for port 1

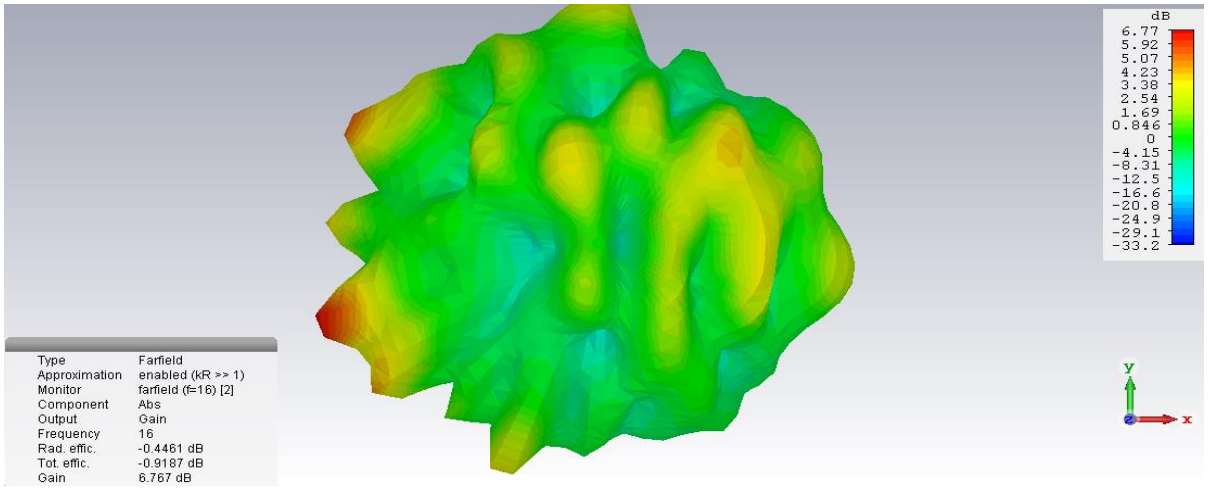

Figure 4.11: Gain pattern of human face shaped MIMO antenna for port 2.

`

Maximum gain and maximum directivity at 16 GHz for various antenna structures are shown in Table 4.3. As observed from the table, the human face shaped MIMO antenna in position 3 has better gain and directivity. The radiation efficiency, total efficiency, gain and directivity at various frequencies for port 1 and port 2 are shown in Table 4.4 and Table 4.5. The gain and directivity are maximum at f= 16 GHz for both the ports. For port 1, the maximum values of the gain and directivity are 7.079 dB and 7.609 dBi, respectively. For port 2, the maximum values of the gain and directivity are 6.765 dB and 7.212 dBi, respectively.

Table 4.3: Gain and directivity of various antenna structures

Antenna Positions	**Position 1 (port 1)**	**Position 1 (port 2)**	**Position 2 (port 1)**	**Position 2 (port 2)**	**Position 3 (port 1)**	**Position 3 (port 2)**
Gain (dB) (f=16 GHz)	5.723	6.181	6.593	4.468	7.080	6.767
Directivity (dBi) (f= 16 GHz)	6.291	6.798	7.194	5.815	7.609	7.212

Table 4.4: Radiation efficiency, total efficiency, gain and directivity at various frequencies for port 1

Frequency (GHz)	**4 GHz**	**10 GHz**	**12 GHz**	**14 GHz**	**16 GHz**
Radiation Efficiency	-1.551 dB	-0.826 dB	-1.213 dB	-0.735 dB	-0.529 dB
Total Efficiency	-1.879 dB	-0.985 dB	-1.320 dB	-0.926 dB	-0.914 dB
Gain	2.911dB	5.062 dB	4.326 dB	5.314 dB	7.079 dB
Directivity	4.462 dBi	5.888 dBi	5.539 dBi	6.050 dBi	7.609 dBi

`

Table 4.5: Radiation efficiency, total efficiency, gain and directivity at various frequencies for port 2

Frequency	4 GHz	10 GHz	12 GHz	14 GHz	16 GHz
Radiation Efficiency	-1.570 dB	-0.8763 dB	-1.131 dB	-0.678 dB	-0.447 dB
Total Efficiency	-1.825 dB	-1.068 dB	-1.238 dB	-0.906 dB	-0.919 dB
Gain	1.976 dB	5.201 dB	4.051 dB	6.227 dB	6.765 dB
Directivity	3.546 dBi	6.078 dBi	5.182 dBi	6.906 dBi	7.212 dBi

4.2.2.4 Comparison of human face shaped MIMO antennas with existing antennas

Table 4.6 shows the comparison between the human face shaped MIMO antenna in position 3 with the existing antennas. From this table, it is evident that proposed human face shaped MIMO antenna has high gain, wide bandwidth and high isolation.

Table 4.6: Comparison of human face shaped MIMO antenna with some existing antennas

Reference	[4]	[5]	[92]	[95]	[101]	Position 3 Antenna
Max Gain (dB)	5	2.5	7	5.9	6.3	7.080
Bandwidth (%)	124.32	109.48	112.42	120	117.8	140.7
Size (mm *mm)	26*31	40*68	38*25	29*23	66.25*66.25	39.1*70.2
Isolation (dB)	>25	>15	>15	>15	>9.8	>19.8

4.2.2.4 VSWR

Figure 4.12 shows the VSWR versus frequency plot for port 1. The maximum value is 3.6, which is at the notched frequency at f=5.5 GHz. The minimum value of VSWR is 1.1.

`

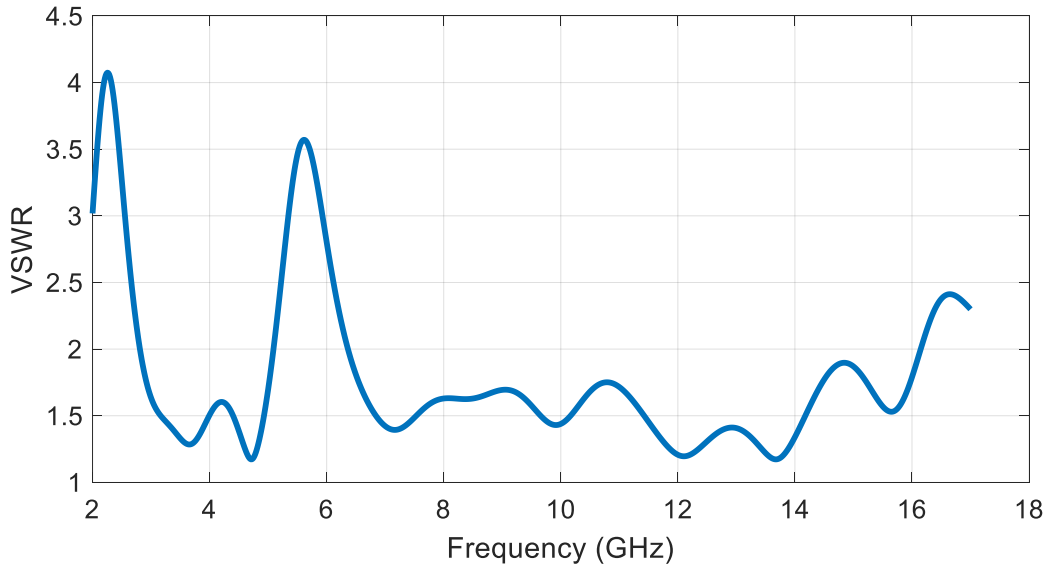

Figure 4.12: VSWR vs frequency plot for port 1

Figure 4.13 shows the VSWR versus frequency plot for port 2. The maximum value is 3.7, which is at the notched frequency at f=5.6 GHz. The minimum value of VSWR is 1.1. From the VSWR plot it is evident that the value of VSWR is less than 2 from 2.8 GHz to 16.1 GHz except at 5 - 6.4 GHz for both the ports.

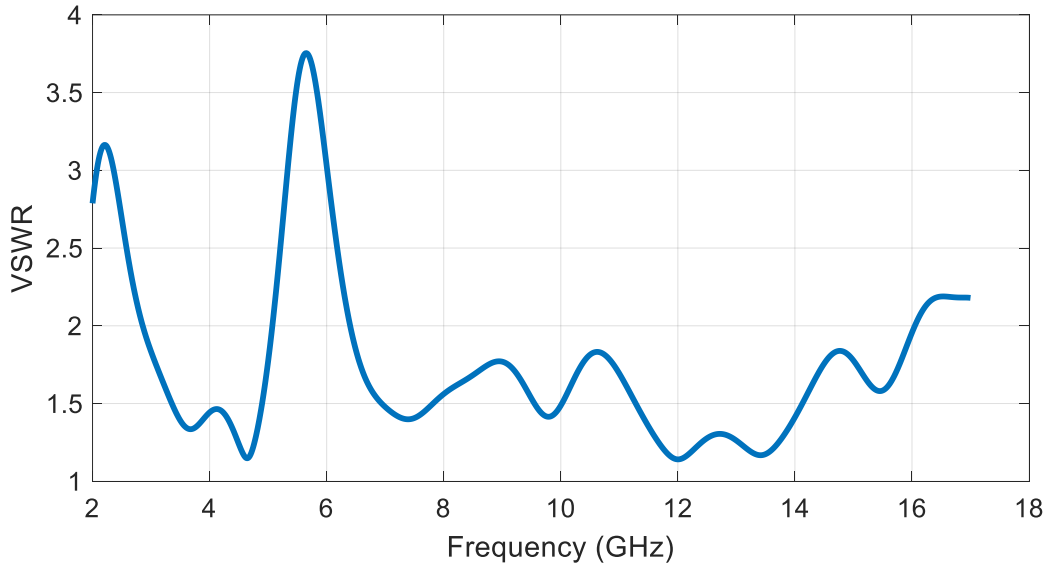

Figure 4.13: VSWR vs frequency plot for port 2

`

4.2.2.5 Gain and directivity of the antenna

The maximum gain and directivity of the antenna are shown in Figure 4.14. As shown from the figure, the maximum gain and maximum directivity of the human face shaped MIMO antenna for port 1 are 7.1 dB and 7.609 dBi, respectively. The maximum gain and maximum directivity of the human face shaped MIMO antenna for port 2 are 6.765 dB and 7.212 dBi, respectively.

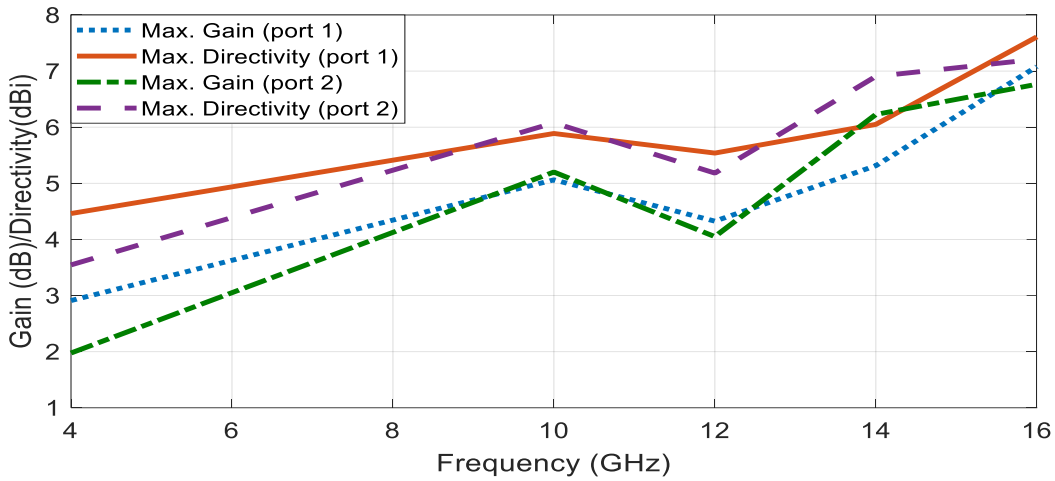

Figure 4.14: Gain and directivity plot of human face shaped MIMO antenna

4.2.3 Fabrication and measured results

To verify the design of the antenna, the MIMO antenna is fabricated on FR4 substrate with relative permittivity of 4.4 and thickness of 1.6 mm with an area of 39.1 * 70.2 mm. FR4 is used as substrate as it is cheap and easily available. The top view and the bottom view of the fabricated antenna are shown in Figure 4.15 (a) and Figure 4.15 (b), respectively. On the top side of the antenna, a microstrip line having a width of 3.4 mm feeds the antenna. The antenna is excited by a 50 Ω SMA connector.

`

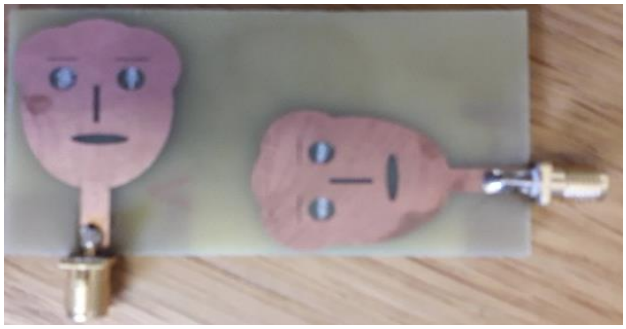

(a)

(b)

Figure 4.15: Fabricated Antenna (a) top view (b) bottom view

4.2.3.1 Reflection coefficient

Figure 4.16 shows the simulated and measured reflection coefficient plot up to 13 GHz. The comparison of measured and simulated results shows good agreement. As seen from the figure, the human face shaped MIMO antenna has the bandwidth from 2.8 GHz to 16.1 GHz with a notch band from 5 GHz to 6.4 GHz.

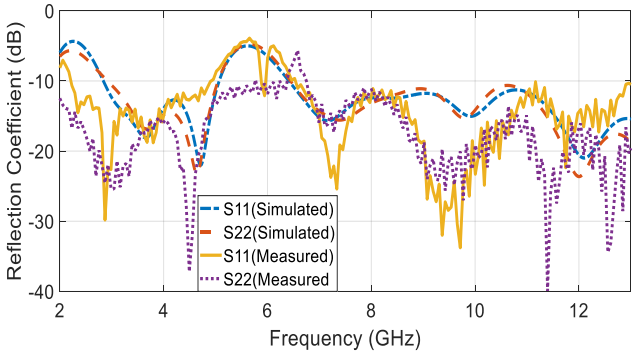

Figure 4.16: Simulated and measured reflection coefficient plot of fabricated antenna

`

4.2.3.2 Two-dimensional radiation patterns

The normalized radiation patterns of the proposed human face shaped MIMO antenna are shown in Figure 4.17. The normalized pattern in phi= 0 degree and phi= 90 degree plane at 4 GHz, 8 GHz, 10 GHz and 12 GHz for port 1 are depicted in Figure 4.17 (a), Figure 4.17 (b), Figure 4.17 (c) and Figure 4.17 (d), respectively. The normalized pattern in phi= 0 degree and phi = 90 degree plane at 4 GHz, 8 GHz, 10 GHz and 12 GHz for port 2 are depicted in Figure 4.17 (e), Figure 4.17 (f), Figure 4.17 (g) and Figure 4.17 (h), respectively. The simulated and measured patterns show agreement with minor deviation. It may be connector and other losses etc. The co-polar and cross-polar simulated patterns of the antenna for both ports at 6 GHz are depicted in Figure 4.18. From these patterns, it can be observed that the cross-polarization is relatively low. From Figure 4.18, it can be noted that the minimum values of cross polarization in the major lobe for port-1 and port-2 are -38.54 dB and -18.79 dB, respectively.

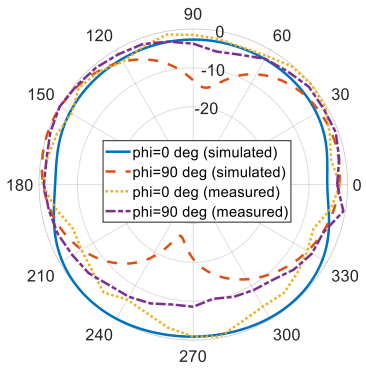

(a)

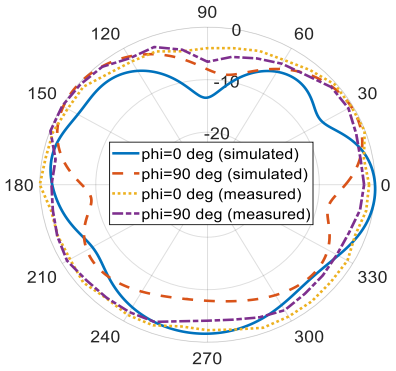

(b)

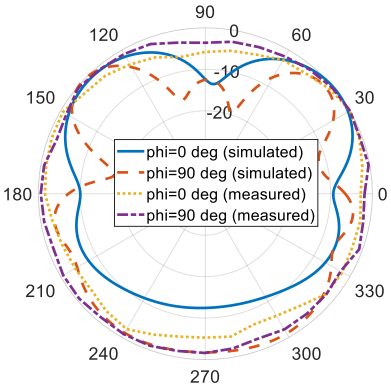

(c)

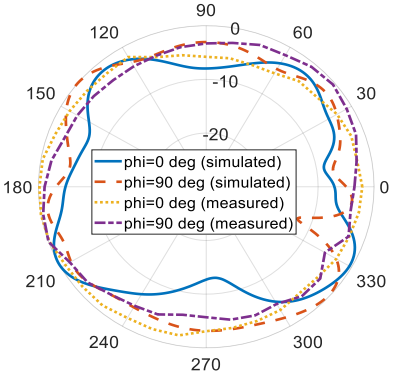

(d)

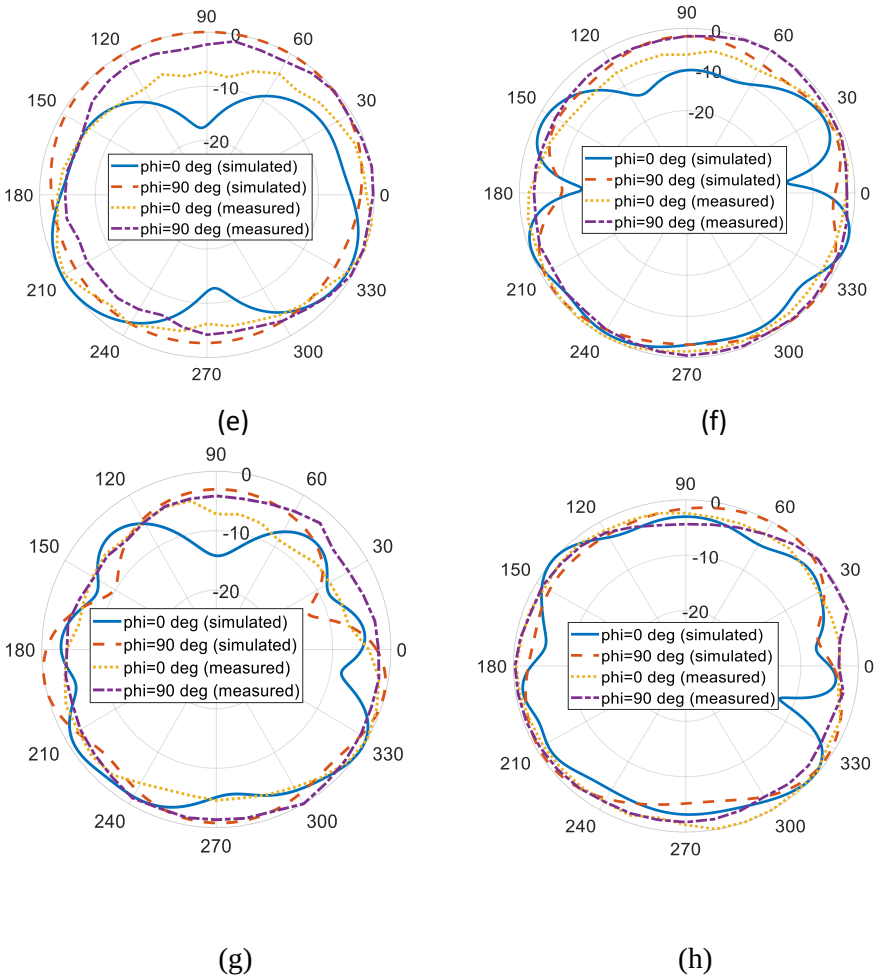

Figure 4.17: Radiation patterns of the antenna at (a) f=4 GHz (port 1), (b) f=8 GHz (port 1), (c) f=10 GHz (port 1), (d) f=12 GHz (port 1), (e) f=4 GHz (port 2), (f) f=8 GHz (port 2) (g) f=10 GHz (port 2), (h) f=12 GHz (port 2)

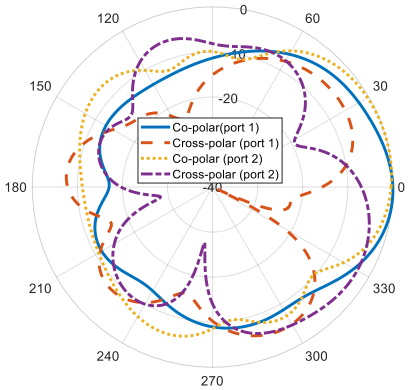

Figure 4.18: Co-polar and cross-polar patterns

`

4.3 Chapter summary

A human face shaped dual polarized MIMO patch antenna for UWB applications with elimination of 5 GHz - 6 GHz WLAN signals has been presented. Two identical human faced antennas are placed orthogonally at a distance of 0.39 λ0. To achieve a wide bandwidth and high isolation, the slots in the patch along with DGS are utilized. The position of the antennas is optimized to further improve the performance of the antenna. The antenna is simulated, optimized, fabricated and measured. The simulated and measured parameters are presented and discussed. The presented antenna has a wide impedance bandwidth from 2.8 GHz to 16.1 GHz with a notch to avoid interference from 5 GHz - 6 GHz WLAN signals. The maximum gain and maximum directivity of the presented human face shaped antenna are 7.079 dB and 7.609 dBi, respectively. The presented human face shaped MIMO patch antenna is suitable for UWB communications.

`

CHAPTER 5: CONCLUSION AND FUTURE WORK

5.1 Conclusion

Ultra-wideband technology in wireless communication plays an important role as it provides large bandwidth with low power consumption. Microstrip antennas are commonly used antennas in various application due to their low profile and compact size, but these antennas suffer from narrow bandwidth and poor gain. Antennas for UWB technology require a wide bandwidth. In this study, the bandwidth is improved by using the concept of defected ground structure and slots in elliptical patch. The design of three human face shaped microstrip patch antennas for ultra-wideband applications have been presented in this study. In the first design, a compact human face shaped microstrip patch antenna, that can operate from 5.9 GHz to 11.2 GHz, is presented. The antenna has a minimum reflection coefficient of -35.11 dB with a size of 25.2 mm * 38.2 mm. The maximum gain and the directivity of the antenna are 6.219 dB and 6.268 dBi, respectively. The human face shaped antenna has the rectangular defects in the ground plane to achieve the wide bandwidth. In the second design, a human face shaped microstrip patch antenna, which covers the frequency from 3 GHz to 14.7 GHz with a notch from 5 GHz to 6.3 GHz to reject WLAN signals, is presented. The minimum reflection coefficient, maximum gain, maximum directivity of the human face shaped antenna with enhanced bandwidth are 5.945 dB, 6.411 dBi and -35.4 dB, respectively. The human face shaped antenna is small in size with the dimensions of 24.6 mm * 38.6 mm and is easy to fabricate. The antenna has rectangular and triangular defects in the ground plane to achieve wide bandwidth. In the third design, a MIMO antenna, which operates from 2.8 GHz to 16.1 GHz with a notch band from 5 GHz to 6.4 GHz, is presented. In MIMO antenna, two human face shaped antennas are placed orthogonally to achieve dual polarization. The human face shaped antennas are separated at a distance of 0.39 λ0. The antenna has a size of 39.1 mm x 70.2 mm with a minimum reflection coefficient of -22 dB. The maximum gain and maximum directivity of the MIMO antenna are 7.079 dB and 7.609 dBi, respectively.

To achieve the wide bandwidth and high isolation, the slots in the patch along with rectangular and triangular defects in the ground plane are utilized. Polarization diversity concept is used to design antenna for MIMO applications. The antennas are simulated using CST microwave studio and various antenna parameters like reflection coefficient, VSWR, radiation

`

pattern, gain, directivity, total efficiency, radiation efficiency etc are presented and discussed. The antennas are fabricated and measured. The measured parameters are also presented and discussed. The proposed antennas are suitable for ultra-wideband applications.

5.2 Future work

Further improvements can be achieved through this work, in regard to enhancing the parameters like gain, directivity and bandwidth of the antennas. Different feeding techniques like proximity feed, aperture feed to increase the bandwidth of the antenna can be investigated. Other techniques like lowering the Q factor of the patch, increasing the height of the substrate can be analyzed to improve the impedance bandwidth of the antenna. Impedance matching techniques using quarter wavelength microstrip impedance transformer, microstrip stubs, microstrip inset feed can be investigated. Multi-layer dielectric substrates can be used to increase the gain of the antenna. Antennas can also be combined in array to improve the gain and obtain high directivity. To reduce the size of the antennas and to increase the isolation between the antennas, the concept of metamaterial can be used. Metamaterials are artificially made by combining two or more naturally occurring materials and has unusual electromagnetic properties. The use of parasitic elements, complementary split ring resonator, decoupling networks to decrease the mutual coupling between the antenna ports can be analyzed.

`

REFERENCES

[1] C. A. Balanis, “Antenna theory analysis & design”, 4rd ed, John Wiley and Sons, New York, 2016.

[2] K. Siwiak, D. McKeown, “Ultra-wideband radio technology”, Wiley, Hoboken, NJ, 2004.

[3] P. Kumar, “Design of low cross-polarized patch antenna for ultra-wideband applications", *International Journal on Communications Antenna and Propagation*, Vol. 7, 265-270, 2017.

[4] N. Malekpour, M. A. Honarvar, “Design of high isolation compact MIMO antenna for UWB application", *Progress In Electromagnetics Research C*, Vol. 62, 119-129, 2016.

[5] A. Najam, Y. Duroc, S. Tedjni, “UWB-MIMO antenna with novel stub structure", *Progress In Electromagnetics Research C*, Vol. 19, 245-257, 2011.

[6] A. K. Arya, M. V. Kartikeyan, A. Patnaik, “Efficiency enhancement of microstrip patch antenna with defected ground structure", *International Conference on Recent Advances in Microwave Theory and Applications*, 729-731, 2008.

[7] A. Choudhary, S. Moya, “A review paper on MIMO antenna isolation improving techniques”, *Journals for International Shodh in Engineering and Technology*, Vol. 2, 2017.

[8] T. S. Bird, “Definition and Misuse of Return Loss”, *IEEE Antennas and Propagation Magazine*, Vol. 51, 166-167, April 2009.

[9] Q. Wang, H. N. Dai, Z. Zheng, M. Imran, A. V. Athanasios, “On connectivity of wireless sensor networks with directional antennas”, Sensors, Vol. 17, 1-22, 2017.

[10] G. Misra, A. Agarwal, K. Agarwal, “Design and performance evaluation of microstrip antenna for ultra-wideband applications using microstrip feed”, *American Journal of Electrical and Electronic Engineering*, Vol. 3, 93-99, 2015.

[11] M. A. Layegh, C. Ghobadi, J. Nourinia, “The optimization design of a novel slotted microstrip patch antenna with multi-bands using adaptive network-based fuzzy interference system”, *Preprints*, Vol. 5, 1-75, 2017

[12] A. D. Khaleel, “Design tri-band single and dual patch array antenna with band suppression”, Master Thesis, Universiti Tenaga Nasional, 2012.

[13] M. Rahman, “Small size coupling feed and inductive shorting antenna for wide bandwidth, increased gain and efficiency with low specific absorption rate (SAR) operation”, Master Thesis, Michigan Technological University, 2016.

[14] Y. I. A. Al-Yasir, A. S. Abdullah, “Design and analysis of corrugated printed antenna for mobile communication applications”, BSc Project Thesis, University of Basra, 2012.

`

[15] M. R. Hasan, A. Al. Suman, "Substrate height and dielectric constant dependent performance analysis of circular microstrip patch array antennas for broadband wireless access", *American Academic and Scholarly Research Journal*, Vol. 4, 43–49, 2012.

[16] M. B. Hossain, S. Datto, "Improvement of antenna performance using stacked microstrip patch antenna", *2nd International Conference on Electrical, Computer & Telecommunication Engineering (ICECTE)*, 1-4, 2016.

[17] S. F. Nurjihan, A. Munir, "Effect of DGS incorporation for bandwidth enhancement of UWB microstrip BPF", *3rd International Conference on Wireless and Telematics*, 39-42, 2017.

[18] U. Kumar, D. K. Upadhyay, B. L. Shahu, "Improvement of performance parameters of rectangular patch antenna using metamaterial", *IEEE International Conference on Recent Trends in Electronics Information Communication Technology*, 1011-1015, 2016.

[19] R. Yahya, A. Nakamura, M. Itami, T. A. Denidni, "A novel UWB FSS-based polarization diversity antenna", *IEEE Antennas and Wireless Propagation Letters*, Vol. 16, 2525-2528, 2017.

[20] Y. M. Madany, "Bandwidth enhancement of compact UWB microstrip patch antenna using EBG structures", *IEEE Antennas and Propagation Society International Symposium*, 402-403, 2013.

[21] F. Alizadeh, J. Nournia, Ch. Ghobadi, B. Mohammadi, "A dual-band rejection UWB antenna using EBG", *IEEE 4th International Conference on Knowledge-Based Engineering and Innovation (KBEI)*, 192-193, 2017.

[22] L. H. Weng, Y. C. Guo, X. W. Shi, X. Q. Chen, "An overview on defective ground structures", *Progress in Electromagnetics Research*, Vol. 7, 173-189, 2008.

[23] P. K. Deb, T. Moyra, P. Bhowmik, "Return loss and bandwidth enhancement of microstrip antenna using defective ground structure (DGS)", *2nd International Conference on Signal Processing and Integrated Networks (SPIN)*, 25-29, 2015.

[24] C. Garg, M. Kaur, "A review of defected ground structure (DGS) in microwave design*", International Journal of Innovative Research in Electrical, Electronics, Instrumentation and Control Engineering*, Vol. 2, 1285-1290, 2014.

[25] C. S. Kim, J. S. Park, D. Ahn, J. B. Lim, "A novel 1-D periodic defected ground structure for planar circuits", *IEEE Microwave and Wireless Components Letters*, Vol. 10, 131–133, 2000.

[26] M. K. Mandal, S. Sanyal, "A novel defected ground structure for planar circuits", *IEEE Microwave and Wireless Components Letters*, Vol. 16, 93–95, 2006.

[27] C. S. Kim, J. S. Lim, S. Nam, K. Y. Kang, D. Ahn, "Equivalent circuit modelling of spiral defected ground structure for microstrip line", *Electronics Letters*, Vol. 38, 1109–1110, 2002.

`

[28] D. J. Woo, T. K. Lee, J. W. Lee, C. S. Pyo, W. K. Choi, "Novel U-slot and V-slot DGS for bandstop filter with improved Q factor", *IEEE Transactions on Microwave Theory and Techniques*, Vol. 54, 2840–2847, 2006.

[29] A. Balalem, A. R. Ali, J. Machac, A. Omar, "Quasi-elliptic microstrip low-pass filters using an interdigital DGS slot", *IEEE Microwave Wireless Components Letters*, Vol. 17, 586-588, 2007.

[30] Z. Z. Hou, "Novel wideband filter with a transmission zero based on split-ring resonator DGS", *Microwave Optical Technology Letters*, Vol. 50, 1691-1693, 2008.

[31] S. N. Burokur, M. Latrach, S. Toutain, "A novel type of microstrip coupler utilizing a slot split ring resonator defected ground plane", *Microwave and Optical Technology Letters*, Vol. 48, 138-141, 2005.

[32] H. W. Liu, Z. F. Li, X. W. Sun, "A novel fractal defected ground structure and its application to the low-pass filter", *Microwave and Optical Technology Letters*, Vol. 39, 453-456, 2003.

[33] J. K. Xiao, Y. F. Zhu, "New U shaped DGS bandstop filters", *Progress in Electromagnetics Research*, Vol. 25, 179-191, 2012.

[34] M. K. Khandelwal, B. K. Kanaujia, S. Kumar, "Defected ground structure: fundamentals, analysis, and applications in modern wireless trends", *International Journal of Antennas and Propagation*, Vol. 2017, 1- 22, 2017.

[35] A. Kunwar, A. K. Gautam, B. K. Kanaujia, K. Rambabu, "Circularly polarized D-shaped slot antenna for wireless applications", *International Journal of RF and Microwave Computer Aided Engineering*, 1-10, 2018.

[36] J.-Y.Jan, J.-W.Su, "Bandwidth enhancement of a printed wide-slot antenna with a rotated slot", *IEEE Transactions on Antennas and Propagation*, Vol. 53, 2111–2114, 2005.

[37] N. Ojaroudi, "Compact UWB monopole antenna with enhanced bandwidth using rotated L-shaped slots and parasitic structures", *Microwave and Optical Technology Letters*, Vol. 56, 175–178, 2014.

[38] C. Zhang, J. Zhang, L. Li, "Triple band-notched UWB antenna based on SIR-DGS and fork-shaped stubs", *Electronics Letters*, Vol. 50, 67-69, 2014.

[39] H. Elftouh, N. A. Touhami, M. Aghoutane, S.E. Amrani, "Miniaturized microstrip patch antenna with defected ground structure", *Progress in Electromagnetics Research C*, Vol. 55, 25-33, 2014.

[40] S. I. H. Shah, S. Bashir, S. D. H. Shah, "Compact multiband microstrip patch antenna using defected ground structure (DGS)", *IEEE International Seminar/Workshop on Direct and Inverse Problems of Electromagnetic and Acoustic Wave Theory*, 96-99, 2014.

`

[41] C. Kumar, D. Guha, “Defected ground structure (DGS)-integrated rectangular microstrip patch for improved polarization purity with wide impedance bandwidth”, *IET Microwaves, Antennas and Propagation,* Vol. 8, 589–596, 2014.

[42] Z. L. Zhang, K. Wei, J. Xie, J. Y. Li, “The MIMO antenna array with mutual coupling reduction and cross-polarization suppression by defected ground structures”, *Radio Engineering,* Vol. 27, 969-975, 2018.

[43] A. Ghosh, B. Basu, “Defected ground structure integrated rectangular microstrip patch antenna on semi-insulating substrate for improved polarization purity”, *Smart Computational Strategies: Theoretical and Practical Aspects. Springer,* 175-183, 2019.

[44] X. L. Liang, “Ultra-Wideband Antenna and Design”, *IntechOpen,* 2012.

[45] K. P. Ray, “Design aspects of printed monopole antennas for ultra-wideband applications”, *International Journal of Antennas and Propagation,* Vol. 2008, 1-8, 2008.

[46] O. Lodge, “Electric telegraphy”, 1898.

[47] P. S. Carter, “Wideband, short wave antenna and transmission line system”, U.S. Patent 2,181, 870, 1939.

[48] N. E. Lindenblad, “Wideband antenna”, U.S. Patent 2, 239, 724, 1941.

[49] X. L. Liang, “Ultra-wideband antenna and design”, *Ultra-Wideband Current Status and Future Trends, Intech,* Chapter 12*, 2012.*

[50] L. Paulsen, J. B. West, W. F. Perger, J. Kraus, “Recent investigations on the volcano smoke antenna”, *IEEE Antennas and Propagation International Symposium (Digest),* Columbus, OH, 845-848, 2003.

[51] A. P. King, “Transmission, radiation, and reception of electromagnetic waves”, U.S. Patent 2, 283, 935 (May 26, 1942)

[52] H. G. Schantz, “A brief history of UWB antennas”, *IEEE Aerospace and Electronic Systems Magazine,* 22-26, 2004.

[53] W. Stohr, “Broadband ellipsoidal dipole antenna”, U.S. Patent 3, 364, 491, 1968.

[54] G. Dubost, S. Zisler, “Antennas a large bande”, New York: Masson, 1976.

[55] N. P. Agrawall, G. Kumar, K. P. Ray, “Wide-band planar monopole antennas”, IEEE *Transactions on Antennas and Propagation,* Vol. 46, 294-295, 1998.

[56] J. A. Evans, M. J. Amunann, “Planar trapezoidal and pentagonal monopoles with impedance bandwidth in excess 10:1”, *IEEE Antennas and Propagation International Symposium (Digest),* 1558-1561, 1999.

[57] S. Y. Suh, W. L. Stutzman, W. A. Davis, “New ultra-wideband printed monopole antenna, planar inverted cone antenna”, *IEEE Transactions on Antennas and Propagation,* Vol. 52, 1361-1364, 2004.

`

[58] X. F. Bai, S. S. Zhong, X.L. Liang, “Leaf-shaped monopole antenna with extremely wide bandwidth”, *Microwave and Optical Technology Letters*, Vol. 48, 1247-1250, 2006.

[59] S. H. Choi, J. K. Park, S.K. Kim, J. Y. Park, “A new ultra-wideband antenna for UWB applications”, *Microwave and Optical Technology Letters*, Vol. 40, 399-401, 2004.

[60] J. Liang, C. C. Chiau, X. Chen, C. G. Parini, “Study of a printed circular disc monopole antenna for UWB systems”, *IEEE Transactions on Antennas and Propagation*, Vol. 53, 3500-3504, 2005.

[61] B. L. Ooi, G. Zhao, M. S. Leong, K. M. Chua, C. W. L. Albert, “Wideband LTCC CPW-fed two layered monopole antenna”, *Electronics Letters*, Vol. 41, 889-890, 2005.

[62] L. Lizzi, R. Azaro, G. Oliveri, A. Massa, “Printed UWB antenna operating for multiple mobile wireless standards”, *IEEE Antennas and Wireless Propagation Letters*, Vol. 10, 1429-1432, 2010.

[63] J. Kim, T. Yoon, J. Kim, J. Choi, “Design of an ultra-wide-band printed monopole antenna using FDTD and genetic algorithm”, *IEEE Microwave and Wireless Components Letters*, Vol. 15, *395-397*, 2005.

[64] Z. N. Low, J. H. Cheong, C. L. Law, “Low-cost PCB antenna for UWB applications”, *IEEE Antennas and Wireless Propagation Letters*, Vol. 4, 237-239, 2005.

[65] O. Ahmed, A. R. Sebak, “A printed monopole antenna with two steps circular slot for UWB applications”, *IEEE Antennas and Wireless Propagation Letters*, Vol. 7, 411-413, 2008.

[66] Y.W. Jang, “Experimental study of large bandwidth three offset microstrip line-fed slot antenna”, *IEEE Microwave and Wireless Components Letters*, Vol. 11, 425-427, 2011.

[67] F. W. Yao, S. S. Zhong, W. Wang, X. L. Liang, “Wideband slot antenna with a novel microstrip feed”, *Microwave Optical Technology Letters*, Vol. 46, 275-278, 2005.

[68] M. Lapierre, Y. M. M. Antar, A. Ittipiboon, A. Petosa, "Ultra-wideband monopole/dielectric resonator antenna", *IEEE Microwave and Wireless Components Letters*, Vol. 15, 7-9, 2005.

[69] Y. F Ruan, Y. X. Guo, X. Q. Shi, “Double annular-ring dielectric resonator antenna for ultra- wideband application”, *Microwave and Optical Technology Letters*, Vol. 49, 362-366, 2007.

[70] M. N. Jazi, T. A. Denidni, “Design and implementation of an ultrawideband hybrid skirt monopole dielectric resonator antenna”, *IEEE Antennas and Wireless propagation Letters*, Vol 7, 493-496, 2008.

[71] Y. Kim, D. H. Kwon, “CPW-fed planar ultra-wideband antenna having a frequency band notch function”, *Electronic Letters*, Vol. 40, 403-405, 2004.

`

[72] K. Chung, J. Kim, J. Choi, “Wideband microstrip-fed monopole antenna having frequency band-notch function”, *IEEE Microwave and Wireless Components Letters,* Vol. 15, 766-768, *2005.*

[73] M. Ojaroudi, G. Ghanbari, N. Ojaroudi, C. Ghobadi, “Small square monopole antenna for UWB applications with variable frequency band notch function”, *IEEE Antennas and Wireless Propagation Letters,* Vol. 15, 133-144, 2009.

[74] J. B. Jiang, Y. Song, Z. H. Yan, X. Zhang, “Band-notch UWB printed antenna with an inverted-L-slotted ground”, *Microwave and Optical Technology Letters,* Vol. 51, 260 – 263, 2009.

[75] C. Y. D. Sim, W. T. Chung, C. H. Lee, “An octagonal UWB antenna with 5 band-notch function”, *Microwave and Optical Letters,* Vol. 51, 74-78, 2009.

[76] I. T. Tang, D. B. Lin, G. H. Liou, J. H. Horng, “Miniaturized 5.2 GHz notched UWB CPW-fed antenna using dual reverse split trapezoid slots”, *Microwave and Optical Letters,* Vol. 50, 652-655, 2009.

[77] J. Ghimire, D. Y. Choi, “Design of a compact ultra-wideband U-shaped slot etched on a circular patch antenna with notch band characteristics for ultra-wideband applications”, *International Journal of Antennas and Propagation*, Vol. 2019, 1-10, 2019.

[78] X. Liu, Y. Z. Yin, J. H. Wang, J. J. Xie, “Compact dual band-notched UWB antenna with parasitic microstrip lines and T-shape Stub”, *Progress in Electromagnetics Research C,* Vol. 41, 55-56, 2013.

[79] F. Guichi, M. Challal, T. A. Denidni, “A novel dual band-notch ultra-wideband monopole antenna using parasitic stubs and slot”, *Microwave Optical Technology Letters,* Vol. 60, 1737– 1744, 2018.

[80] Y. Li, W. Li, Q. Ye, “A reconfigurable triple-notch-band antenna integrated with defected microstrip structure band-stop filter for ultra-wideband cognitive radio applications”, *International Journal of Antennas and Propagation*, Vol. 2013, 1-13, 2013.

[81] D. Guha, S. Biswas, C. Kumar, “Printed antenna designs using defected ground structures: a review of fundamentals and state-of-the-art developments”, *Forum for Electromagnetic Research Methods and Application Technologies (FERMAT),* 1-13, 2014.

[82] M. Mabaso, P. Kumar, “A dual band patch antenna for bluetooth and wireless local area networks applications”, *International Journal of Microwave and Optical Technology,* Vol. 13, 393-400, 2018

[83] N. Kumprasert, “Theoretical study of dual-resonant frequency and circular polarization of elliptical microstrip antennas", *IEEE Antennas and Propagation Society International Symposium*, Vol. 2, 1015-1020, 2000.

`

[84] D. Ahn, J. S. Park, C. S. Kim, J. Kim, Y. Qian, T. Itoh, "A design of the low-pass filter using the novel microstrip defected ground structure", *IEEE Transactions On Microwave Theory And Techniques*, Vol. 49, 86-93, 2001.

[85] R. Kumar, Virendra, A. Saxena, "Elliptical micro-strip patch antenna for circular polarization design using HFSS", *International Research Journal of Engineering and Technology (IRJET)*, Vol. 03, 1408-1411, 2016.

[86] P. A. Ambresh, P. M. Hadalgi, P. V. Hunagund, "Effect of slots on microstrip patch antenna characteristics", *2011 International Conference on Computer, Communication and Electrical Technology (ICCCET)*, 239-241, *2011*.

[87] Q. Nassir, "Patch antenna performance improvement using circular slots", *2017 International Conference on Wireless Networks and Mobile Communications (WINCOM)*, 1-5, 2017.

[88] A. A. Ibrahim, M. A. Abdalla, "Compact size UWB antenna with multi-band notched characteristics for wireless applications", *IEEE International Symposium on Antennas and Propagation*, 1819-1820, 2016.

[89] M. A. Ullah, F. B. Ashraf, T. Alam, M. S. Allam, S. Kibria, M. T. Islam, "A compact triangular shaped microstrip patch antenna with triangular slotted ground for UWB application", *2016 International Conference on Innovations in Science, Engineering and Technology*, 1-4, 2016.

[90] M. Senapati, P. Kumar, V. Bara, "Design of microstrip patch antenna for application in UWB region", *10th International Conference on Intelligent Systems and Control*, 1-3, 2016.

[91] G. P. Singh, M. Kumar, R. Saxena, J. A. Ansari, "Bandwidth analysis of boomerang slot rectangular microstrip patch antenna", *2nd International Conference on Telecommunication and Networks*, 1-4, 2017.

[92] S. Naser, N. Dib, "A compact printed UWB pacman-shaped MIMO antenna with two frequency rejection bands", *Jordanian Journal of Computers and Information Technology (JJCIT)*, Vol. 2, 1-16, 2016.

[93] K. J. Babu, B. K. Kumar, S. R. Boddu, K. S. R Krishna, "Design of a compact octagonal UWB MIMO antenna employing polarization diversity technique", *Progress in Electromagnetics Research Symposium – Fall (PIERS – FALL)*, 1785-1789, 2017.

[94] J. Y. Zhang, F. Zhang, W. P. Tian, Y. L. Luo, "ACS-fed UWB-MIMO antenna with shared radiator", *Electronics Letters*, Vol. 51, 1301–1302, 2015.

[95] M. S. Khan, A. D. Capobianco, S. M. Asif, D. E. Anagnostou, R. M. Shubair, B. D. Braaten, "A compact CSRR-enabled UWB diversity antenna", *IEEE Antennas Wireless Propagation Letters*, Vol. 16, 808–812, 2017.

[96] G. S. Lin, C. H. Sung, J. L. Chen, L. S. Chen, M. P. Houng, "Isolation improvement in UWB MIMO antenna system using carbon black film", *IEEE Antennas Wireless Propagation. Letters*, Vol. 16, 222–225, 2017.

`

[97] P. Kumar, J. L. Masa-Campos, “Dual polarized monopole patch antennas for UWB Applications with elimination of WLAN signals”, *Advanced Electromagnetics*, Vol. 5, 46-52, 2016.

[98] D. Bhattacharya, M. Joshi, “DGS based mutual coupling reduction in an ultra wideband microstrip patch antenna array”, *International Conference on Innovations in Information, Embedded and Communication*, 1-4, 2017.

[99] J. Ghosh, S. Ghosal, D. Mitra, S. R. B. Chaudhuri, “Mutual coupling reduction between closely placed microstrip patch antenna using meander line resonator”, *Progress in Electromagnetics Research Letters*, Vol. 59, 115–122, 2016.

[100] J. OuYang, F. Yang, Z. M. Wang, “Reducing mutual coupling of closely spaced microstrip MIMO antennas for WLAN application”, *IEEE Antennas and Wireless Propagation Letters*, Vol. 10, 310–313, 2011.

[101] R. Kumar, R. V. S Ram Krishna, “A dual polarized UWB slot antenna with kite shaped slot for high isolation*”, International Conference on Microwave, Optical and Communication Engineering*, 261-263, 2015.